

University of Groningen

## Detection and staging of solid tumors with FDG-PET and FLT-PET

Cobben, David Catharina Petrus

**IMPORTANT NOTE: You are advised to consult the publisher's version (publisher's PDF) if you wish to cite from it. Please check the document version below.**

*Document Version*

Publisher's PDF, also known as Version of record

*Publication date:*

2004

[Link to publication in University of Groningen/UMCG research database](#)

*Citation for published version (APA):*

Cobben, D. C. P. (2004). *Detection and staging of solid tumors with FDG-PET and FLT-PET*. [S.n.].

### Copyright

Other than for strictly personal use, it is not permitted to download or to forward/distribute the text or part of it without the consent of the author(s) and/or copyright holder(s), unless the work is under an open content license (like Creative Commons).

The publication may also be distributed here under the terms of Article 25fa of the Dutch Copyright Act, indicated by the "Taverne" license. More information can be found on the University of Groningen website: <https://www.rug.nl/library/open-access/self-archiving-pure/taverne-amendment>.

### Take-down policy

If you believe that this document breaches copyright please contact us providing details, and we will remove access to the work immediately and investigate your claim.

*Downloaded from the University of Groningen/UMCG research database (Pure): <http://www.rug.nl/research/portal>. For technical reasons the number of authors shown on this cover page is limited to 10 maximum.*

# Detection and staging of solid tumors with FDG-PET and FLT-PET



David C.P. Cobben

**Detection and staging of solid tumors  
with FDG-PET and FLT-PET**

**David Catharina Petrus Cobben**

The research of this thesis was supported by the Dutch Cancer Association. Grant no. 2000-2299.

Financial support for this thesis was kindly provided by  
Stichting Trace 2000  
Eurotec  
Siemens Medical Systems  
Groningen University Institute for Drug Exploration  
University of Groningen

Cover: FDG-PET (left) and FLT-PET scan of a patient with metastatic non-small cell lung cancer

Ponsen & Looijen, Wageningen, The Netherlands  
© 2004 D.C.P. Cobben

Thesis University Groningen  
ISBN 90-367-1996-8

## Stellingen

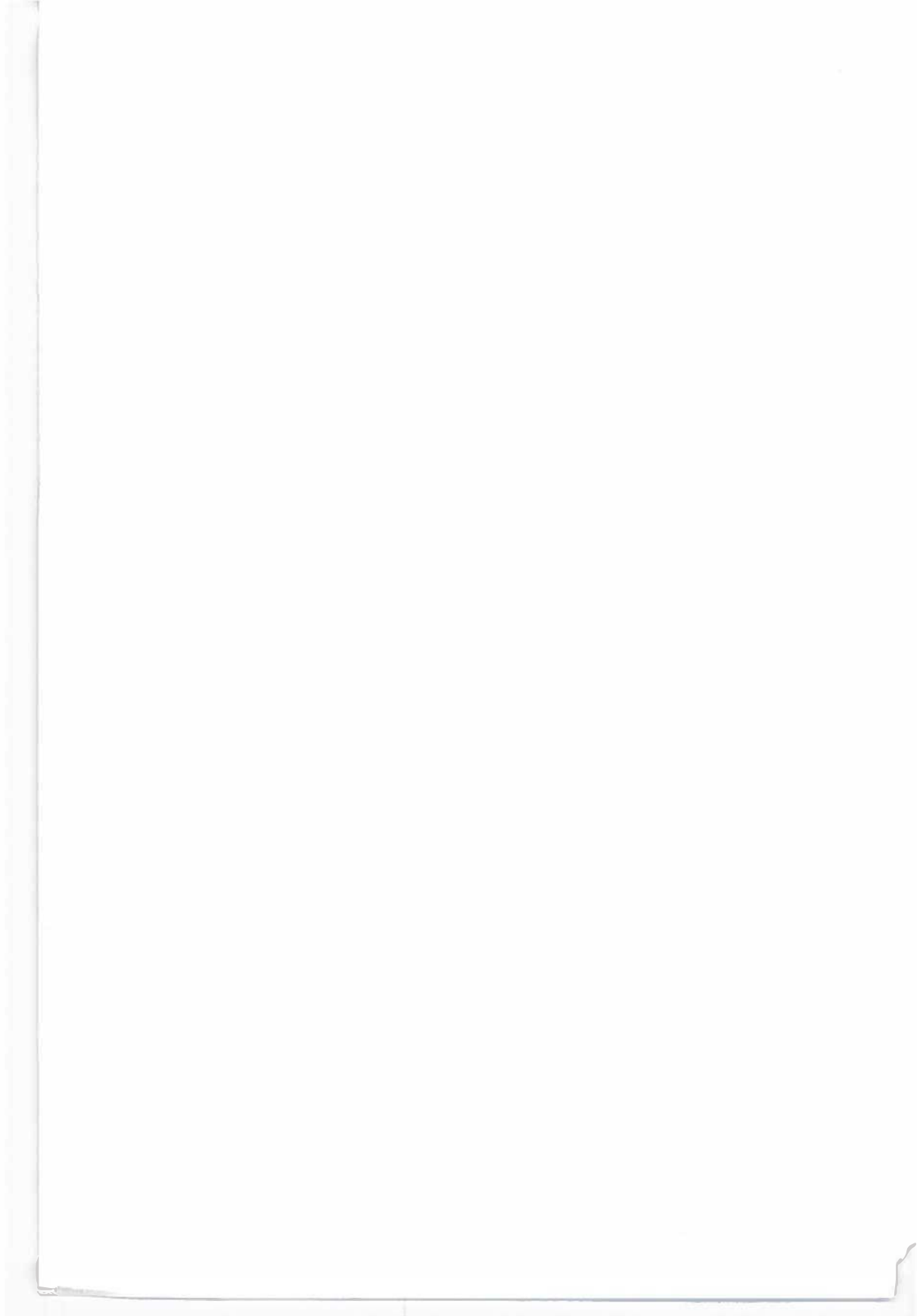
behorende bij het proefschrift

'Detection and staging of solid tumors with FDG-PET and FLT-PET'

1. FLT-PET meet de celproliferatie indirect.
2. De toekomst van FLT-PET ligt eerder op het gebied van de therapie-evaluatie dan op het gebied van tumordetectie en stadiëring.
3. De berekeningsmethode is het enige gestandaardiseerde aan de Standardized Uptake Value (SUV).
4. Vergelijking van "PET-data" wordt vaak bemoeilijkt door de summiere omschrijving van de methodologie in publicaties.
5. De ontwikkeling van de medische praktijk is een zaak van lange adem; PET en de ontwikkeling van diverse toepasbare tracers zijn hiervan voorbeelden.
6. De resectie-marge van het melanoom is nog steeds omstreden.
7. Na kinderen en ouderen met kanker, verdienen nu de adolescenten aandacht.
8. De epidemische toename van overgewicht lijkt gepaard te gaan met een endemische behoefte aan bariatrische chirurgie.
9. Er is een toenemende behoefte aan "novel food".
10. "Het zou misschien kunnen dat machines beslissen, maar we hebben nog steeds de dokter nodig om te helen". (Atul Gawande, 2002)
11. In de toekomst is het niet ondenkbaar dat de patiënt eerst informeert naar het aantal "Nintendo-uren" van de chirurg, alvorens enige vorm van "sleutelgatchirurgie" te willen ondergaan. (James Rosser, 2004)

David C. P. Cobben

Groningen, 12 mei 2004



Rijksuniversiteit Groningen

**Detection and staging of solid tumors with FDG-PET and FLT-PET**

Proefschrift

ter verkrijging van het doctoraat in de  
Medische Wetenschappen  
aan de Rijksuniversiteit Groningen  
op gezag van de  
Rector Magnificus, dr. F. Zwarts,  
in het openbaar te verdedigen op  
woensdag 12 mei 2004  
om 13.15 uur

door

**David Catharina Petrus Cobben**

geboren op 8 juni 1974  
te Maastricht

**Promotores**

Prof. Dr. H.J. Hoekstra

Prof. Dr. W. Vaalburg

**Copromotores**

Dr. P.H. Elsinga

Dr. A.J.H. Suurmeijer

**Beoordelingscommissie**

Prof. Dr. H.J. Machulla

Prof. Dr. W.J.G. Oyen

Prof. Dr. J.L.N. Roodenburg



**Paranimfen**

Ing. B. Maas

Drs. M.F. Lutke Holzik

## CONTENTS

- 9     **Chapter 1**   Introduction
- 29    **Chapter 2**   New diagnostic techniques in staging in the surgical treatment of cutaneous malignant melanoma  
*European Journal of Surgical Oncology 2002; 28: 692-700*
- 51    **Chapter 3**   Fluorodeoxyglucose-positron emission tomography and sentinel lymph node biopsy in staging primary cutaneous melanoma  
*European Journal of Surgical Oncology 2003; 2: 662-664*
- 61    **Chapter 4**    $^{18}\text{F}$ -3'-fluoro-3'-deoxy-L-thymidine; a new tracer for staging metastatic melanoma?  
*Journal of Nuclear Medicine 2003; 44: 1927-1932*
- 77    **Chapter 5**   Selectivity of 3'-deoxy-3'-[ $^{18}\text{F}$ ]fluorothymidine (FLT) and 2-[ $^{18}\text{F}$ ]fluoro-2-deoxy-D-glucose (FDG) for tumor versus inflammation in a rodent model  
*Journal of Nuclear Medicine – in press*
- 93    **Chapter 6**   Detection and grading of soft tissue sarcomas of the extremities with  $^{18}\text{F}$ -3'-fluoro-3'-deoxy-L-thymidine  
*Clinical Cancer Research 2004; 10: 1685-90*
- 109   **Chapter 7**   FLT-PET for the visualization of laryngeal cancer: a comparison with FDG-PET  
*Journal of Nuclear Medicine 2004; 45: 226-231*
- 123   **Chapter 8**   Is  $^{18}\text{F}$ -3'-fluoro-3'-deoxy-L-thymidine useful for staging and restaging of patients with non-small cell lung cancer?  
*Submitted*

<b>138</b>	<b>Chapter 9</b>	Summary
<b>144</b>	<b>Chapter 10</b>	Samenvatting
<b>150</b>		Dankwoord
<b>155</b>		Curriculum vitae
<b>156</b>		List of publications



# **Chapter 1**

## **Introduction**

The number of patients diagnosed with cancer is still increasing. In the Netherlands, approximately 328.000 new cancer patients are expected yearly and approximately 184.000 cancer patients die of their disease.<sup>1</sup> One of the most important causes is the proportional increase of the aging population. While accuracy and the impact of many novel diagnostic tools on survival of cancer patients are still under investigation, other new diagnostic tools are already being implemented and developed. The TNM-staging system, which is the universal approach for diagnosing and staging cancer, forms the basis for the development of those new diagnostic tools. This approach will be discussed and used to explain some of the major technological advances in the diagnosis and staging of cancer. Positron Emission Tomography, which is one of these technological advances, will be discussed in detail.

### **TNM staging of cancer**

Anti-cancer treatment depends on histological diagnosis and staging system of the anatomical site, size and extent of the tumor and presence of lymphatic and/or haematogenic metastases. The TNM-staging system is the universal staging method for all kinds of malignancies, which has been developed and updated since 1943 by international cancer societies. The goal of the TNM-staging system is to serve as a 'common language' for oncologists. The TNM-staging does not only stage cancer patients, but can also help with treatment planning, give an indication of prognosis, assist in treatment evaluation, facilitate exchange of information between treatment centers and contribute to the continuing investigation of human cancer.

The TNM-staging system consists of 3 levels. The **T**umor stage, stands for the local progression of the tumor, **N**odal stage for regional metastasis in the lymph node and the **M** stage for distant metastasis. Local progression of the tumor is expressed in numbers or as 'is'. T<sub>is</sub> stands for 'carcinoma in situ' and T<sub>1</sub>, T<sub>2</sub>, T<sub>3</sub> or T<sub>4</sub>, express the increasing local progression of the tumor. In the same fashion does N<sub>0</sub>, stand for no presence of regional lymphatic metastasis and N<sub>1</sub>, N<sub>2</sub> and N<sub>3</sub> for progression of regional lymphatic metastasis. M<sub>0</sub> stands for no haematogenic metastasis present and M<sub>1</sub> for presence of haematogenic metastasis. The application of the TNM system in the clinical practice and the value of several diagnostic techniques will be discussed in the next paragraphs.

## **Clinical pathological staging**

The clinical pathological staging of cancer is improving with the development of techniques such as immunohistochemistry (IHC) using antibodies and reverse transcriptase polymerase chain reaction (RT-PCR) for the sensitive detection of malignant cells in the pathological diagnosis of cancer. Computed tomography (CT), magnetic resonance imaging (MRI), ultrasonography (US) and positron emission tomography (PET) play a role in the anatomical or functional detection of tumors. However, all these techniques have their limitations. Fine needle aspiration can often distinguish between a benign and malignant process. To obtain a final histopathological diagnosis, a biopsy or an excision of the tumor is required. The pathologist will examine the specimen on several parameters, e.g. resemblance with normal tissue, number of mitotic figures, amount of necrosis and additional specific tissue or cell staining. The results of these examinations are histological specification and differentiation. The difficulty of obtaining a tissue biopsy of a tumor is the sampling error, especially in a non-palpable lesion. In addition the biopsy may not always be representative for the whole tumor regarding malignancy and proliferation activity, because many large tumors are heterogeneous with regard to proliferation activity and contain area(s) of necrosis.

## **Tumor extent**

CT, MRI, US and surgery (e.g. laparotomy, laparoscopy and/or endoscopy) are used to investigate the extent of the tumor into the surrounding tissues. The difficulty of CT, MRI and US is that they play a very modest role in discriminating between malignant and normal tissue, especially in tumors that are highly differentiated and/or with a low proliferation grade. Furthermore, the detection of a recurrent malignancy on MRI and CT after previous cancer treatment is difficult, due to the tissue changes after surgery, radiation therapy and/or chemotherapy. These tissue changes are mostly caused by fibrosis, which can mimic or enclose malignant tissue. Surgery is in general a too invasive procedure to investigate the extent of the tumor prior to therapy.

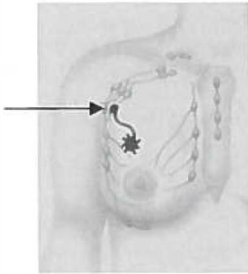
## Lymphatic metastases

CT, MRI, US and the sentinel lymph node (SLN) procedure can be used for the detection of lymphatic metastases. The method of choice, depends on the location of the primary tumor and location of the expected lymphatic metastases. The diagnosis of lymphatic metastases by MRI, CT and US depends mainly on the detection of enlarged lymph nodes. MRI, CT or US categorize lymph nodes larger than 1 cm as suspect for malignancy. However, enlarged lymph nodes can be reactive without containing metastatic cells and non-enlarged (< 1 cm) lymph nodes can contain metastatic cells. With respect to the last, it is interesting to mention new developments with lymph targeted MRI contrast agents, which may detect very small lymph node metastases.<sup>2</sup>

The advantage of the SLN technique is that it can detect the first echelon lymph node, which is thoroughly investigated by the pathologist with haematoxylin and eosin (HE) staining and if necessary, immunohistochemical (IHC) staining. However, the only indication for the sentinel node procedure is currently, limited and clinical node negative breast cancer. In the Netherlands, the clinical applications for melanomas, vulvar and cervical cancer, resectable non-small cell lung cancer, renal cell carcinoma and rhabdomyosarcoma, are still under investigation. The concept of the SLN represents a major opportunity to stratify patients for appropriate treatment, since the status of the SLN has been incorporated in the TNM classification of breast cancer and of melanoma. In short<sup>3</sup>, blue dye or [<sup>99m</sup>Tc]-nano-colloid is injected intradermally (melanoma) or around the tumor or intradermally above the tumor (breast cancer) and taken up by the lymphatic system and transported to the lymph nodes. Scintigraphy detects [<sup>99m</sup>Tc]-nano-colloid in the first draining lymph node(s) on the day prior to the surgery and its location(s) is/are marked on the skin. During surgery the draining lymph nodes may be stained blue and, when still radioactive, can be detected by the gamma probe, and is in this way indicated as "sentinel lymph node(s)" (Figure 1). The sentinel lymph node is excised and sent to the pathologist for histological and immunohistochemical analysis. When the sentinel lymph node contains malignant cells, all regional lymph nodes are excised, since these nodes have an increased risk to contain metastatic cells as well.



**Figure 1. Sentinel lymph node in breast cancer**



The blue dye and [ $^{99m}\text{Tc}$ ]-nano-colloid are injected in the tumor and drain to the first lymph node: "sentinel lymph node" (arrow).

### **Haematogenic metastases**

The presence of haematogenic metastases can be established by several techniques, depending on the site of the metastasis. Liver metastases can be detected by CT, MRI or US. Metastases in the lungs can be detected by conventional X-ray or CT and bone metastasis by [ $^{99m}\text{Tc}$ ]-technetium-phosphate scintigraphy, conventional X-ray, CT and MRI. A drawback is that each site requires its own optimal technique(s) for detection of haematogenic metastases. In cancer patients disseminated tumor cells in the blood and bone marrow can often be detected by highly sensitive techniques such as RT-PCR. The presence (of subtypes) of these cells can be an indication for the prognosis. However, more studies with larger patient groups and the same design are needed, before the presence of metastatic cells in the blood and bone marrow can be incorporated in a staging system such as the TNM-staging system.

### **Restaging and therapy evaluation**

Restaging of cancer patients and therapy monitoring, is solely based on a decrease in tumor size, which is not always feasible or quantifiable. US, CT and MRI are used to estimate the tumor response, based on change in tumor size. However, decrease in tumor size does not have to occur directly after treatment. Often a delay between response and tumor shrinkage can be seen. Furthermore, the size of tumor, increased or decreased, does not correlate with the presence or the amount of viable cancer cells. During and even after therapy tumors can consist of fibrosis, necrosis and/or viable cancer cells, which can differ in proliferation activity.

## **Developments in diagnostic tools**

Because of the limitations of the current diagnostics for cancer, technological advances have led to new and improved diagnostic methods for staging cancer during the last decade. Especially the SLN biopsy and advanced radiodiagnostic imaging methods are recent developments in clinical oncology. The SLN procedure has been established as a reliable method for detection of lymphatic metastases in breast cancer and has reached the last investigational phase in melanoma. Functional imaging, such as functional CT, functional MRI, magnetic resonance spectroscopy, functional US and positron emission tomography (PET) are major recent advances in oncology.<sup>4-9</sup> Functional CT, MRI and US focus on the quantification and alteration in the tumor vascularity. These techniques measure the behavior of specific and non-specific contrast agents in time in the tumor and may contribute in lesion characterization, tumor grading, predicting and monitoring of the response in radiation and chemotherapy, determine tumor prognosis and direct the optimal site for biopsy. However, today these techniques are not yet available in most clinical surroundings and are used mainly as a research tool.

Another functional imaging technique, Positron Emission Tomography (PET), has been investigated extensively in the last decades. PET has proven to be useful in diagnosing and staging of several cancers and is used increasingly in clinical oncology.

In general, the goal of all the individual and combined staging techniques is to provide an accurate diagnosis and TNM stage for the cancer patient for individually tailored cancer treatment.

## **Positron Emission Tomography**

Positron Emission Tomography uses positron emitting radionuclides, which are incorporated into compounds that take part in physiological processes (tracers). Positron emitting radionuclides are generally produced by bombarding target materials with highly accelerated particles (deuterons or protons), using a cyclotron. The most frequently used radionuclides are carbon-11 ( $^{11}\text{C}$ ), nitrogen-13, ( $^{13}\text{N}$ ), oxygen-15 ( $^{15}\text{O}$ ) and fluorine-18 ( $^{18}\text{F}$ ), which possess short physical half-lives (2-110 min.). These radioactive products can be used for the synthesis of radiolabeled tracers.

PET radionuclides have a surplus of positively charged particles in their nucleus (protons). To achieve stability within the nucleus, a positron is emitted. After travelling a small distance through the body, the positron encounters an electron and 'annihilates'.

During this process, the mass of these two photons is converted into energy ( $E=mc^2$ ). This energy is liberated as two photons, each charged with 511 keV of energy, which emit under an angle of nearly 180 degrees.

The PET camera, which mostly consists of a full ring of detectors, registers only the simultaneously detected two photons (within 10 nanoseconds) on two opposite detectors. This is also known as coincidence detection. The camera is able to register the radiation in different angles, allowing establishment of the underlying distribution of radioactivity. When a radiopharmaceutical is administered (intravenously, orally or via inhalation) to a patient lying in the camera, the distribution of radioactivity within the field of view can be monitored in time, also known as a dynamic scan. By moving the bed, the whole body of the patient can be scanned to make a static “whole body” scan, which is used for tumor and metastases detection.

The PET imaging method has technical limitations. The resolution of the current generation of PET-cameras is 4-5 mm and is therefore unable to detect small tumors and micrometastases as is possible with the sentinel lymph node procedure.<sup>10,11</sup> Moreover partial volume effects, influence the accuracy of the radioactivity measurement in small lesions by causing a spread of the signal over a larger area than it actually occupies. Depending on the spatial resolution of the camera the tracer accumulation can be significantly underestimated in small tumors.<sup>12,13</sup>

Thus, PET visualizes metabolic processes as opposed to conventional imaging methods (CT, MRI and US), which are currently used for TNM staging and depend on structural or anatomical abnormalities.

### **Glucose metabolism**

The most widely used PET tracer in oncology is 2- $^{18}\text{F}$ -fluoro-2-deoxy-D-glucose (FDG) and measures glucose utilization.<sup>14-17</sup> FDG is a glucose analogue, that enters the cells via the same membrane transporters as glucose (Figure 2). Glucose as well as FDG are phosphorylated by the enzyme hexokinase. In contrast to glucose-6-phosphate, FDG-6-phosphate is not a substrate for further metabolism in the glycolytic pathway. Therefore FDG-6-phosphate is trapped in the cells, in proportion to their glycolytic activity.

The indications for the use of FDG-PET in oncology are e.g. the diagnosis of pulmonary nodules, staging of lung cancer, end of treatment evaluation in lymphoma and

restaging of a suspected relapse of colon cancer.<sup>9,18</sup> Furthermore, FDG-PET seems promising for staging stage III, IV and recurrent melanoma.<sup>19-21</sup>

FDG is not a tumor-specific tracer. It is also physiologically taken up in the heart and the brain and is excreted through the urinary system. The physiological uptake in the brain makes detection and interpretation of brain tumors difficult, while physiological uptake in the heart and urinary system makes the interpretation of lesions inside or in the vicinity of these organs difficult as well. High physiological FDG uptake, causing false positive results, can be seen in muscle tissue, macrophages and other cells in (local) inflammatory processes or activated after chemotherapy or radiation therapy. Decreased uptake can cause false negative results in hyperglycemic patients.<sup>9,10,22</sup>

Therefore, there is a need for more specific tracers. Most research has been focused on the applicability of amino acid tracers and of pyrimidine analogues such as thymidine, which have the potential to be more specific. Besides these approaches several tracers, based on other molecular uptake mechanisms related to cancer, have been synthesized and evaluated. Examples are listed in Table 1. Some of these approaches are still in a preclinical phase, others have been investigated in small groups of patients.

**Figure 2. Trapping principles of FDG and FLT**

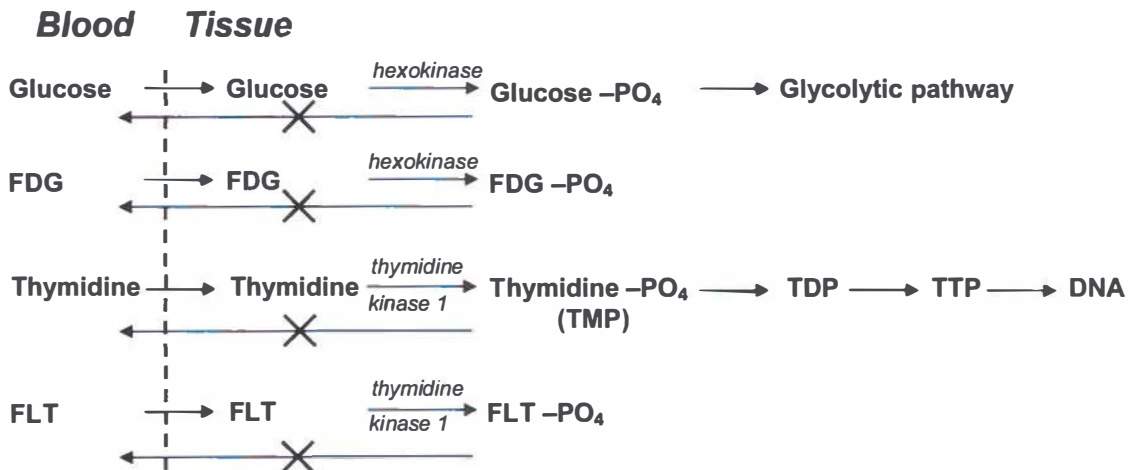


**Table 1. Tracers and uptake mechanisms**

Tracer	Uptake Mechanism
[ <sup>18</sup> F]-FDG <sup>18</sup> , [ <sup>11</sup> C]-glucose <sup>23</sup>	Glucose consumption
[ <sup>18</sup> F]-Fluoroethyltyrosine <sup>24</sup> , [ <sup>11</sup> C]-tyrosine <sup>25</sup> , [ <sup>11</sup> C]-methionine <sup>26</sup>	Protein synthesis
[ <sup>11</sup> C]-thymidine <sup>27</sup> , [ <sup>18</sup> F]-Fluorouracil <sup>28</sup> , [ <sup>18</sup> F]-Fluorothymidine <sup>29</sup>	DNA-synthesis
[ <sup>11</sup> C]-Choline <sup>30</sup> , [ <sup>18</sup> F]-Fluoroethylcholine <sup>31</sup>	Membrane synthesis
[ <sup>18</sup> F]-Fluoromisonidazole <sup>32</sup>	Oxygenation
[ <sup>18</sup> F]-octreotide <sup>33</sup> , [ <sup>18</sup> F]-Fluoroestradiol <sup>34</sup> , [ <sup>18</sup> F]-neuropeptides <sup>35</sup>	Signal transduction
[ <sup>18</sup> F]-phosphonium salts <sup>36</sup>	Membrane potential
[ <sup>18</sup> F]-Fluorodihydroxyphenylalanine <sup>37</sup>	Excretion of neurotransmitters

### Protein synthesis

Protein synthesis and amino acid transport are increased in tumors.<sup>26</sup> To measure these phenomena with PET, several amino acid tracers have been developed. The radiolabeled amino acids differ with regard to the production method and pharmacokinetics *in vivo*. For these reasons, mainly [<sup>11</sup>C]-methionine (MET) has been studied in clinical trials.<sup>26</sup> MET is transported into the tumor cell, metabolized and irreversible incorporated into proteins. Low physiological uptake of MET can be seen in the brain, somewhat higher uptake in the pituitary gland, pancreas, salivary glands, lacrimal glands, bone marrow and occasionally in the myocardium. Abdominal uptake in the liver and the pancreas can be seen as well as uptake in the intestines of varying degree. Preclinical data showed that MET is a selective tracer, which correlates with proliferative activity. However, preclinical data on the applicability of MET for evaluation of chemotherapy and radiation therapy are inconsistent.<sup>38-42</sup> More *in vivo* data are needed to investigate the background of MET-uptake for evaluation of several therapies. In clinical oncology MET has been applied in head and neck cancer, lung cancer and brain tumors.<sup>43-49</sup> The physiological uptake in liver and salivary glands, makes MET a less attractive tracer for the detection of liver malignancies, liver metastases or metastases of head and neck cancer. The increased uptake in the pancreas makes it difficult for the detection of pancreatic cancer. From these studies can be concluded that FDG is a slightly more accurate tracer than MET, with the exception of brain tumors.<sup>26</sup> Most studies included few patients and did not investigate the value of MET for the detection of metastases. In nearly all tumor types more research is required, in larger patient series and in well defined clinical settings.

MET and other amino acid tracers, such as  $^{11}\text{C}$ -tyrosine, also show non-specific uptake in ischaemic brain areas, stroke, scar tissue, abscess, irradiated areas, sarcoidosis and many other benign processes.<sup>26</sup> The tumor specific nature of amino acids is probably better than for FDG, but there is room for improvement.

## DNA synthesis

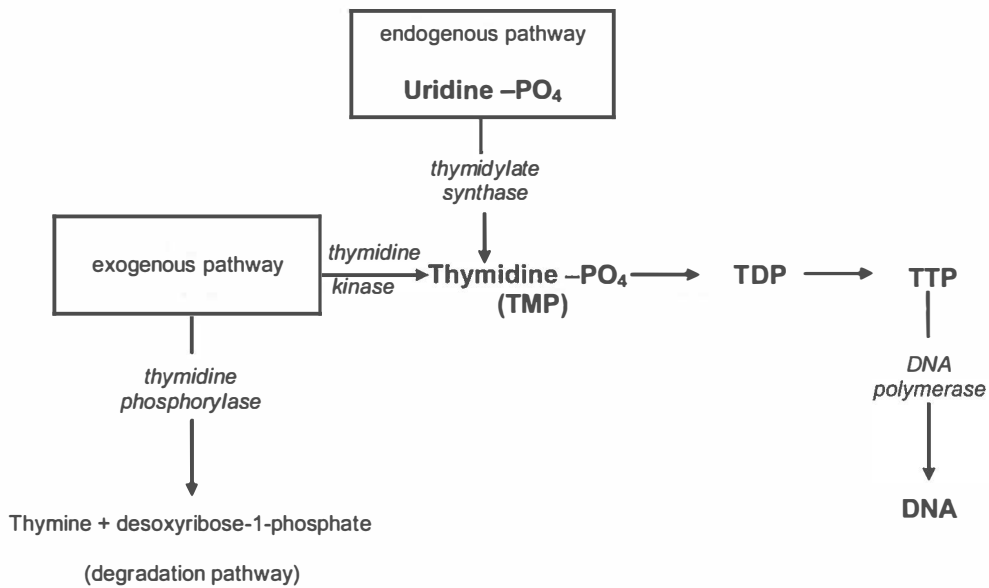
Since amino acid tracers and FDG seemed not specific enough, pyrimidine analogues, such as thymidine, were investigated. Pyrimidine analogues take part in the DNA synthesis and could therefore be more specific than the amino acid tracers. DNA is synthesized from nucleotides of four bases: cytosine, guanine, adenine and thymidine. Since thymidine is the only nucleotide that is not incorporated in the synthesis of RNA, using labeled thymidine as a substrate for growing cells, is a logical choice for specifically measuring cell proliferation. There are two pathways for the metabolism of thymidine (Figure 3). Thymidine is transported via facilitated diffusion by NBMPR-sensitive (*es*) and NBMPR-insensitive (*is*) transporters.<sup>50</sup> Once inside the cell, thymidine can be phosphorylated by thymidine kinase (TK), to thymidine monophosphate (TMP), followed by phosphorylation to thymidinediphosphate (TDP) and thymidinetriphosphate (TTP), prior to incorporation into the DNA. This is called the exogenous (salvage) pathway, since it allows the cell to use sources of thymidine produced elsewhere. Some of the thymidine used by cells is produced by endogenous (de novo) synthesis from uridylate. Deoxyuridine monophosphate is methylated to make TMP by thymidylate synthase (TS). Both TK and TS levels generally increase 5-10 times as cells enter the S-phase, which is the DNA synthesis phase of the cell.<sup>27</sup> Thymidine tracers take part in the exogenous pathway and are therefore dependent on the thymidine kinase concentration.

Labeled thymidine has been investigated in cell culture and animal studies for years. It seemed to be rapidly incorporated into newly synthesized DNA. [Methyl- $^{11}\text{C}$ ]-thymidine and [2- $^{11}\text{C}$ ]-thymidine have both been applied clinically in brain tumors, head and neck cancers, sarcomas, renal cancers and non-Hodgkin's lymphoma.<sup>51,51-59</sup> However, [ $^{11}\text{C}$ ]-thymidine is metabolized very rapidly and, depending on its labeling position, metabolites are being formed in tissue and blood. Therefore proliferation imaging with [ $^{11}\text{C}$ ]-thymidine requires correction for labeled metabolites. Models have been developed for reliable estimates of cellular proliferation by measuring thymidine flux from the blood into DNA in tumors.<sup>27</sup> Because of the rapid metabolism, only a fraction of the

injected [ $^{11}\text{C}$ ]-thymidine is incorporated into DNA and labeled metabolites impair image interpretation. Furthermore the short half-life of 20 min of carbon-11 and the relatively complicated production method prevents widespread use in a clinical setting. These aspects make thymidine difficult to apply as a tracer in general and in centers without a cyclotron in particular.

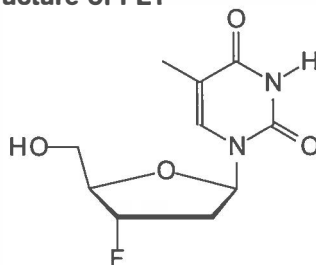
In the ongoing search for a new tracer that would not have the drawbacks of FDG, amino acid tracers and [ $^{11}\text{C}$ ]-thymidine, [ $^{18}\text{F}$ ]-fluoro-3'-deoxy-3'-L-fluorothymidine (FLT) was developed (Figure 4).<sup>29</sup>

**Figure 3. Biochemical pathways related to thymidine**



TDP=thymidine diphosphate; TTP= thymidine triphosphate

**Figure 4. Chemical structure of FLT**



## FLT-PET

Shields et al. developed and tested FLT in canines and humans. FLT is resistant to degradation and was retained in proliferating tissues by the action of thymidine kinase 1 (TK<sub>1</sub>), which causes phosphorylation of FLT (Figure 2 and 3). Approximately 30% of the circulating FLT is metabolized in the liver into its glucuronated form. FLT produced high-contrast images, visualizing normal bone marrow, liver and tumors. Thymidine kinase 1 (TK<sub>1</sub>) is a principal enzyme in the DNA-salvage pathway (Figure 3) in cells,<sup>60</sup> and is especially upregulated just before and during the S-phase of the cell cycle.<sup>61,62</sup> The TK<sub>1</sub> concentration increases 5-10-fold as cells enter the S-phase.<sup>61</sup>

*In vitro* research indicated that FLT uptake in tumor cells reflected TK<sub>1</sub> activity, percentage of cells in S-phase and tumor cell proliferation.<sup>60</sup> Little uptake of [<sup>3</sup>H]FLT (0.2%) was seen in DNA. The correlation between [<sup>3</sup>H]FLT uptake and percentage of cells in the S-phase varied between 0.76 and 0.91 and 0.86 for [<sup>3</sup>H]thymidine. Correlation between the [<sup>3</sup>H]FLT uptake and TK<sub>1</sub> activity was 0.63 in parental A549 (lung cancer) cells, 0.45 in A549 cells that were irradiated and 0.86 in A549 cells with abrogated p53 tumor suppressor gene.

Recently, the correlation between FLT uptake and proliferation has been investigated *in vivo* by the research groups of Buck, Veselle, Barthel and Wagner.<sup>63-65</sup> The groups of Buck (n=30) and Veselle (n=11) confirmed in patients with solitary pulmonary nodules, that FLT uptake correlated with proliferation. The correlation between SUV and proliferation fraction varied between 0.78 and 0.87. The correlation between SUV and S-phase fraction varied between 0.36 and 0.69. Wagner et al. demonstrated a strong correlation with proliferation in B-cell lymphoma in mice and patients.<sup>64</sup> Barthel et al. used FLT for therapy evaluation in SCID mice with fibrosarcoma. They found a strong correlation between FLT and proliferation (r=0.71) and the therapeutic effect was better to evaluate with FLT than with FDG.<sup>65</sup> FLT may not have the same drawbacks as FDG (increased uptake in inflammation and benign lesions and little or no uptake in cancer of hyperglycemic patients) and amino acid tracers (physiological uptake in especially abdominal organs and salivary glands), and is correlated with proliferation. FLT may therefore be an interesting tracer for the detection and therapy evaluation of cancer.



## **Summary**

Many diagnostic techniques are used and developed to investigate the extent of the tumor and the presence of lymphatic and haematogenic metastases in cancer patients. Especially, the sentinel lymph node (SLN) technique and functional imaging techniques, such as positron emission tomography (PET) are increasingly used. The SLN technique is a standard of care for staging breast cancer and might become a staging technique for other forms of cancers such as melanoma. FDG-PET, which measures glucose metabolism and is the most widely used PET-method in oncology. However, FDG is not a tumor-specific tracer. FLT-PET, which measures DNA-synthesis, has the potential to become a more specific tracer to apply in for the diagnosis and therapy evaluation of cancer.

## **Aim of this thesis**

To investigate the scope and limitations of FLT-PET in solid tumors. Since FLT may be a more specific tracer than FDG, the applicability of FLT-PET for differentiation between tumor inflammation, tumor detection, tumor grading and tumor staging, was investigated. In all studies FLT-PET was compared with the standard diagnostic tool for the investigated type of cancer. In cancer types where FDG-PET is used routinely, FLT-PET is compared with FDG-PET as well. In order to fulfill these objectives the following studies have been carried out:

- Review the new diagnostic techniques for the staging of melanomas: sentinel lymph node biopsy, FDG-PET and pathology from a surgical point of view (chapter 2).
- To compare FDG-PET with sentinel lymph node biopsy for staging patients with melanoma (chapter 3).
- To investigate the value of FLT-PET for the detection of metastatic melanoma and staging melanoma patients with metastases (chapter 4).
- To investigate if FLT-PET can differentiate between cancer and inflammation in a rat model in comparison to FDG-PET (chapter 5).
- To study the correlation between FLT uptake and proliferation activity of low and high grade soft tissue sarcomas (chapter 6).
- To compare the value of FLT-PET with FDG-PET, CT and histopathology for the detection of primary and recurrent laryngeal cancer (chapter 7).

- To explore the value of FLT-PET with FDG-PET for staging patients with non-small cell lung cancer (NSCLC) (chapter 8).
- To summarize and describe the future perspectives of FLT-PET (chapter 9).

## References

1. Dijck van, J. A. A. M, Coebergh, J. W. W., Siesling, and Visser, O. Trends of cancer in the Netherlands 1989-1998; Report of the Netherlands Cancer Registry. 1-57. 2002. Utrecht, Vereniging van Integrale Kanker Centra.
2. Harisinghani, M. G., Barentsz, J., Hahn, P. F., Deserno, W. M., Tabatabaei, S., van de Kaa, C. H., de la, R. J., and Weissleder, R. Noninvasive detection of clinically occult lymph-node metastases in prostate cancer. *N.Engl.J Med*, 348: 2491-2499, 2003.
3. Nieweg, O. E., Tanis, P. J., and Kroon, B. B. The definition of a sentinel node. *Ann.Surg.Oncol.*, 8: 538-541, 2001.
4. Gluecker, T. M. and Fletcher, J. G. CT colonography (virtual colonoscopy) for the detection of colorectal polyps and neoplasms. current status and future developments. *Eur.J Cancer*, 38: 2070-2078, 2002.
5. Padhani, A. R. Functional MRI for anticancer therapy assessment. *Eur.J Cancer*, 38: 2116-2127, 2002.
6. Miles, K. A. Functional computed tomography in oncology. *Eur.J Cancer*, 38: 2079-2084, 2002.
7. Griffiths, J. R., Tate, A. R., Howe, F. A., and Stubbs, M. Magnetic Resonance Spectroscopy of cancer-practicalities of multi-centre trials and early results in non-Hodgkin's lymphoma. *Eur.J Cancer*, 38: 2085-2093, 2002.
8. Blomley, M. J. and Eckersley, R. J. Functional ultrasound methods in oncological imaging. *Eur.J Cancer*, 38: 2108-2115, 2002.
9. Jerusalem, G., Hustinx, R., Beguin, Y., and Fillet, G. PET scan imaging in oncology. *Eur.J Cancer*, 39: 1525-1534, 2003.
10. Cobben, D. C., Koopal, S., Tiebosch, A. T., Jager, P. L., Elsinga, P. H., Wobbes, T., and Hoekstra, H. J. New diagnostic techniques in staging in the surgical treatment of cutaneous malignant melanoma. *Eur.J Surg.Oncol.*, 28: 692-700, 2002.
11. Mijnhout, G. S., Hoekstra, O. S., Van Lingen, A., Van Diest, P. J., Ader, H. J., Lammertsma, A. A., Pijpers, R., Meijer, S., and Teule, G. J. How morphometric analysis of metastatic load predicts the (un)usefulness of PET scanning: the case of lymph node staging in melanoma. *J Clin.Pathol.*, 56: 283-286, 2003.
12. Avril, N., Rose, C. A., Schelling, M., Dose, J., Kuhn, W., Bense, S., Weber, W., Ziegler, S., Graeff, H., and Schwaiger, M. Breast imaging with positron emission tomography and fluorine-18 fluorodeoxyglucose: use and limitations. *J Clin.Oncol.*, 18: 3495-3502, 2000.
13. Avril, N., Bense, S., Ziegler, S. I., Dose, J., Weber, W., Laubenbacher, C., Romer, W., Janicke, F., and Schwaiger, M. Breast imaging with fluorine-18-FDG PET: quantitative image analysis. *J Nucl Med*, 38: 1186-1191, 1997.
14. Hustinx, R., Benard, F., and Alavi, A. Whole-body FDG-PET imaging in the management of patients with cancer. *Semin.Nucl.Med.*, 32: 35-46, 2002.
15. Hustinx, R. and Alavi, A. Tumor imaging. *In* M. J. Welch and C. S. Redvandy (eds.), *Handbook of Radiopharmaceuticals*, 1 ed, pp. 629-642. Chippenham, England: John Wiley & sons, Ltd, 2003.
16. Bomanji, J. B., Costa, D. C., and Ell, P. J. Clinical role of positron emission tomography in oncology. *Lancet Oncol.*, 2: 157-164, 2001.
17. Gambhir, S. S., Czernin, J., Schwimmer, J., Silverman, D. H., Coleman, R. E., and Phelps, M. E. A tabulated summary of the FDG PET literature. *J Nucl.Med.*, 42: 1-93S, 2001.

18. Pieterman, R. M., van Putten, J. W., Meuzelaar, J. J., Mooyaart, E. L., Vaalburg, W., Koeter, G. H., Fidler, V., Pruim, J., and Groen, H. J. Preoperative staging of non-small-cell lung cancer with positron-emission tomography. *N.Engl.J.Med.*, 343: 254-261, 2000.
19. Tyler, D. S., Onaitis, M., Kherani, A., Hata, A., Nicholson, E., Keogan, M., Fisher, S., Coleman, E., and Seigler, H. F. Positron emission tomography scanning in malignant melanoma. *Cancer*, 89: 1019-1025, 2000.
20. Prichard, R. S., Hill, A. D., Skehan, S. J., and O'Higgins, N. J. Positron emission tomography for staging and management of malignant melanoma. *Br.J Surg.*, 89: 389-396, 2002.
21. Mijnhout, G. S., Hoekstra, O. S., van Tulder, M. W., Teule, G. J., and Deville, W. L. Systematic review of the diagnostic accuracy of (18)F- fluorodeoxyglucose positron emission tomography in melanoma patients. *Cancer*, 97: 1530-1542, 2001.
22. Strauss, L. G. Fluorine-18 deoxyglucose and false-positive results: a major problem in the diagnostics of oncological patients. *Eur.J.Nucl.Med.*, 23: 1409-1415, 1996.
23. Spence, A. M., Muzi, M., Graham, M. M., O'Sullivan, F., Krohn, K. A., Link, J. M., Lewellen, T. K., Lewellen, B., Freeman, S. D., Berger, M. S., and Ojemann, G. A. Glucose metabolism in human malignant gliomas measured quantitatively with PET, 1-[C-11]glucose and FDG: analysis of the FDG lumped constant. *J Nucl Med*, 39: 440-448, 1998.
24. Weber, W. A., Wester, H. J., Grosu, A. L., Herz, M., Dzewas, B., Feldmann, H. J., Molls, M., Stocklin, G., and Schwaiger, M. O-(2-[18F]fluoroethyl)-L-tyrosine and L-[methyl-11C]methionine uptake in brain tumours: initial results of a comparative study. *Eur.J Nucl Med*, 27: 542-549, 2000.
25. Kole, A. C., Plaat, B. E., Hoekstra, H. J., Vaalburg, W., and Molenaar, W. M. FDG and L-[1-11C]-tyrosine imaging of soft-tissue tumors before and after therapy. *J Nucl Med*, 40: 381-386, 1999.
26. Jager, P. L., Vaalburg, W., Pruim, J., de Vries, E. G., Langen, K. J., and Piers, D. A. Radiolabeled amino acids: basic aspects and clinical applications in oncology. *J Nucl Med*, 42: 432-445, 2001.
27. Krohn, K. A., Mankoff, D. A., and Eary, J. F. Imaging cellular proliferation as a measure of response to therapy. *J Clin.Pharmacol., Suppl.* 96S-103S, 2001.
28. Bading, J. R., Alauddin, M. M., Fissekis, J. D., Shahinian, A. H., Joung, J., Spector, T., and Conti, P. S. Blocking catabolism with eniluracil enhances PET studies of 5-[18F]fluorouracil pharmacokinetics. *J Nucl Med*, 41: 1714-1724, 2000.
29. Shields, A. F., Grierson, J. R., Dohmen, B. M., Machulla, H. J., Stayanoff, J. C., Lawhorn-Crews, J. M., Obradovich, J. E., Muzik, O., and Mangner, T. J. Imaging proliferation in vivo with [F-18]FLT and positron emission tomography. *Nat.Med.*, 4: 1334-1336, 1998.
30. de Jong, I. J., Pruim, J., Elsinga, P. H., Vaalburg, W., and Mensink, H. J. 11C-choline positron emission tomography for the evaluation after treatment of localized prostate cancer. *Eur.Urol.*, 44: 32-38, 2003.
31. Hara, T. 18F-fluorocholeline: a new oncologic PET tracer. *J Nucl Med*, 42: 1815-1817, 2001.
32. Rajendran, J. G., Wilson, D. C., Conrad, E. U., Peterson, L. M., Bruckner, J. D., Rasey, J. S., Chin, L. K., Hofstrand, P. D., Grierson, J. R., Eary, J. F., and Krohn, K. A. [(18)F]FMISO and [(18)F]FDG PET imaging in soft tissue sarcomas: correlation of hypoxia, metabolism and VEGF expression. *Eur.J Nucl Med Mol.Imaging*, 30: 695-704, 2003.
33. Wester, H. J., Schottelius, M., Scheidhauer, K., Meisetschlager, G., Herz, M., Rau, F. C., Reubi, J. C., and Schwaiger, M. PET imaging of somatostatin receptors: design, synthesis and preclinical evaluation of a novel (18)F-labelled, carbohydrate analogue of octreotide. *Eur.J Nucl Med Mol.Imaging*, 30: 117-122, 2003.

34. Jonson, S. D. and Welch, M. J. PET imaging of breast cancer with fluorine-18 radiolabeled estrogens and progestins. *Q.J Nucl Med*, 42: 8-17, 1998.
35. Varagnolo, L., Stokkel, M. P., Mazzi, U., and Pauwels, E. K. 18F-labeled radiopharmaceuticals for PET in oncology, excluding FDG. *Nucl Med Biol.*, 27: 103-112, 2000.
36. Madar, I., Weiss, L., and Izbicki, G. Preferential accumulation of (3)H-tetraphenylphosphonium in non-small cell lung carcinoma in mice: comparison with (99m)Tc-MIBI. *J Nucl Med*, 43: 234-238, 2002.
37. Jacob, T., Grahek, D., Younsi, N., Kerrou, K., Aide, N., Montravers, F., Balogova, S., Colombet, C., De, B., V, and Talbot, J. N. Positron emission tomography with [(18)F]FDOPA and [(18)F]FDG in the imaging of small cell lung carcinoma: preliminary results. *Eur.J Nucl Med Mol.Imaging*, 2003.
38. Kubota, K., Ishiwata, K., Kubota, R., Yamada, S., Tada, M., Sato, T., and Ido, T. Tracer feasibility for monitoring tumor radiotherapy: a quadruple tracer study with fluorine-18-fluorodeoxyglucose or fluorine-18-fluorodeoxyuridine, L-[methyl-14C]methionine, [6-3H]thymidine, and gallium-67. *J Nucl Med*, 32: 2118-2123, 1991.
39. Schaidler, H., Haberkorn, U., Berger, M. R., Oberdorfer, F., Morr, I., and van Kaick, G. Application of alpha-aminoisobutyric acid, L-methionine, thymidine and 2-fluoro-2-deoxy-D-glucose to monitor effects of chemotherapy in a human colon carcinoma cell line. *Eur.J Nucl Med*, 23: 55-60, 1996.
40. Minn, H., Clavo, A. C., Grenman, R., and Wahl, R. L. In vitro comparison of cell proliferation kinetics and uptake of tritiated fluorodeoxyglucose and L-methionine in squamous-cell carcinoma of the head and neck. *J Nucl Med*, 36: 252-258, 1995.
41. Higashi, K., Clavo, A. C., and Wahl, R. L. In vitro assessment of 2-fluoro-2-deoxy-D-glucose, L-methionine and thymidine as agents to monitor the early response of a human adenocarcinoma cell line to radiotherapy. *J Nucl Med*, 34: 773-779, 1993.
42. Sato, K., Kameyama, M., Ishiwata, K., Katakura, R., and Yoshimoto, T. Metabolic changes of glioma following chemotherapy: an experimental study using four PET tracers. *J Neurooncol.*, 14: 81-89, 1992.
43. Leskinen-Kallio, S., Lindholm, P., Lapela, M., Joensuu, H., and Nordman, E. Imaging of head and neck tumors with positron emission tomography and [11C]methionine. *Int.J Radiat.Oncol.Biol.Phys.*, 30: 1195-1199, 1994.
44. Lindholm, P., Leskinen, S., and Lapela, M. Carbon-11-methionine uptake in squamous cell head and neck cancer. *J Nucl Med*, 39: 1393-1397, 1998.
45. Nettelbladt, O. S., Sundin, A. E., Valind, S. O., Gustafsson, G. R., Lamberg, K., Langstrom, B., and Bjornsson, E. H. Combined fluorine-18-FDG and carbon-11-methionine PET for diagnosis of tumors in lung and mediastinum. *J Nucl Med*, 39: 640-647, 1998.
46. Jansson, T., Westlin, J. E., Ahlstrom, H., Lilja, A., Langstrom, B., and Bergh, J. Positron emission tomography studies in patients with locally advanced and/or metastatic breast cancer: a method for early therapy evaluation? *J Clin.Oncol.*, 13: 1470-1477, 1995.
47. Huovinen, R., Leskinen-Kallio, S., Nagren, K., Lehtikainen, P., Ruotsalainen, U., and Teras, M. Carbon-11-methionine and PET in evaluation of treatment response of breast cancer. *Br.J Cancer*, 67 : 787-791, 1993.
48. Ogawa, T., Shishido, F., Kanno, I., Inugami, A., Fujita, H., Murakami, M., Shimosegawa, E., Ito, H., Hatazawa, J., Okudera, T., and . Cerebral glioma: evaluation with methionine PET. *Radiology*, 186: 45-53, 1993.

49. Mosskin, M., von Holst, H., Bergstrom, M., Collins, V. P., Eriksson, L., Johnstrom, P., and Noren, G. Positron emission tomography with <sup>11</sup>C-methionine and computed tomography of intracranial tumours compared with histopathologic examination of multiple biopsies. *Acta Radiol.*, 28: 673-681, 1987.
50. Belt, J. A., Marina, N. M., Phelps, D. A., and Crawford, C. R. Nucleoside transport in normal and neoplastic cells. *Adv.Enzyme Regul.*, 33: 235-252, 1993.
51. Vander Borgh T., Pauwels, S., Lambotte, L., Labar, D., De Maeght, S., Stroobandt, G., and Laterre, C. Brain tumor imaging with PET and 2-[carbon-11]thymidine. *J Nucl Med*, 35: 974-982, 1994.
52. Shields, A. F., Lim, K., Grierson, J., Link, J., and Krohn, K. A. Utilization of labeled thymidine in DNA synthesis: studies for PET. *J Nucl Med*, 31: 337-342, 1990.
53. Martiat, P., Ferrant, A., Labar, D., Cogneau, M., Bol, A., Michel, C., Michaux, J. L., and Sokal, G. In vivo measurement of carbon-11 thymidine uptake in non-Hodgkin's lymphoma using positron emission tomography. *J Nucl Med*, 29: 1633-1637, 1988.
54. van Eijkeren, M. E., De Schryver, A., Goethals, P., Poupeye, E., Schelstraete, K., Lemahieu, I., and De Potter, C. R. Measurement of short-term <sup>11</sup>C-thymidine activity in human head and neck tumours using positron emission tomography (PET). *Acta Oncol.*, 31: 539-543, 1992.
55. Eary, J. F., Mankoff, D. A., Thompson, J. A., Gold, P., and Krohn, K. A. Tumor metabolism and proliferation using quantitative PET imaging in renal cell carcinoma patients treated with IL-2. *Proc ASCO*, 13: 338a, 1999.
56. Eary, J. F., Mankoff, D. A., Spence, A. M., Berger, M. S., Olshen, A., Link, J. M., O'Sullivan, F., and Krohn, K. A. 2-[<sup>11</sup>C]thymidine imaging of malignant brain tumors. *Cancer Res.*, 59: 615-621, 1999.
57. Shields, A. F., Mankoff, D. A., Link, J. M., Graham, M. M., Eary, J. F., Kozawa, S. M., Zheng, M., Lewellen, B., Lewellen, T. K., Grierson, J. R., and Krohn, K. A. Carbon-11-thymidine and FDG to measure therapy response. *J Nucl Med*, 39: 1757-1762, 1998.
58. van Eijkeren, M. E., Thierens, H., Seuntjens, J., Goethals, P., Lemahieu, I., and Strijckmans, K. Kinetics of [methyl-<sup>11</sup>C]thymidine in patients with squamous cell carcinoma of the head and neck. *Acta Oncol.*, 35: 737-741, 1996.
59. Mankoff, D. A., Shields, A. F., Link, J. M., Graham, M. M., Muzi, M., Peterson, L. M., Eary, J. F., and Krohn, K. A. Kinetic analysis of 2-[<sup>11</sup>C]thymidine PET imaging studies: validation studies. *J Nucl Med*, 40: 614-624, 1999.
60. Eriksson, S., Kierdaszuk, B., Munch-Petersen, B., Oberg, B., and Johansson, N. G. Comparison of the substrate specificities of human thymidine kinase 1 and 2 and deoxycytidine kinase toward antiviral and cytostatic nucleoside analogs. *Biochem.Biophys.Res.Commun.*, 176: 586-592, 1991.
61. Sherley, J. L. and Kelly, T. J. Regulation of human thymidine kinase during the cell cycle. *J.Biol.Chem.*, 263: 8350-8358, 1988.
62. Toyohara, J., Waki, A., Takamatsu, S., Yonekura, Y., Magata, Y., and Fujibayashi, Y. Basis of FLT as a cell proliferation marker: comparative uptake studies with [<sup>3</sup>H]thymidine and [<sup>3</sup>H]arabinothymidine, and cell-analysis in 22 asynchronously growing tumor cell lines. *Nucl.Med.Biol.*, 29: 281-287, 2002.
63. Buck, A. K., Schirrmeister, H., Hetzel, M., Von Der, H. M., Halter, G., Glatting, G., Mattfeldt, T., Liewald, F., Reske, S. N., and Neumaier, B. 3-deoxy-3-[(<sup>18</sup>F)]fluorothymidine-positron emission tomography for noninvasive assessment of proliferation in pulmonary nodules. *Cancer Res.*, 62: 3331-3334, 2002.
64. Wagner, M., Seitz, U., Buck, A., Neumaier, B., Schultheiss, S., Bangerter, M., Bommer, M., Leithauser, F., Wawra, E., Munzert, G., and Reske, S. N. 3'-[<sup>18</sup>F]fluoro-3'-deoxythymidine ([<sup>18</sup>F]-FLT) as positron

emission tomography tracer for imaging proliferation in a murine B-Cell lymphoma model and in the human disease. *Cancer Res.*, 63: 2681-2687, 2003.

65. Barthel, H., Cleij, M. C., Collingridge, D. R., Hutchinson, O. C., Osman, S., He, Q., Luthra, S. K., Brady, F., Price, P. M., and Aboagye, E. 3'-deoxy-3'-[<sup>18</sup>F]Fluorothymidine as a new marker for monitoring tumor response to antiproliferative therapy *in vivo* with positron emission tomography. *Cancer Res.*, 63: 3791-3798, 2003.
66. Vesselle, H., Grierson, J., Muzi, M., Pugsley, J. M., Schmidt, R. A., Rabinowitz, P., Peterson, L. M., Vallieres, E., and Wood, D. E. In Vivo Validation of 3'-deoxy-3'-[<sup>18</sup>F]fluorothymidine ([<sup>18</sup>F]FLT) as a Proliferation Imaging Tracer in Humans: Correlation of [<sup>18</sup>F]FLT Uptake by Positron Emission Tomography with Ki-67 Immunohistochemistry and Flow Cytometry in Human Lung Tumors. *Clin.Cancer Res.*, 8: 3315-3323, 2002.
67. Francis, D. L., Visvikis, D., Costa, D. C., Arulampalam, T. H., Townsend, C., Luthra, S. K., Taylor, I., and Eil, P. J. Potential impact of [<sup>18</sup>F]3'-deoxy-3'-fluorothymidine versus [<sup>18</sup>F]fluoro-2-deoxy- d-glucose in positron emission tomography for colorectal cancer. *Eur.J Nucl.Med.Mol.Imaging*, 2003.





## Chapter 2

### **New Diagnostic techniques in staging in the surgical treatment of cutaneous malignant melanoma**

D.C.P. Cobben<sup>1,4</sup>, S. Koopal<sup>1</sup>, A.T.M.G. Tiebosch<sup>2</sup>, P.L. Jager<sup>3,4</sup>, P.H. Elsinga<sup>4</sup>,  
Th. Wobbes<sup>5</sup>, H.J. Hoekstra<sup>1</sup>

Departments of Surgical Oncology<sup>1</sup>, Pathology and Laboratory Medicine<sup>2</sup>, Nuclear Medicine<sup>3</sup> and PET-center<sup>4</sup> of the Groningen University Hospital and the department of Surgery<sup>5</sup>, University Medical Centre, Nijmegen, The Netherlands.

*European Journal of Surgical Oncology 2002; 28: 692-700*

## **Summary**

The emphasis of the research on the surgical treatment of melanoma has been on the resection margins, the role of elective lymph node dissection in high risk patients and the value of adjuvant regional treatment with hyperthermic isolated lymph perfusion with melphalan. Parallel to this research, new diagnostic techniques, such as Positron Emission Tomography and the introduction of the sentinel lymph node biopsy with advanced laboratory methods such as immuno-histochemical markers, and reverse transcriptase polymerase chain reaction, have been developed to facilitate early detection of metastatic melanoma. The role of these new techniques on the staging and surgical treatment of melanoma is discussed in this paper.

## **Introduction**

The incidence of cutaneous malignant melanoma (CMM) in the Netherlands is 14 per 100.000, as compared to an incidence of approximately 33 in the United States, and is increasing approximately 5% per year.<sup>1,2</sup> There have been changes in the distribution with regard to anatomic location, histology, race, socio-economic status and stage of CMM at diagnosis during the past decade, with an increase in thinner lesions, which have a more favourable outcome.<sup>2,4</sup> The main problem in the surgical treatment of melanoma is the high tendency for recurrence local, regional or distant. The impact of surgical wounding and wound healing of melanoma with respect to tumour development and metastatic outgrowth is still unknown.<sup>5</sup>

During the last two decades extensive research has been performed on the surgical treatment of melanoma, with the focus on the extent of resection margins<sup>6-12</sup>, the role of elective lymph node dissection in high risk melanoma patients<sup>13-16</sup>, and the value of adjuvant regional treatment with hyperthermic isolated limb perfusion (HILP) with melphalan.<sup>17-23</sup>

New diagnostic techniques for the detection of melanoma and its metastases, such as Positron Emission Tomography (PET), as well as the sentinel lymph node (SLN) biopsy, with or without new laboratory methods such as immuno-histochemical (IHC) markers, and reverse transcriptase polymerase chain reaction (RT-PCR), made their introduction into the clinic. Their impact on the current surgical treatment of melanoma and their current status for the general surgical practice are reviewed and discussed in this paper.

## **Sentinel Lymph Node (SLN) Biopsy**

Recently Morton et al defined that the first drainage lymph node from the primary tumour site and the first site of any nodal metastases, is the blue stained sentinel node, based on a standardised approach for the intra-operative lymphatic mapping with Tc-99m sulphur colloid and patent blue dye.<sup>24</sup>

The concept of the sentinel lymph node represents a major opportunity to stratify patients for appropriate surgery in cancer and is explained in detail by Keshtgar et al and by Nieweg et al.<sup>25,26</sup> In short, blue dye or 99mTc-nano-colloid is injected in or around the tumour or subdermally above the tumour and taken up by the lymphatic system and transported to the lymph nodes.<sup>27,28</sup> Scintigraphy detects 99mTc-nano-colloid in the first

draining lymph node(s) on the day prior to the surgery and its location is/are marked on the skin (Figure 1).

During surgery the draining lymph nodes may be stained blue and when radioactive can be detected by the gamma probe, and indicated as “sentinel lymph node(s)”. The sentinel node is excised and sent to the pathologist for histological and immunohistochemical analysis. The gamma probe together with patent blue dye can identify more SLNs (99.5%) than lymphatic mapping with patent blue dye alone (84%).<sup>29</sup> Because of the limited sensitivity (38%), frozen section analysis, is generally not performed from the SLN, since adequate histological analysis can be performed with HE and additional immunohistochemical staining only.<sup>30-32</sup> The accuracy of the SLN biopsy technique is increased if a more detailed and specific histopathological analysis of the SLN specimen is performed, using evaluation of multiple serial sections with hematoxylin and eosin (H&E), as well as IHC using antibodies detecting melanocytic antigens (S-100 and anti-HMB-45 proteins). In addition the SLN specimen may be evaluated using RT-PCR detecting mRNA for amongst others MART-1 and tyrosinase. This will be discussed more in detail in the paragraph on pathology.

**Figure 1.**



Figure 1. (A) Posterior image 5 min after intradermal injection of Tc99m-nanocolloid around a melanoma scar, located on the lower back, showing tracer transport from the injection site through two lymph vessels to the left, and one to the right. (B) Anterior image of the same patient with body contours, obtained 2 hrs later, showing the injection site shining through from the back, and multiple sentinel nodes in both groins.

Accurate sentinel lymph node mapping requires close co-ordination and communication between surgeons, nuclear medicine physicians, and pathologists. Most institutions have established guidelines for the safe use of radioactive materials during localisation and resection of the SLN. Meticulously performed scintigraphy is essential to ensure correct imaging of the SLN.

The results of clinical research confirm the high accuracy and good clinical applicability of the SLN concept. In a study of Berman et al, all metastases were found in regional nodal basins, which were visualised by lymphoscintigraphy.<sup>33</sup> This was confirmed in a multicenter trial, in which the accuracy of lymphatic mapping and sentinel lymphadenectomy with blue dye and radiocolloid was 99.1%.<sup>31</sup> Studies world-wide have confirmed the validity of the SLN concept, the accuracy of the SLN biopsy as a staging procedure, the biologic significance and therapeutic considerations. Most investigators report a high success rate for identification of the SLN (96-99,5%).<sup>28,29,31,34</sup> The SLN concept, a minimal *invasive* surgical procedure allows to determine the nodal status accurately without the morbidity associated with lymphadenectomy. When applied in stage I and II patients, approximately 20% will have positive SLNs, similar to what would be expected after elective lymph node dissection (ELND).<sup>16,28,35</sup> Regional nodal recurrence of early stage melanoma is rare when the SLN is negative. Therefore the SLN biopsy is an alternative to routine ELND or “watch and wait” policy.<sup>36-38</sup> The importance of the prognostic role of a positive lymph node has been underlined and incorporated in the completely revised staging system for CMM.<sup>39-41</sup> Intra-operative SLN mapping and SLN biopsy is a cost-effective procedure, that allows an accurate identification of regional lymph nodes that contain metastatic disease.<sup>42</sup>

Anatomical location and previous wide local excision (WLE), in which the defect was covered by flap rotation, influence the predictability of the lymph drainage pattern. Melanomas located on the lower and upper limb drain to a predictable area, the inguinal groin or the axilla, while those located at the proximal trunk, head and neck area often drain contralaterally and to unpredictable areas, such as internal mammary, para-aortic, chest wall lymph nodes, triangular intermuscular space and often to more than one lymphatic basin.<sup>43-46</sup> Previous WLE of the melanoma does not appear to negate the reliability of the SLN biopsy, provided that no flap rotation was used to cover the defect.<sup>47</sup>

In case of a negative SLN, close attention should be paid to all blue lymph nodes and lymph nodes with a low radioactivity. In a substudy of the Sunbelt trial an analysis was performed to determine the frequency of metastatic disease in less radioactive lymph nodes, when the most radioactive or “hottest” node did not contain metastatic disease, in order to determine which sentinel nodes should be removed. If only the most radioactive of all sentinel nodes in each basin would have been removed, 13.1% of the nodes would still contain micrometastases. However, it appeared that when all sentinel nodes, with a

radioactivity level greater than 10% of the ex vivo count of the most radioactive node, were removed, no positive nodes were missed. Therefore it is recommended that all such nodes and all blue nodes should be removed.<sup>48</sup> Interval nodes are sentinel nodes in an unexpected node field between the primary lesion and the usual regional basin. These nodes have the same chance of harbouring micrometastatic disease as a sentinel node in this usual node field.<sup>49,50</sup>

The status of the SLN is the best predictor of recurrence and therefore of utmost importance for the prognosis and treatment planning. A study of 565 patients with melanoma and identified SLN, unequivocally demonstrated that the disease free survival rates of the 85 patients with positive sentinel nodes were significantly worse than in the group of 480 patients with negative sentinel nodes.<sup>35</sup> Besides the detection of positive lymph nodes by ELND, even more and unexpected lymph nodes can be detected by SLNB. In fact in multivariate analysis, SLN status is the strongest predictor of recurrence. Therefore a positive SLN biopsy identifies patients most likely to benefit from therapeutic lymph-node dissection and adjuvant therapy. These are patients with nodal metastases.

The role of SLN mapping in the surgical treatment is currently further investigated in two major multi-institutional prospective trials. In the first study the SLN concept is studied. In a prospective randomised trial, consisting of wide local excision of the primary melanoma versus wide local excision and SLN biopsy, the therapeutic value of lymph node dissection in clinical node negative patients is investigated.<sup>51</sup> The objective of the study is to determine if this surgical strategy can prolong the disease free and overall survival of melanoma patients. The value of regional lymphadenectomy and adjuvant interferon alfa-2b therapy in clinical node negative patients with occult nodal metastasis, detected by SLN biopsy, is being studied in the Sunbelt Melanoma Trial.<sup>52</sup> Results of both studies are still pending.

The impact of the SLN on the final treatment and survival of melanoma patients is unknown and reason for controversy. Although in 20-25% of the patients nodal involvement is found and the patients therefore are upstaged, in 75% of the patients, undergoing this invasive procedure, the stage remained unchanged. One of the arguments of Thomas and Patocskai, who stated that SLNB should be confined to patients in clinical trials, is that there is no postsurgical treatment, which prolongs survival.<sup>53</sup> The arguments in favour of SLNB are described by McMasters et al.<sup>54</sup> One of the arguments is, that SLNB identifies patients eligible for adjuvant therapy with interferon alpha-2b. There is still some

controversy about the effect of interferon alpha-2b on survival.<sup>55-58</sup> Therefore it is our belief that trials of patients to be treated with interferon alpha-2b and other novel agents, should continue to be based on a positive sentinel lymph node.

### **Positron Emission Tomography (PET)**

Nearly together with the introduction of the sentinel lymph node concept, PET has emerged as another clinical modality to study staging, restaging and therapy monitoring of melanoma patients. Its high sensitivity and specificity may add to patient management, perhaps more than clinical examination and techniques that depict anatomy, such as computed tomography (CT), magnetic resonance imaging (MRI) and ultrasound. Clinical examination and techniques that depict anatomy (CT, MRI, ultrasound) are not adequate for the detection of metastatic melanoma.<sup>59,60</sup>

Tumour metabolism may be a more accurate parameter to detect tumour deposits and to monitor the effect of various forms of therapy on tumour viability. Positron Emission Tomography (PET) is an excellent technique to investigate metabolism in vivo. The radiopharmaceutical <sup>18</sup>F-fluoro-2-deoxy-D-glucose (FDG) is used worldwide for this purpose.

FDG is a glucose analogue that is taken up by cells, which are metabolically active and especially in tumour cells. It is trapped in the first step of glucose metabolism and accumulates in the cell after phosphorylation.<sup>61</sup> Most melanomas have a very high glucose utilisation. In in vitro experiments melanoma cells demonstrate higher uptake than other tumour types.<sup>62</sup>

In means of sensitivity and specificity for the detection of metastatic melanoma FDG-PET has shown to be superior to conventional imaging techniques (CT, MRI and ultrasound). PET demonstrated uptake of FDG in untreated melanoma deposits within lymph nodes and viscera.<sup>62</sup> Initial clinical experience in the mid-nineties of FDG-PET in CMM suggested that PET scanning was an accurate modality to detect melanoma metastases with the exception of metastases in the brain.<sup>62-65</sup> The effectiveness of PET scanning for detecting melanoma metastases was compared to CT and MRI in a series of 76 melanoma patients, AJCC Stage II to IV. The sensitivity was 94.2% and the specificity 83.3% for PET scanning, compared to only 55.3 and 84.4 respectively for CT scanning. There were only four false negative scans, which was probably due to very small areas of melanoma. PET scanning was particularly able to detect regional lymph node metastases.

The smallest nodules detected were 4-5 mm in diameter.<sup>59</sup> FDG-PET compared to clinical examination, CT, ultrasound, radiography, and liver function tests and pathological routine examinations or clinical follow up, proved to be a more sensitive method for detecting widespread metastases from malignant melanoma and useful as a supplement to clinical examination in melanoma staging (Figure 2).<sup>60</sup>

**Figure 2.**

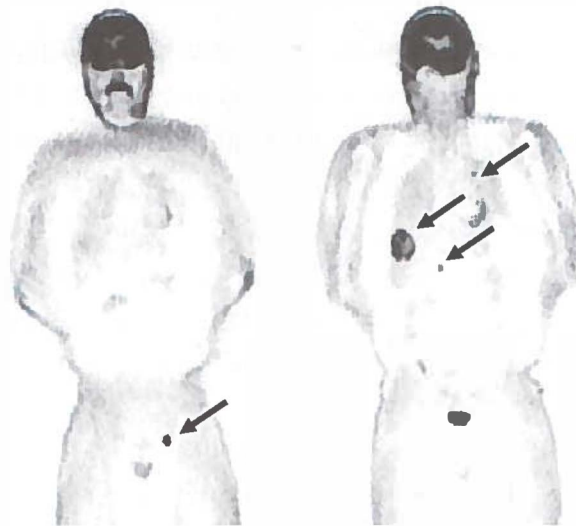


Figure 2. (A) Coronal FDG-PET image of a 44 year old patient with a penile melanoma, 7 months after partial amputation of the penis and right inguinal and para-iliacal lymph node dissections. A new lymph node metastasis in left inguinal area is clearly positive (arrow). (B) More dorsal slice of the same patient. A large metastasis with central necrosis can be found in the liver, and additional metastases in the left lung and para-aortic region (arrows). Further lymph node dissections were cancelled.

Despite this good performance of PET in staging of melanoma, sentinel lymph node biopsy proved to be even superior for the detection of metastases in regional lymph nodes in clinically node negative patients. FDG-PET imaging of regional lymph nodes in clinically node negative patients with AJCC stage I, II, and III melanoma, localised to the skin, was prospectively compared to SLN biopsy. Sensitivity of SLNB for detection of occult regional lymph node metastases was 94.4%, specificity 100%, positive predictive value (PPV) 100% and negative predictive value (NPV) 98.6%. The sensitivity of FDG-PET, however, was only 16.7%, specificity 95.8%, PPV 50% and NPV 81.9%.<sup>66</sup> As could be expected, the



failure to detect micrometastatic disease is the result of limitations of the imaging equipment and technique.<sup>67-69</sup>

A number of factors may interfere with the accuracy of PET scanning for metastatic melanoma. Apart from the detection limit of about 5 mm, false negatives may occur in patients with hyperglycaemia or after radiotherapy. Previous recent chemotherapy may influence the uptake of FDG due to cytostatic or cytolytic effects as well. False positives may be caused by non-specific uptake in inflammatory lesions, or mistaken for urinary excretion.<sup>59</sup>

While less suited for primary staging, FDG-PET may be of value in stage III or IV, or for patients with recurrent melanoma.<sup>69,70</sup> Patients may benefit from surgical removal of recurrences as long as no further metastases are present. To exclude the presence of additional metastases, FDG-PET may be useful, although more evidence is needed before FDG-PET data will influence therapeutic decision making.<sup>69,71,72</sup> Detection of metastatic melanoma with new tracers needs to be further investigated, although it remains doubtful whether micrometastases will ever be detected, like in the sentinel node procedure.

## **Pathology**

There are currently over 25 prognostic factors for CMM based on variables from the primary tumour. Tumour size, especially Breslow-thickness, invasion, ulceration, and site are the most important prognostic factors. There is also a growing interest in the impact of angiogenesis as a critical contributor to tumour growth, prognosis, and especially to metastatic potential. Based on multiple regression analysis the lymph node status of the melanoma patient is still the most powerful predicting factor for recurrence and survival.<sup>35,39,41</sup>

The technique of examining the SLN has improved and different techniques are used for the detection of micrometastatic disease. Routine histological evaluation is based on conventional HE staining of one or two sections from the central cross-section of the node, and examination involves less than 1% of the volume of the node and thus could easily miss micrometastatic disease. Histological examination of a lymph node at several levels clearly results in an increased sensitivity.<sup>38,73,74</sup> In addition, other techniques can be applied in order to increase the detection rate of (micro)metastatic cells.<sup>75</sup> Theoretically the presence of metastatic melanoma cells can be determined by demonstrating specific proteins using immunohisto- or cytochemistry; by demonstrating the presence of specific

changes in the DNA (translocations, mutations) using polymerase chain reaction (PCR), or detecting gene expression in the metastatic cells by identifying specific mRNAs using RT-PCR. In addition, relevance of serum tumour markers using immunochemical techniques in evaluation of therapy response and/or prognosis are investigated.<sup>76,77</sup>

Using immunohistochemistry, 1 tumour cell in  $10^5$  cells in lymph nodes can be detected.<sup>78</sup> Using the SLN biopsy technique only one or two lymph nodes are analysed in detail for micrometastatic disease. Serial sectioning and immunohistochemical staining with the S-100 and the HMB-45 antibodies will increase the number of positive nodes identified (Figure 3).<sup>73,79</sup> However, the S100 protein is a non-specific marker since it is also expressed in amongst others Schwann cells and dendritic reticulum cells normally present in the lymph nodes.<sup>80</sup> HMB-45 is variably expressed in melanomas.<sup>81</sup> No melanoma specific antigen has been described yet.

**Figure 3.**

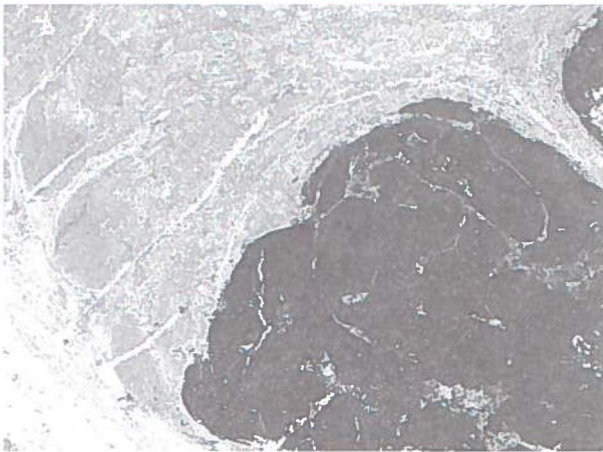


Figure 3. Metastatic melanoma cells in a lymph node: Immunohistochemical staining using anti HMB-45. Original magnification: 5x.

A breakthrough was the development of a highly sensitive method to reduce the already low false-negative rates of lymph nodes, by examining the lymph nodes for the presence of tyrosinase messenger RNA by RT-PCR. Fifty-eight percent of the histologic-negative SLN was upstaged with the RT-PCR.<sup>82</sup> RT-PCR is an extremely sensitive, and reproducible, and efficient technique for the identification of micrometastases in melanoma patients.<sup>83-85</sup> The technique of RT-PCR is also already successfully used on SLN's.<sup>84-87</sup> With IHC or PCR techniques 9-44% of the negative lymph nodes by routine HE staining,

will be upstaged. Investigators have reported additional positive lymph nodes in lymphadenectomy specimens in 10-52% of cases.<sup>74,84,85,88</sup> Tyrosinase is expressed in non-malignant melanocytes and Schwann cells, which can be present in lymph nodes.<sup>81</sup> Tyrosinase expression in lymph nodes can also be caused by 'illegitimate transcription', caused by imperfect transcription, as well.<sup>89,90</sup> These two causes for tyrosinase expression in lymph nodes can cause false positive results and it is therefore advisable to use a panel of markers to increase the specificity.<sup>52,81,91,92</sup>

Heterogeneity and specificity of gene expression and the importance of morphological control will influence test results. Regarding specificity, target genes should be selected that are exclusively expressed in the tumour cells and not in lymphatic cells. Examples are "illegal" expression of gp100, which was considered as a melanocytic lineage specific gene.<sup>93</sup> Finally, it is important to compose the right primer sets for the PCR to avoid amplification of pseudogenes<sup>94,95</sup>, which may lead to false positive results. Regarding the heterogeneity of gene expression one should realise that most tumours, especially the poorly undifferentiated ones, may contain tumour cells which do not express specific differentiation genes as tyrosinase and MART-1.<sup>96</sup> Approximately 17% of the advanced primary melanomas and melanoma metastases did not show positive tumour cells for any of these two differentiation markers.<sup>96</sup> In such cases the detection of tumour specific markers, i.e. MAGE's may yield useful.<sup>97</sup> The search for genes which play a role in malignant melanoma is difficult, but several important discoveries have been made.<sup>98-100</sup> Several studies have compared the sensitivity of IHC and the RT-PCR on lymph node tissue and showed that PCR is more sensitive<sup>74,84,85,88,101</sup> A disadvantage of PCR is that there is no morphological control and false positives can occur. Furthermore, we should realise that in most of these studies IHC was performed on only one single thin section while for PCR several thick sections are used, increasing the odds of a positive PCR.

S100, Melanoma Inhibiting Activity (MIA) and tumour-associated antigen (TA90) have been detected as serum markers for malignant melanoma, which are valuable in therapy monitoring and in detecting tumour progression.<sup>76,77</sup> Recently, a prospective study with 1,007 patients, confirmed that the new luminescence immuno assay (LIA) assay of S100-B protein in serum is correlated with clinical stage and is an independent prognostic marker in clinical stages II and III.<sup>102</sup> RT-PCR based detection of tyrosinase in peripheral blood shows limitations in clinical relevance, and reproducibility.<sup>92,103,104</sup> The use of a panel of markers will allow a better insight in prognostic classification.<sup>105-107</sup>

Nevertheless, 25% of the negative stage I and II melanoma patients will recur and die of their disease within 5 years of diagnosis, suggesting that some of these patients already have hematogenous metastases.

The value of the upstaging of the SLN with IHC or RT-PCR with respect to disease free survival, or the consequences for a lymph node dissection is currently unknown, but a combination of a panel with tumour specific markers with morphology will increase the accuracy. The search for specific makers, which indicate the genetic defects for melanoma, is still pending and will increase the accuracy as well. In addition proliferating markers of tumour progression may be of additional value. The place of the melanoma tumour marker S100-B via LIA in the clinical decision making of CMM needs further investigation.

## **Conclusions**

The presence or absence of lymph node metastases is the most powerful predicting factor for recurrence and survival of melanoma. The 5 year survival rates for localised tumours for AJCC Stage I and II are 92.5 and 74.8%, respectively, Stage III 49.0%, and Stage IV only 17.9%.<sup>3</sup> These figures have changed in the revised AJCC classification, because of the change in tumour-node-metastasis (TNM) criteria and stage groupings.<sup>41</sup> The 5-years survival rate following therapeutic lymph node dissection ranges in the literature from 19% to 38%.<sup>108</sup> Lymphatic metastases are generally followed by hematogeneous metastases. Surgery for metastatic melanoma is usually palliative only, but in a selected group of patients with metastasis it prolongs survival, even for years.<sup>109</sup> At present surgery is the only curative treatment option for metastatic disease.<sup>110</sup>

Clinical research confirms the high accuracy and good clinical applicability of the SLN concept.<sup>31,33,111</sup> The importance of the prognostic role of a positive SLN has been underlined by incorporation of the SLN status in the revised staging system for CMM.<sup>39</sup> Because the impact of the SLN on the final treatment and survival of melanoma patients is still unknown, we believe that more research is needed in that area.

FDG-PET is superior to conventional imaging techniques for staging metastatic melanoma (ultrasound, MRI and CT).<sup>59,60</sup> FDG-PET has proven to be especially useful in stage III and IV disease.<sup>69-72</sup> The accuracy of detecting metastases can be interfered by different factors.<sup>59</sup> As expected, FDG-PET is inferior to SLN biopsy in clinically negative lymph node patients with AJCC stage I and II, especially because of the inability to detect

micrometastasis.<sup>66-68</sup> FDG-PET as a diagnostic tool may especially be useful for stage III and IV disease.<sup>69,70,72</sup>

The techniques of examining the SLN have improved the last decade, especially by increasing the number of dissection levels and using IHC and RT-PCR.<sup>38,73,74</sup> By using immunohistochemical staining with S-100 and HMB-45, and RT-PCR on tyrosinase mRNA the number of positive nodes has increased to almost 50%.<sup>74,79,82,84,85,88</sup> Nevertheless, in 25% of negative stage I and II patients the melanoma will recur and patients die within 5 years of diagnosis.

For the detection of metastatic cells in lymph nodes and in peripheral blood, it is advisable to use a panel of makers to increase specificity<sup>81,91,92,105-107,112</sup> in combination with morphological control. The search for specific genes, which play a role in malignant melanoma, is ongoing, but several discoveries have been made.<sup>98-100</sup>

The surgical treatment of primary and recurrent melanomas, as well as lymphogenic and/or metastatic disease is well defined. The SNB concept is improving the staging of melanomas, but the clinical status is still experimental. The interferon therapy in an adjuvant setting is still not accepted as a standard therapy. PET has the potential to provide more insight in the amount of metastatic deposits in stage III and IV patients. Surgery is still the major corner stone in the treatment of melanoma. Further clinical and fundamental research may provide more insight in the treatment of a disease with a fast growing incidence. Melanoma is still an unimaginable and unpredictable disease.

## References

- 1 Visser O, Coebergh JWW, Schouten LJM, Dijck van JAAM. Incidence of cancer in the Netherlands 1997; Ninth report of the Netherlands cancer registry. *Dutch Cancer Registry* 2001.
- 2 Jemal A, Devesa SS, Hartge P, Tucker MA. Recent trends in cutaneous melanoma incidence among whites in the United States. *J Natl Cancer Inst* 2001; 93: 678-83.
- 3 Chang AE, Karnell LH, Menck HR. The National Cancer Data Base report on cutaneous and noncutaneous melanoma: a summary of 84,836 cases from the past decade. The American College of Surgeons Commission on Cancer and the American Cancer Society. *Cancer* 1998; 83: 1664-78.
- 4 Epstein DS, Lange JR, Gruber SB, Mofid M, Koch SE. Is physician detection associated with thinner melanomas? *JAMA* 1999; 281: 640-3.
- 5 Hofer SO, Molema G, Hermens RA, Wanebo HJ, Reichner JS, Hoekstra HJ. The effect of surgical wounding on tumour development. *Eur J Surg Oncol* 1999; 25: 231-43.
- 6 Veronesi U, Cascinelli N, Adamus J, Balch C, Bandiera D, Barchuk A, Bufalino R, Craig P, De Marsillac J, Durand JC. Thin stage I primary cutaneous malignant melanoma. Comparison of excision with margins of 1 or 3 cm. *N Engl J Med* 1988; 318: 1159-62.
- 7 Balch CM, Urist MM, Karakousis CP, Smith TJ, Temple WJ, Drzewiecki K, Jewell WR, Bartolucci AA, Mihm MC, Jr., Barnhill R. Efficacy of 2-cm surgical margins for intermediate-thickness melanomas (1 to 4 mm). Results of a multi-institutional randomized surgical trial. *Ann Surg* 1993; 218: 262-7.
- 8 Balch CM, Soong SJ, Smith T, Ross MI, Urist MM, Karakousis CP, Temple WJ, Mihm MC, Barnhill RL, Jewell WR, Wanebo HJ, Desmond R. Long-term results of a prospective surgical trial comparing 2 cm vs. 4 cm excision margins for 740 patients with 1-4 mm melanomas. *Ann Surg Oncol* 2001; 8: 101-8.
- 9 NIH Consensus Conference. Diagnosis and treatment of early melanoma. *JAMA* 1992; 268: 314-9.
- 10 Kroon BB, Nieweg OE, Hoekstra HJ, Lejeune FJ. Principles and guidelines for surgeons: management of cutaneous malignant melanoma. European Society of Surgical Oncology Brussels. *Eur J Surg Oncol* 1997; 23: 550-8.
- 11 Cascinelli N. Margin of resection in the management of primary melanoma. *Semin Surg Oncol* 1998; 14: 272-5.
- 12 Randomised trial of width of excision of thick cutaneous melanoma. *Melanoma Study Group (MSG)/British Association of Plastic Surgeons* 2001.
- 13 Veronesi U, Adamus J, Bandiera DC, Brennhovd IO, Caceres E, Cascinelli N, Claudio F, Ikonopisov RL, Javorskj VV, Kirov S, Kulakowski A, Lacoub J, Lejeune F, Mechl Z, Morabito A, Rode I, Sergeev S, van Slooten E, Szczygiel K, Trapeznikov NN. Inefficacy of immediate node dissection in stage I melanoma of the limbs. *N Engl J Med* 1977; 297: 627-30.
- 14 Sim FH, Taylor WF, Ivins JC, Pritchard DJ, Soule EH. A prospective randomized study of the efficacy of routine elective lymphadenectomy in management of malignant melanoma. Preliminary results. *Cancer* 1978; 41: 948-56.
- 15 Balch CM, Soong SJ, Bartolucci AA, Urist MM, Karakousis CP, Smith TJ, Temple WJ, Ross MI, Jewell WR, Mihm MC, Barnhill RL, Wanebo HJ. Efficacy of an elective regional lymph node dissection of 1 to 4 mm thick melanomas for patients 60 years of age and younger. *Ann Surg* 1996; 224: 255-63.
- 16 Cascinelli N, Morabito A, Santinami M, MacKie RM, Belli F. Immediate or delayed dissection of regional nodes in patients with melanoma of the trunk: a randomised trial. WHO Melanoma Program. *Lancet* 1998; 351: 793-6.

- 17 Schraffordt Koops HS, Vaglini M, Suci S, Kroon BB, Thompson JF, Gohl J, Eggermont AM, Di Filippo F, Krementz ET, Ruiter D, Lejeune FJ. Prophylactic isolated limb perfusion for localized, high-risk limb melanoma: results of a multicenter randomized phase III trial. European Organization for Research and Treatment of Cancer Malignant Melanoma Cooperative Group Protocol 18832, the World Health Organization Melanoma Program Trial 15, and the North American Perfusion Group Southwest Oncology Group-8593. *J Clin Oncol* 1998; 16: 2906-12.
- 18 Steinmann G, Eggermont AM. Boehringer Ingelheim trial 152.70. An open randomised, prospective trial to compare the efficacy and safety of TNF-alfa and melphalan with melphalan alone via isolated limb perfusion for metastatic melanoma of the limb (stage IIA, IIB, IIIA and IIIAB). *Boehringer Ingelheim trial 152 70* 1999.
- 19 Fraker DL. NCI-trial: Phase III randomized study of hyperthermic isolated limb perfusion and melphalan with or without tumor necrosis factor in patients with localized, advanced, extremity melanoma. *ACOSOG-Z0020* 2001.
- 20 Baas PC, Hoekstra HJ, Schraffordt Koops H, Oosterhuis JW, Weele van der LT, Oldhoff J. Results of hyperthermic isolated regional perfusion of locally metastasized melanoma of the lower extremity with melphalan with or without dactinomycin using different dosage methods. *Reg Cancer Treat* 1989; 2: 87-91.
- 21 Hafstrom L, Rudenstam CM, Blomquist E, Ingvar C, Jonsson PE, Lagerlof B, Lindholm C, Ringborg U, Westman G, Ostrup L. Regional hyperthermic perfusion with melphalan after surgery for recurrent malignant melanoma of the extremities. Swedish Melanoma Study Group. *J Clin Oncol* 1991; 9: 2091-4.
- 22 Hoekstra HJ, Schraffordt Koops H.S, de Vries EGE, van Weerden TW, Oldhoff J. Toxicity of hyperthermic isolated limb perfusion with cisplatin for recurrent melanoma of the lower extremity after previous perfusion treatment. *Cancer* 1993; 72: 1224-9.
- 23 Brady MS. Phase II Study of Isolated Limb Infusion With Melphalan and Dactinomycin in Patients With Primary or Recurrent, Unresectable Regional Melanoma or Soft Tissue Sarcoma of the Extremity. *NCI-trial* 2001.
- 24 Morton DL, Bostick PJ. Will the true sentinel node please stand? *Ann Surg Oncol* 1999; 6: 12-4.
- 25 Keshtgar MR, Eli PJ. Sentinel lymph node detection and imaging. *Eur J Nucl Med* 1999; 26: 57-67.
- 26 Nieweg OE, Tanis PJ, Kroon BB. The definition of a sentinel node. *Ann Surg Oncol* 2001; 8: 538-41.
- 27 Robinson DS, Sample WF, Fee HJ, Holmes C, Morton DL. Regional lymphatic drainage in primary malignant melanoma of the trunk determined by colloidal gold scanning. *Surg Forum* 1977; 28: 147-8.
- 28 Morton DL, Wen DR, Wong JH, Economou JS, Cagle LA, Storm FK, Foshag LJ, Cochran AJ. Technical details of intraoperative lymphatic mapping for early stage melanoma. *Arch Surg* 1992; 127: 392-9.
- 29 Kapteijn BA, Nieweg OE, Liem I, Mooi WJ, Balm AJ, Muller SH, Peterse JL, Valdes Olmos RA, Hoefnagel CA, Kroon BB. Localizing the sentinel node in cutaneous melanoma: gamma probe detection versus blue dye. *Ann Surg Oncol* 1997; 4: 156-60.
- 30 Koopal SA, Tiebosch ATMG, Piers AD, Schraffordt Koops H, Hoekstra HJ. Frozen section analysis of sentinel lymph nodes in melanoma patients. *Cancer* 2000; 89: 1720-5.
- 31 Morton DL, Thompson JF, Essner R, Elashoff R, Stern SL, Nieweg OE, Roses DF, Karakousis CP, Mozzillo N, Reintgen D, Wang HJ, Glass EC, Cochran AJ. Validation of the accuracy of intraoperative lymphatic mapping and sentinel lymphadenectomy for early-stage melanoma: a multicenter trial. Multicenter Selective Lymphadenectomy Trial Group. *Ann Surg* 1999; 230: 453-63.

- 32 Tanis PJ, Boom RP, Koops HS, Faneyte IF, Peterse JL, Nieweg OE, Rutgers EJ, Tiebosch AT, Kroon BB. Frozen section investigation of the sentinel node in malignant melanoma and breast cancer. *Ann Surg Oncol* 2001; 8: 222-6.
- 33 Berman CG, Norman J, Cruse CW, Reintgen DS, Clark RA. Lymphoscintigraphy in malignant melanoma. *Ann Plast Surg* 1992; 28: 29-32.
- 34 Albertini JJ, Cruse CW, Rapaport D, Wells K, Ross M, DeConti R, Berman CG, Jared K, Messina J, Lyman G, Glass F, Fenske N, Reintgen DS. Intraoperative radio-lympho-scintigraphy improves sentinel lymph node identification for patients with melanoma. *Ann Surg* 1996; 223: 217-24.
- 35 Gershenwald JE, Thompson W, Mansfield PF, Lee JE, Colome MI, Tseng CH, Lee JJ, Balch CM, Reintgen DS, Ross MI. Multi-institutional melanoma lymphatic mapping experience: the prognostic value of sentinel lymph node status in 612 stage I or II melanoma patients. *J Clin Oncol* 1999; 17: 976-83.
- 36 Morton DL, Wen DR, Cochran AJ. Management of early-stage melanoma by intra-operative lymphatic mapping and selective lymphadenectomy or "watch and see". *Surg Oncol Clin N Am* 1992; 247-59.
- 37 Reintgen D, Cruse CW, Wells K, Berman C, Fenske N, Glass F, Schroer K, Heller R, Ross M, Lyman G. The orderly progression of melanoma nodal metastases. *Ann Surg* 1994; 220 : 759-67.
- 38 Gershenwald JE, Colome MI, Lee JE, Mansfield PF, Tseng C, Lee JJ, Balch CM, Ross MI. Patterns of recurrence following a negative sentinel lymph node biopsy in 243 patients with stage I or II melanoma. *J Clin Oncol* 1998; 16: 2253-60.
- 39 Balch CM, Buzaid AC, Atkins MB, Cascinelli N, Coit DG, Fleming ID, Houghton A, Jr., Kirkwood JM, Mihm MF, Morton DL, Reintgen D, Ross MI, Sober A, Soong SJ, Thompson JA, Thompson JF, Gershenwald JE, McMasters KM. A new American Joint Committee on Cancer staging system for cutaneous melanoma. *Cancer* 2000; 88: 1484-91.
- 40 Balch CM, Buzaid AC, Soong SJ, Atkins MB, Cascinelli N, Coit DG, Fleming ID, Gershenwald JE, Houghton A, Jr., Kirkwood JM, McMasters KM, Mihm MF, Morton DL, Reintgen DS, Ross MI, Sober A, Thompson JA, Thompson JF. Final version of the american joint committee on cancer staging system for cutaneous melanoma. *J Clin Oncol* 2001; 19 : 3635-48.
- 41 Balch CM, Soong SJ, Gershenwald JE, Thompson JF, Reintgen DS, Cascinelli N, Urist M, McMasters KM, Ross MI, Kirkwood JM, Atkins MB, Thompson JA, Coit DG, Byrd D, Desmond R, Zhang Y, Liu PY, Lyman GH, Morabito A. Prognostic factors analysis of 17,600 melanoma patients: validation of the American Joint Committee on Cancer melanoma staging system. *J Clin Oncol* 2001; 19: 3622-34.
- 42 Reintgen D, Rapaport D, Tanabe KK, Ross M. Lymphatic mapping and sentinel node biopsy in patients with malignant melanoma. *J Fla Med Assoc* 1997; 84: 188-93.
- 43 Uren RF, Howman-Giles R, Thompson JF, Quinn MJ, O'Brien C, Shaw HM, Bosch CM, McCarthy WH. Lymphatic drainage to triangular intermuscular space lymph nodes in melanoma on the back. *J Nucl Med* 1996; 37: 964-6.
- 44 Norman J, Cruse CW, Espinosa C, Cox C, Berman C, Clark R, Saba H, Wells K, Reintgen D. Redefinition of cutaneous lymphatic drainage with the use of lymphoscintigraphy for malignant melanoma. *Am J Surg* 1991; 162: 432-7.
- 45 Uren RF, Howman-Giles RB, Shaw HM, Thompson JF, McCarthy WH. Lymphoscintigraphy in high-risk melanoma of the trunk: predicting draining node groups, defining lymphatic channels and locating the sentinel node. *J Nucl Med* 1993; 34: 1435-40.
- 46 Uren RF, Howman-Giles RB, Thompson JF, Shaw HM, McCarthy WH. Lymphatic drainage from periumbilical skin to internal mammary nodes. *Clin Nucl Med* 1995; 20: 254-5.



- 47 Karakousis CP, Grigoropoulos P. Sentinel node biopsy before and after wide excision of the primary melanoma. *Ann Surg Oncol* 1999; 6: 785-9.
- 48 McMasters KM, Reintgen DS, Ross MI, Wong SL, Gershenwald JE, Krag DN, Noyes RD, Viar V, Cerrito PB, Edwards MJ. Sentinel lymph node biopsy for melanoma: how many radioactive nodes should be removed? *Ann Surg Oncol* 2001; 8: 192-7.
- 49 Uren RF, Howman-Giles R, Thompson JF, McCarthy WH, Quinn MJ, Roberts JM, Shaw HM. Interval nodes: the forgotten sentinel nodes in patients with melanoma. *Arch Surg* 2000; 135: 1168-72.
- 50 Thelmo MC, Morita ET, Treseler PA, Nguyen LH, Allen RE, Jr., Sagebiel RW, Kashani-Sabet M, Leong SP. Micrometastasis to in-transit lymph nodes from extremity and truncal malignant melanoma. *Ann Surg Oncol* 2001; 8: 444-8.
- 51 Morton DL. NCI trial: Multicenter Selective Lymphadenectomy Trial. *NCI grant PO1 CA 29605* 2001.
- 52 McMasters KM, Reintgen DD, Edwards MJ, Cerrito P, Krag DN, Ross MI. Sunbelt Melanoma Trial: A multicenter trial of adjuvant interferon alfa-2b for melanoma in patients with early lymph node metastasis detected by lymphatic mapping and sentinel lymph node biopsy. *Sunbelt Melanoma Trial (SMT)* 1996.
- 53 Thomas JM, Patocskai EJ. The argument against sentinel node biopsy for malignant melanoma. *BMJ* 2000; 321: 3-4.
- 54 McMasters KM, Reintgen DS, Ross MI, Gershenwald JE, Edwards MJ, Sober A, Fenske N, Glass F, Balch CM, Coit DG. Sentinel lymph node biopsy for melanoma: controversy despite widespread agreement. *J Clin Oncol* 2001; 19: 2851-5.
- 55 Eggermont AMM, Kleeberg UR, Ruiter DJ, Suci S. European Organization for Research and Treatment of Cancer Melanoma Group trial experience with more than 2,000 patients, evaluating adjuvant treatment with low or intermediate doses of interferon alpha-2b. *ASCO conference* 2001.
- 56 Kirkwood JM. Adjuvant therapy of high-risk resected melanoma: relapse-free and overall survival effects of high dose interferon alpha-2b in randomized controlled multicenter trials E1684 and E2696 and intergroup trials E1690 and E1694. *ASCO conference* 2001.
- 57 Kirkwood JM, Ibrahim JG, Sosman JA, Sondak VK, Agarwala SS, Ernstoff MS, Rao U. High-dose interferon alfa-2b significantly prolongs relapse-free and overall survival compared with the GM2-KLH/QS-21 vaccine in patients with resected stage IIB-III melanoma: results of intergroup trial E1694/S9512/C509801. *J Clin Oncol* 2001; 19: 2370-80.
- 58 Cascinelli N, Belli F, MacKie RM, Santinami M, Bufalino R, Morabito A. Effect of long-term adjuvant therapy with interferon alpha-2a in patients with regional node metastases from cutaneous melanoma: a randomised trial. *Lancet* 2001; 358: 866-9.
- 59 Holder WD, Jr., White RL, Jr., Zuger JH, Easton EJ, Jr., Greene FL. Effectiveness of positron emission tomography for the detection of melanoma metastases. *Ann Surg* 1998; 227: 764-9.
- 60 Eigtved A, Andersson AP, Dahlstrom K, Rabol A, Jensen M, Holm S, Sorensen SS, Drzewiecki KT, Hojgaard L, Friberg L. Use of fluorine-18 fluorodeoxyglucose positron emission tomography in the detection of silent metastases from malignant melanoma. *Eur J Nucl Med* 2000; 27: 70-5.
- 61 Som P, Atkins HL, Bandyopadhyay D, Fowler JS, MacGregor RR, Matsui K, Oster ZH, Sacker DF, Shiue CY, Turner H, Wan CN, Wolf AP, Zabinski SV. A fluorinated glucose analog, 2-fluoro-2-deoxy-D-glucose (F-18): nontoxic tracer for rapid tumor detection. *J Nucl Med* 1980; 21: 670-5.
- 62 Gritters LS, Francis IR, Zasadny KR, Wahl RL. Initial assessment of positron emission tomography using 2-fluorine-18- fluoro-2-deoxy-D-glucose in the imaging of malignant melanoma. *J Nucl Med* 1993; 34: 1420-7.

- 63 Damian DL, Fulham MJ, Thompson E, Thompson JF. Positron emission tomography in the detection and management of metastatic melanoma. *Melanoma Res* 1996; 6: 325-9.
- 64 Wagner JD, Schauwecker D, Hutchins G, Coleman JJ, III. Initial assessment of positron emission tomography for detection of nonpalpable regional lymphatic metastases in melanoma. *J Surg Oncol* 1997; 64: 181-9.
- 65 Rinne D, Baum RP, Hor G, Kaufmann R. Primary staging and follow-up of high risk melanoma patients with whole- body 18F-fluorodeoxyglucose positron emission tomography: results of a prospective study of 100 patients. *Cancer* 1998; 82: 1664-71.
- 66 Wagner JD, Schauwecker D, Davidson D, Coleman JJ, III, Saxman S, Hutchins G, Love C, Hayes JT. Prospective study of fluorodeoxyglucose-positron emission tomography imaging of lymph node basins in melanoma patients undergoing sentinel node biopsy. *J Clin Oncol* 1999; 17: 1508-15.
- 67 Macfarlane DJ, Sondak V, Johnson T, Wahl RL. Prospective evaluation of 2-[18F]-2-deoxy-D-glucose positron emission tomography in staging of regional lymph nodes in patients with cutaneous malignant melanoma. *J Clin Oncol* 1998; 16: 1770-6.
- 68 Acland KM, Healy C, Calonje E, O'Doherty M, Nunan T, Page C, Higgins E, Russell-Jones R. Comparison of positron emission tomography scanning and sentinel node biopsy in the detection of micrometastases of primary cutaneous malignant melanoma. *J Clin Oncol* 2001; 19: 2674-8.
- 69 Wagner JD, Schauwecker DS, Davidson D, Wenck S, Jung SH, Hutchins G. FDG-PET sensitivity for melanoma lymph node metastases is dependent on tumor volume. *J Surg Oncol* 2001; 77: 237-42.
- 70 Tyler DS, Onaitis M, Kherani A, Hata A, Nicholson E, Keogan M, Fisher S, Coleman E, Seigler HF. Positron emission tomography scanning in malignant melanoma. *Cancer* 2000; 89: 1019-25.
- 71 Schwimmer J, Essner R, Patel A, Jahan SA, Shepherd JE, Park K, Phelps ME, Czernin J, Gambhir SS. A review of the literature for whole-body FDG PET in the management of patients with melanoma. *Q J Nucl Med* 2000; 44: 153-67.
- 72 Mijnhout GS, Hoekstra OS, van Tulder MW, Teule GJ, Deville WL. Systematic review of the diagnostic accuracy of (18)F- fluorodeoxyglucose positron emission tomography in melanoma patients. *Cancer* 2001; 91: 1530-42.
- 73 Robert ME, Wen DR, Cochran AJ. Pathological evaluation of the regional lymph nodes in malignant melanoma. *Semin Diagn Pathol* 1993; 10: 102-15.
- 74 Bostick PJ, Morton DL, Turner RR, Huynh KT, Wang HJ, Elashoff R, Essner R, Hoon DS. Prognostic significance of occult metastases detected by sentinel lymphadenectomy and reverse transcriptase-polymerase chain reaction in early-stage melanoma patients. *J Clin Oncol* 1999; 17: 3238-44.
- 75 Jung R, Ahmad-Nejad P, Wimmer M, Gerhard M, Wagener C, Neumaier M. Quality management and influential factors for the detection of single metastatic cancer cells by reverse transcriptase polymerase chain reaction. *Eur J Clin Chem Clin Biochem* 1997; 35: 3-10.
- 76 Djukanovic D, Hofmann U, Sucker A, Rittgen W, Schadendorf D. Comparison of S100 protein and MIA protein as serum marker for malignant melanoma. *Anticancer Res* 2000; 20: 2203-7.
- 77 Kelley MC, Gupta RK, Hsueh EC, Yee R, Stern S, Morton DL. Tumor-associated antigen TA90 immune complex assay predicts recurrence and survival after surgical treatment of stage I-III melanoma. *J Clin Oncol* 2001; 19: 1176-82.
- 78 Hatta N, Takata M, Takehara K, Ohara K. Polymerase chain reaction and immunohistochemistry frequently detect occult melanoma cells in regional lymph nodes of melanoma patients. *J Clin Pathol* 1998; 51: 597-601.

- 79 Cochran AJ, Wen DR, Morton DL. Occult tumor cells in the lymph nodes of patients with pathological stage I malignant melanoma. An immunohistological study. *Am J Surg Pathol* 1988; 12: 612-8.
- 80 Bautista NC, Cohen S, Anders KH. Benign melanocytic nevus cells in axillary lymph nodes. A prospective incidence and immunohistochemical study with literature review. *Am J Clin Pathol* 1994; 102: 102-8.
- 81 Clarkson KS, Sturdge IC, Molyneux AJ. The usefulness of tyrosinase in the immunohistochemical assessment of melanocytic lesions: a comparison of the novel T311 antibody (anti-tyrosinase) with S-100, HMB45, and A103 (anti-melan-A). *J Clin Pathol* 2001; 54: 196-200.
- 82 Wang X, Heller R, VanVoorhis N, Cruse CW, Glass F, Fenske N, Berman C, Leo-Messina J, Rappaport D, Wells K. Detection of submicroscopic lymph node metastases with polymerase chain reaction in patients with malignant melanoma. *Ann Surg* 1994; 220: 768-74.
- 83 Reintgen D, Albertini J, Berman C, Cruse CW, Fenske N, Glass LF, Puleo C, Wang X, Wells K, Rapaport D, DeConti R, Messina J, Heller R. Accurate Nodal Staging of Malignant Melanoma. *Cancer Control* 1995; 2: 405-14.
- 84 Blaheta HJ, Schitteck B, Breuninger H, Sotlar K, Ellwanger U, Thelen MH, Maczey E, Rassner G, Bueltmann B, Garbe C. Detection of melanoma micrometastasis in sentinel nodes by reverse transcription-polymerase chain reaction correlates with tumor thickness and is predictive of micrometastatic disease in the lymph node basin. *Am J Surg Pathol* 1999; 23: 822-8.
- 85 Blaheta HJ, Schitteck B, Breuninger H, Garbe C. Detection of micrometastasis in sentinel lymph nodes of patients with primary cutaneous melanoma. *Recent Results Cancer Res* 2001; 158: 137-46.
- 86 Palmieri G, Ascierio PA, Cossu A, Mozzillo N, Motti ML, Satriano SM, Botti G, Caraco C, Celentano E, Satriano RA, Lissia A, Tanda F, Pirastu M, Castello G. Detection of occult melanoma cells in paraffin-embedded histologically negative sentinel lymph nodes using a reverse transcriptase polymerase chain reaction assay. *J Clin Oncol* 2001; 19: 1437-43.
- 87 Goydos JS, Ravikumar TS, Germino FJ, Yudd A, Bancila E. Minimally invasive staging of patients with melanoma: sentinel lymphadenectomy and detection of the melanoma-specific proteins MART-1 and tyrosinase by reverse transcriptase polymerase chain reaction. *J Am Coll Surg* 1998; 187: 182-8.
- 88 Shivers SC, Wang X, Li W, Joseph E, Messina J, Glass LF, DeConti R, Cruse CW, Berman C, Fenske NA, Lyman GH, Reintgen DS. Molecular staging of malignant melanoma: correlation with clinical outcome. *JAMA* 1998; 280: 1410-5.
- 89 Chelly J, Concordet JP, Kaplan JC, Kahn A. Illegitimate transcription: transcription of any gene in any cell type. *Proc Natl Acad Sci U S A* 1989; 86: 2617-21.
- 90 Battyani Z, Xerri L, Hassoun J, Bonerandi JJ, Grob JJ. Tyrosinase gene expression in human tissues. *Pigment Cell Res* 1993; 6: 400-5.
- 91 Shivers SC, Li W, Haddad F, Reintgen DS. Molecular staging of melanoma. *Ann Surg Oncol* 1999; 6: 225-6.
- 92 Calogero A, Timmer-Bosscha H, Schraffordt KH, Tiebosch AT, Mulder NH, Hospers GA. Limitations of the nested reverse transcriptase polymerase chain reaction on tyrosinase for the detection of malignant melanoma micrometastases in lymph nodes. *Br J Cancer* 2000; 83: 184-7.
- 93 Brouwenstijn N, Slager EH, Bakker AB, Schreurs MW, Van der Spek CW, Adema GJ, Schrier PI, Figdor CG. Transcription of the gene encoding melanoma-associated antigen gp100 in tissues and cell lines other than those of the melanocytic lineage. *Br J Cancer* 1997; 76: 1562-6.
- 94 Neumaier M, Gerhard M, Wagener C. Diagnosis of micrometastases by the amplification of tissue-specific genes. *Gene* 1995; 159: 43-7.

- 95 Dingemans AM, Brakenhoff RH, Postmus PE, Giaccone G. Detection of cytokeratin-19 transcripts by reverse transcriptase- polymerase chain reaction in lung cancer cell lines and blood of lung cancer patients. *Lab Invest* 1997; 77: 213-20.
- 96 de Vries TJ, Fourkour A, Wobbles T, Verkroost G, Ruiter DJ, van Muijen GN. Heterogeneous expression of immunotherapy candidate proteins gp100, MART-1, and tyrosinase in human melanoma cell lines and in human melanocytic lesions. *Cancer Res* 1997; 57: 3223-9.
- 97 Brasseur F, Rimoldi D, Lienard D, Lethe B, Carrel S, Arienti F, Suter L, Vanwijck R, Bourlond A, Humblet Y. Expression of MAGE genes in primary and metastatic cutaneous melanoma. *Int J Cancer* 1995; 63: 375-80.
- 98 Greulich KM, Utikal J, Peter RU, Krahn G. c-MYC and nodular malignant melanoma. A case report. *Cancer* 2000; 89: 97-103.
- 99 Hipfel R, Schittek B, Bodingbauer Y, Garbe C. Specifically regulated genes in malignant melanoma tissues identified by subtractive hybridization. *Br J Cancer* 2000; 82: 1149-57.
- 100 Polsky D, Young AZ, Busam KJ, Alani RM. The transcriptional repressor of p16/Ink4a, Id1, is up-regulated in early melanomas. *Cancer Res* 2001; 61: 6008-11.
- 101 van der Velde-Zimmerman D, Roijers JF, Bouwens-Rombouts A, De Weger RA, de Graaf PW, Tilanus MG, Van den Tweel JG. Molecular test for the detection of tumor cells in blood and sentinel nodes of melanoma patients. *Am J Pathol* 1996; 149: 759-64.
- 102 Martenson ED, Hansson LO, Nilsson B, von Schoultz E, Mansson BE, Ringborg U, Hansson J. Serum S-100b protein as a prognostic marker in malignant cutaneous melanoma. *J Clin Oncol* 2001; 19: 824-31.
- 103 Palmieri G, Strazzullo M, Ascierto PA, Satriano SM, Daponte A, Castello G. Polymerase chain reaction-based detection of circulating melanoma cells as an effective marker of tumor progression. Melanoma Cooperative Group. *J Clin Oncol* 1999; 17: 304-11.
- 104 Schittek B, Blaheta HJ, Ellwanger U, Garbe C. Polymerase chain reaction in the detection of circulating tumour cells in peripheral blood of melanoma patients. *Recent Results Cancer Res* 2001; 158: 93-104.
- 105 Schrader AJ, Probst-Kepper M, Grosse J, Kunter U, Franzke A, Sel S, Atzpodien E, Buer J. Tumour microdissemination and survival in metastatic melanoma. *Anticancer Res* 2000; 20: 3619-24.
- 106 Schrader AJ, Probst-Kepper M, Grosse J, Kunter U, Schenk F, Franzke A, Atzpodien J, Buer J. Molecular and prognostic classification of advanced melanoma: a multi- marker microcontamination assay of peripheral blood stem cells. *Melanoma Res* 2000; 10: 355-62.
- 107 Curry BJ, Myers K, Hersey P. MART-1 is expressed less frequently on circulating melanoma cells in patients who develop distant compared with locoregional metastases. *J Clin Oncol* 1999; 17: 2562-71.
- 108 Karakousis CP. Therapeutic node dissections in malignant melanoma. *Semin Surg Oncol* 1998; 14: 291-301.
- 109 Sharpless SM, Das Gupta TK. Surgery for metastatic melanoma. *Semin Surg Oncol* 1998; 14: 311-8.
- 110 Reintgen D. Establishing a standard of care for the patient with melanoma. *Ann Surg Oncol* 2001; 8: 91.
- 111 Reintgen D. Melanoma nodal metastases: biologic significance and therapeutic considerations. *Surg Oncol Clin N Am* 1996; 5: 105-20.
- 112 Bieligm SC, Ghossein R, Bhattacharya S, Coit DG. Detection of tyrosinase mRNA by reverse

transcription-polymerase chain reaction in melanoma sentinel nodes. *Ann Surg Oncol* 1999; 6: 232-40.



## **Chapter 3**

### **Fluorodeoxyglucose-positron emission tomography and sentinel lymph node biopsy in staging primary cutaneous melanoma**

K. Havenga<sup>1</sup>, D.C.P. Cobben<sup>2</sup>, W.J.G. Oyen<sup>3</sup>, S. Nienhuijs<sup>1</sup>, H.J. Hoekstra<sup>2</sup>, T.J.M. Ruers<sup>1</sup>,  
Th. Wobbes<sup>1</sup>

Departments of Surgery<sup>1</sup> and Nuclear Medicine<sup>3</sup>, University Medical Center Nijmegen,  
P.O. Box 9101, 6500 HB Nijmegen. Division of Surgical Oncology<sup>2</sup>, Groningen University  
Hospital, P.O. Box 30.001, 9700 RB Groningen, The Netherlands.

*European Journal of Surgical Oncology 2003; 2: 662-664*

## Summary

**Aim:** In this study we investigate the value of sentinel lymph node (SLN) biopsy and Fluorodeoxyglucose Positron Emission Tomography (FDG-PET) in relation to SLN biopsy in staging primary cutaneous melanoma.

**Methods:** 55 patients with primary cutaneous melanoma of more than 1.0 mm. Breslow thickness and no palpable regional lymph nodes underwent a FDG-PET scan before SLN biopsy.

**Results:** SLN's were retrieved in 53 patients. Melanoma metastases were found in the SLN of 13 patients. FDG-PET detected the lymph node metastases in two of the 13 patients with SLN metastases. In five patients FDG accumulation was recorded in a regional lymph node basin, while no tumor positive SLN was found. In 8 patients FDG-PET showed increased activity at a site of possible distant metastasis. Only in one patient metastatic disease was confirmed. In five of these patients no possible explanation for the positive FDG-PET result could be found.

**Conclusion:** FDG-PET should not be considered in this group. SLN biopsy reveals regional metastases that are too small to be detected by FDG-PET. The prevalence of distant metastases is too small to justify routine use of FDG-PET.



## Introduction

Accurate staging of patients with cutaneous melanoma is important. After tumor thickness and tumor ulceration, lymph node status is the most important prognostic factor, as is emphasized in the completely revised staging system for cutaneous melanoma (1). Elective lymph node dissection has been proposed to increase survival in patients with isolated regional lymph node metastases. Although some studies failed to demonstrate the benefit of elective lymph node dissection, long term results from the Intergroup Melanoma Surgical Trial show a survival benefit for stratified subgroups of patients with non-ulcerated tumors, tumor thickness between 1.0 mm and 2.0 mm, or melanomas of the limb, undergoing elective regional lymph node dissection. (2). If regional lymph node dissection gives a survival benefit, it is likely to be in patients with metastases confined to the regional lymph node basin. Identification of patients with occult regional lymph node metastases may thus be important. Sentinel lymph node biopsy (SLNB) is widely used for this purpose. The value of early detection of lymph node metastases by SLNB, followed by therapeutic lymph node dissection, is currently prospectively studied in the Multicenter Selective Lymphadenectomy Trial (3) and the Sunbelt Melanoma Trial (protocol on <http://www.sunbeltmelanoma.com/prot2000.htm>). SLNB is an invasive procedure that gives no direct information on possible distant metastases, although a positive SLN has been shown to be the best predictor of tumor recurrence (4).

In recent years fluorodeoxyglucose - positron emission tomography (FDG-PET) may be a sensitive staging tool for melanoma. Initial results comparing FDG-PET with conventional diagnostic tests or with elective or selective regional lymph node dissection suggested a sensitivity and specificity of 90 percent or more (5-7).

This study was designed to investigate the value of FDG-PET scanning in the clinical treatment of primary cutaneous melanoma. The following questions were addressed: does FDG-PET predict lymph node metastasis in the SLN, and does FDG-PET provide useful information about extended disease outside the primary lymph node basin?

## Patients and methods

Patients were selected with primary cutaneous melanoma  $\geq$  1.0 mm Breslow thickness on the extremities or trunk, and no palpable regional lymph nodes. Fifty-five patients were entered in this study; 45 patients were treated at University Medical Center Nijmegen, and 10 patients were treated at the University Hospital Groningen, The

Netherlands. Twenty-six patients (47 percent) were male, 29 patients (53 percent) were female. Age range of the patients was 15 to 77 years, median age was 54 years. The primary lesions were located on the upper extremity in five patients (9 percent), on the lower extremity in 27 patients (49 percent), and on the trunk in 23 patients (42 percent). Mean Breslow thickness was 3.18 mm, ranging from 1.00 mm to 13 mm. Median Breslow thickness was 2.40 mm.

### ***SLNB technique***

All patients were scheduled to undergo sentinel lymph node biopsy. Preoperatively, lymphatic drainage patterns were defined by performing lymphoscintigraphy with  $^{99}\text{Tc}$  nanocolloid. Probable sentinel nodes were marked at the skin. Before the incision, one to two milliliters patent blue dye was injected around the excision scar of the primary lesion. A gamma probe was used to identify the sentinel node during the operation, as is described in detail by Nieweg and Keshtgar (8,9). In Nijmegen a Europrobe (Euromedical Instruments, Le Chesnay, France) was used, in Groningen a Neoprobe 1000 and Neoprobe 2000 (Neoprobe Corporation, Dublin, Ohio, USA).

### ***FDG-PET scanning technique***

All patients underwent a FDG-PET scan before the operation. In Nijmegen, a dedicated, rotating half-ring PET-scanner (ECAT-ART, Siemens/CTI, Knoxville, TN, USA) was used for data acquisition. Prior to FDG-injection, patients were fasting for at least 6 h. Intake of sugar-free liquids was permitted. Immediately prior to the procedure, patients were hydrated with 500 ml of water. One hour after intravenous injection of 200-220 MBq FDG (Mallinckrodt Medical, Petten, The Netherlands) and 20 mg furosemide, emission and transmission images of the area between proximal femora and the base of the skull were acquired (10 minutes per bed position). The images were corrected for attenuation and reconstructed using the ordered-subsets expectation maximisation (OSEM) algorithm.

In Groningen, an ECAT 951/31 or an ECAT HR+ positron camera (Siemens/CTI, Knoxville, TN, USA) was used for data acquisition. After overnight fasting the patients were administered 422 MBq FDG (range 386 - 603 MBq) intravenously. Patients were hydrated in the same fashion.  $^{18}\text{F}$ -FDG was synthesized according to Hamacher by an automated synthesis module.(10,11) Data acquisition started 90 min after injection for 5

min per bed position. Both attenuation corrected and non-attenuation corrected images were reconstructed using OSEM.

## **Results**

### ***Sentinel node***

Sentinel lymph node (SLN) biopsy was performed using <sup>99</sup>Tc nanocolloid in all patients and patent blue in 22 patients. SLN's were retrieved from one lymph node basin in 45 patients, and from a second lymph node basin in eight patients (15%). In two patients (4 percent), a SLN could not be retrieved. Melanoma metastases were found in the SLN of 13 patients (24%). Mean Breslow thickness of the primary tumour was 4.28 mm, ranging from 1.0 to 13.0 mm. Median Breslow thickness was 2.4 mm.

### ***FDG-PET***

FDG-PET detected the lymph node metastasis in only two of the 13 patients with proven SLN metastases. The diameter of the lymph node metastasis was 7 and 8 mm in these patients. The Breslow thickness of the primary tumour was 2.4 and 4.4 mm respectively. In the other 11 regional metastatic sites no abnormal FDG accumulation was seen. The diameter of the metastases in these 11 sentinel lymph node was: ≤ 2 mm (n=8), 4 mm (n=1), 5 mm (n=1), and 11 mm (n=1). In the 32 SLN negative patients FDG-PET was negative in 27. However, in five patients FDG accumulation in a regional lymph node basin was recorded, while no tumor-positive SLN was found.

FDG-PET scan showed increased activity at a site of possible distant metastasis in eight patients.

- In one patient, increased activity in the mediastinum, liver and right adrenal gland was demonstrated to be caused by metastatic disease.
- In one patient increased activity in the mediastinum was demonstrated, later concluded to be due to a lung cancer.
- In two patients, increased activity was seen in the mediastinum and lung hilus. Analysis by CT scan in both patients and mediastinoscopy in one patient did not reveal any abnormalities.
- In one patient increased activity was seen at the splenic flexure of the colon. At colonoscopy no abnormalities were found.

- In one patient, increased activity was seen along the aorta and right iliacal vessels, cranial and posterior to the bladder. Sigmoidoscopy showed a hyperplastic polyp at 20 cm from the anal verge, which may explain the retrovesical hotspot. CT scan showed para-aortal lymph nodes with a diameter of 1.3 cm and several para-aortal, iliac, and peri-rectal lymph nodes with a diameter of 1 cm or less, which did not change in the following years.
- In one patient increased activity was demonstrated in the presacral area. After a follow-up of 38 months, the patient remains with no evidence of metastatic disease.
- In one patient increased activity was demonstrated caudal to the liver. A barium enema study showed a probable malignancy at the hepatic flexure for which the patient underwent a right hemicolectomy. Pathological examination revealed a T1N0 lesion in a large tubulovillous adenoma.

## Discussion

In this study, we evaluated FDG-PET scanning in staging primary cutaneous melanoma  $\geq 1.0$  mm Breslow thickness, and no palpable regional lymph nodes. SLN biopsy identified 13 patients with regional lymph node metastases, six of these patients had a micro metastasis ( $< 2$  mm). FDG-PET scanning identified only two of these patients, with regional metastases of 7 mm and 8 mm in diameter. Furthermore, FDG-PET scanning suggested incorrectly a regional lymph node metastasis in 5 patients. Only one patient with generalized metastatic disease was identified by FDG-PET scanning.

Technical limitations of the FDG-PET are likely to cause these poor results (6,12,13). Only tumor loads of 80 mm<sup>3</sup> or more can be visualized by FDG- PET (13) or expressed as a detection level of 4-5 mm (14). This is in contrast with SLN biopsy, where the pathologist is able to identify micro metastases (15).

Some studies have published favorable results of FDG-PET in staging primary melanoma (5,6). These studies compared FDG-PET with conventional diagnostics or lymph node dissection and not with SLN biopsy. In these studies accuracy rates of 88-98% were reported.

Ackland and co-authors evaluated FDG-PET and SLN biopsy in 50 patients with primary melanoma more than 1 mm in thickness or with lymphatic invasion. Fourteen positive regional lymph nodes were retrieved by SLNB. No regional lymph node metastasis was found with FDG-PET (12). Wagner and co-authors compared FDG-PET to

SLNB in 70 patients with primary melanoma with a thickness more than 1 mm or with localized regional cutaneous recurrence (16). In 17 patients, regional lymph node metastases were found with SLNB while in one additional patient a regional lymph node metastasis was found during follow-up examination. Only three of these 18 regional lymph node metastases were found with FDG-PET. Belhocine and co-authors also evaluated FDG-PET and SLN biopsy in 21 patients. FDG-PET detected only one of six sentinel node metastasis (17).

FDG-PET may be of value in stage III, IV, or for patients with recurrent melanoma (13,18). More research is needed before FDG-PET will influence therapeutic decision making (7,13,19,20).

In conclusion, FDG-PET should not be considered in patients with primary cutaneous melanoma  $\geq 1.0$  mm Breslow thickness, and no palpable regional lymph nodes. SLN biopsy reveals regional metastases that are too small to be detected by FDG-PET. The prevalence of distant metastases in this group of patients is too small to justify routine preoperative FDG-PET.

## References

1. Balch CM, Buzaid AC, Soong Sj et al. Version of the American Joint Committee on Cancer Staging System for Cutaneous Melanoma. *J Clin Oncol* 2001; 19: 3635-48.
2. Balch CM, Soong SJ, Smith T et al. Long-Term Results of a Prospective Surgical Trial Comparing 2 Cm Vs. 4 Cm Excision Margins for 740 Patients With 1-4 Mm Melanomas. *Ann Surg Oncol* 2001; 8: 101-8.
3. Morton DL, Thompson JF, Essner R et al. Validation of the Accuracy of Intraoperative Lymphatic Mapping and Sentinel Lymphadenectomy for Early-Stage Melanoma: a Multicenter Trial. Multicenter Selective Lymphadenectomy Trial Group. *Ann Surg* 1999; 230: 453-63.
4. Gershenwald JE, Thompson W, Mansfield PF et al. Multi-Institutional Melanoma Lymphatic Mapping Experience: the Prognostic Value of Sentinel Lymph Node Status in 612 Stage I or II Melanoma Patients. *J Clin Oncol* 1999; 17: 976-83.
5. Rinne D, Baum RP, Hor G, Kaufmann R. Primary Staging and Follow-Up of High Risk Melanoma Patients With Whole- Body 18F-Fluorodeoxyglucose Positron Emission Tomography: Results of a Prospective Study of 100 Patients. *Cancer* 1998; 82: 1664-71.
6. Macfarlane DJ, Sondak V, Johnson T, Wahl RL. Prospective Evaluation of 2-[18F]-2-Deoxy-D-Glucose Positron Emission Tomography in Staging of Regional Lymph Nodes in Patients With Cutaneous Malignant Melanoma. *J Clin Oncol* 1998; 16: 1770-6.
7. Cobben DC, Koopal S, Tiebosch AT, Jager PL, Elsinga PH, Wobbes Th, Hoekstra HJ. New Diagnostic Techniques in Staging in the Surgical Treatment of Cutaneous Malignant Melanoma. *Eur J Surg Oncol* 2002; 28: 692-700.
8. Nieweg OE, Tanis PJ, Kroon BB. The Definition of a Sentinel Node. *Ann Surg Oncol* 2001; 8: 538-41.
9. Keshtgar MR, Eil PJ. Sentinel Lymph Node Detection and Imaging. *Eur J Nucl Med* 1999; 26: 57-67.
10. Hamacher K, Coenen HH, Stocklin G. Efficient Stereospecific Synthesis of No-Carrier-Added 2-[18F]-Fluoro-2- Deoxy-D-Glucose Using Aminopolyether Supported Nucleophilic Substitution. *J Nucl Med* 1986; 27: 235-8.
11. Medema J, Luurtsema G, Keizer H. Efficient stereospecific synthesis of no-carrier-added 2-[18F]-fluoro-2-deoxy-D-glucose using aminopolyether supported nucleophilic substitution. *Journal of Labelled Computed Radiopharmaceuticals* 42 (suppl), s853-s855. 1994.
12. Acland KM, Healy C, Calonje E et al. Comparison of Positron Emission Tomography Scanning and Sentinel Node Biopsy in the Detection of Micrometastases of Primary Cutaneous Malignant Melanoma. *J Clin Oncol* 2001; 19: 2674-8.
13. Wagner JD, Schauwecker DS, Davidson D, Wenck S, Jung SH, Hutchins G. FDG-PET Sensitivity for Melanoma Lymph Node Metastases Is Dependent on Tumor Volume. *J Surg Oncol* 2001; 77: 237-42.
14. Holder WD, Jr., White RL, Jr., Zuger JH, Easton EJ, Jr., Greene FL. Effectiveness of Positron Emission Tomography for the Detection of Melanoma Metastases. *Ann Surg* 1998; 227: 764-9.
15. Hatta N, Takata M, Takehara K, Ohara K. Polymerase Chain Reaction and Immunohistochemistry Frequently Detect Occult Melanoma Cells in Regional Lymph Nodes of Melanoma Patients. *J Clin Pathol* 1998; 51: 597-601.
16. Wagner JD, Schauwecker D, Davidson D et al. Prospective Study of Fluorodeoxyglucose-Positron Emission Tomography Imaging of Lymph Node Basins in Melanoma Patients Undergoing Sentinel Node Biopsy. *J Clin Oncol* 1999; 17: 1508-15.

17. Belhocine T, Pierard G, De Labrassinne M, Lahaye T, Rigo P. Staging of Regional Nodes in AJCC Stage I and II Melanoma: <sup>18</sup>F FDG PET Imaging Versus Sentinel Node Detection. *Oncologist* 2002; 7: 271-8.
18. Tyler DS, Onaitis M, Kherani A et al. Positron Emission Tomography Scanning in Malignant Melanoma. *Cancer* 2000; 89: 1019-25.
19. Schwimmer J, Essner R, Patel A et al. A Review of the Literature for Whole-Body FDG PET in the Management of Patients With Melanoma. *Q J Nucl Med* 2000; 44: 153-67.
20. Mijnhout GS, Hoekstra OS, van Tulder MW, Teule GJ, Deville WL. Systematic Review of the Diagnostic Accuracy of (18)F- Fluorodeoxyglucose Positron Emission Tomography in Melanoma Patients. *Cancer* 2001; 91: 1530-42.





## Chapter 4

### **$^{18}\text{F}$ -3'-fluoro-3'-deoxy-L-thymidine; a new tracer for staging metastatic melanoma?**

David C.P. Cobben<sup>1,2</sup>, Piet L. Jager<sup>1</sup>, Philip H. Elsinga<sup>1</sup>, Bram Maas<sup>1</sup>,  
Albert J. H. Suurmeijer<sup>3</sup>, Harald J. Hoekstra<sup>2</sup>

PET-center<sup>1</sup>, Departments of Surgical Oncology<sup>2</sup> and Pathology and Laboratory  
Medicine<sup>3</sup>, Groningen University Hospital, Groningen, The Netherlands.

*Journal of Nuclear Medicine 2003 Dec; 44: 1927-1932*

## Summary

In this study the feasibility of  $^{18}\text{F}$ -3'-fluoro-3'-deoxy-L-thymidine positron emission tomography (FLT-PET) for staging patients with clinical stage III melanoma was investigated.

**Methods:** 10 patients with melanoma and metastases to the locoregional draining lymph nodes, clinical stage III, based on physical examination, chest X-ray, LDH and histopathological confirmation underwent a whole-body FLT-PET scan 1 hour after injection of a median 400 (185-430)MBq FLT. Patients were staged according. All FLT-PET lesions were verified using the American Joint Committee on Cancer Staging System which includes physical examination, spiral computed tomography, ultrasound, chest X-ray and histopathological examinations. Size and mitotic rate of metastatic lymph nodes and skin metastases were determined.

**Results:** All histopathological samples and FLT-PET lesions were categorized over anatomical regions and correlated. All locoregional metastases were correctly visualized by FLT-PET. Region based sensitivity for detection of lymph node metastatic disease was 88%. There were 3 true negative and 2 false positive lesions. The detection limit for lymph node metastases appeared to be approximately 6 mm or a mitotic rate of 9 per 2 mm<sup>2</sup>. Two patients were upstaged by FLT-PET, which was confirmed by CT. In three patients, FLT-PET detected a total of 3 additional lesions, with therapeutic consequences, without influencing staging. These lesions were initially missed by clinical staging.

**Conclusion:** FLT-PET seems promising for (re)staging purposes in clinically stage III melanoma. Further research is needed, in which FLT-PET should be compared with FDG-PET.

## Introduction

Positron emission tomography (PET), using  $^{18}\text{F}$ -fluoro-2'-deoxy-D-glucose (FDG), has been accepted as a powerful non-invasive metabolic imaging method for the diagnosis and staging of cancer (1). The enzyme hexokinase causes intracellular entrapment of FDG, reflecting glucose metabolism. (2) FDG is transported into the cells, which are metabolically active, especially in the case of tumor cells (3).

Most melanomas have a very high glucose utilization. In vitro experiments demonstrate a high FDG uptake in melanoma cells (4). Therefore, almost parallel with the introduction of the sentinel lymph node biopsy (SLNB) in the staging of melanoma patients, FDG-PET emerged as a clinical modality for staging, restaging and therapy monitoring. Conventional imaging techniques, such as computed tomography (CT), magnetic resonance imaging (MRI), ultrasound (US) and physical examination are not as accurate for the detection of metastatic melanoma as SLNB and/or FDG-PET (5). For primary locoregional staging, FDG-PET is surpassed by the SLNB (6-9). FDG-PET may be of value in stage III or IV melanoma patients, or for patients with recurrent melanoma (5,10-14).

FDG is not a selective tracer, since it is also taken up in macrophages. Macrophages invade tumors and appear in inflammatory lesions, causing false positive results (15,16). Another problem is a decreased uptake in hyperglycemia (17). Furthermore, routine whole-body FDG-PET lacks sensitivity for imaging brain metastases, because glucose is avidly taken up by the normal brain.

Recently,  $^{18}\text{F}$ -fluoro-3'-deoxy-3'-L-fluorothymidine (FLT) has been introduced as a PET-tracer by Shields and Grierson, which might not have these drawbacks (18,19). This pyrimidine analog, is phosphorylated by the enzyme thymidine kinase 1 ( $\text{TK}_1$ ), which leads to intracellular trapping (19). During DNA synthesis,  $\text{TK}_1$  activity increases almost tenfold and is, therefore, an accurate reflection of cellular proliferation (20). The aim of this study was to investigate the feasibility of FLT-PET for the staging of regionally metastasized melanoma.

## **Materials and Methods**

### ***Patients***

This prospective study consisted of ten consecutive patients with clinically stage III melanoma (locoregional disease). Patients were included from April until November 2002. Two patients had a unknown primary and 2 patients had a primary melanoma, which was too small to assess the Clark level. All patients gave written informed consent. For inclusion, the liver and kidney functions and hematological parameters (Hb, Ht, erythrocytes, thrombocytes, leukocytes and white cell count) had to be within normal limits. Pregnant patients and patients with psychiatric disorders were excluded. All screened patients could be included in the study. The Medical Ethics Committee of the Groningen University Hospital approved the study protocol.

### ***PET studies***

Synthesis of FLT was performed according to the method of Machulla et al.(21) FLT was produced by [<sup>18</sup>F]fluorination of the 4,4'-dimethoxytrityl protected anhydrothymidine, followed by a deprotection step. After purification by reversed phase HPLC, the product was made isotonic and passed through a 0.22µm filter. FLT was produced with a radiochemical purity of >95% and specific activity of >10 TBq/mmol. The radiochemical yield was 6.7±3.7% (decay corrected).

Eight studies were performed using an ECAT EXACT HR+ (Siemens/CTI Inc., Knoxville, TN) and two studies on an ECAT 951/31 (Siemens/CTI Inc., Knoxville, TN). Prior to PET imaging, patients were instructed to fast for at least 6 hours to keep the study comparable with studies performed with FDG (22). They were also instructed to drink one liter of water prior to imaging to stimulate FLT excretion from the renal calyces and stimulate subsequent voiding. Surgery followed FLT-PET after a median period of 26 (7-45) days.

Sixty minutes after injection, a non attenuation-corrected whole-body scan was acquired from crown to femur with 8 minutes per bed position. Because detection or exclusion of malignant lesions, rather than the quantitative determination of uptake, is the main goal of this feasibility study, only non-attenuation corrected PET images were obtained. If the primary tumor was located under the level of the femur, the patient was

scanned from crown to foot. PET-images were iteratively reconstructed (ordered subset expectation maximization) (23).

### ***Pathological evaluation and staging***

The histology of all primary lesions and metastasis were evaluated according to the latest version of the American Joint Committee on Cancer (AJCC).(24) The emphasis of this classification is on tumor thickness, ulceration and number of positive lymph nodes. Breslow thickness and Clark level of the primary lesion were evaluated. In all metastatic lesions (in-transit and lymph node metastases), tumor size and mitotic rate were measured. Tumor size was expressed in mm or as micrometastasis if smaller than 2 mm. Mitotic rate was expressed in number of mitoses per 2 mm<sup>2</sup> at a 400 magnification.

The staging took place according to the last version of the American Joint Committee on Cancer (AJCC) (24). All patients were firstly staged clinically, by physical examination, LDH, chest X-ray and histopathological confirmation of the locoregional lymph node(s). Lastly, the patients were staged on the basis of the FLT-PET images only and finally staged pathologically after surgery. The included patients with stage III melanoma had locoregional metastases in the lymph nodes of the groin or axilla.

### ***Data analysis***

FLT-PET images were analyzed for uptake in malignant lesions and normal anatomical structures. Two experienced PET-physicians (PLJ, DCPC) evaluated the images independently only aware of the original location of the primary lesion, but blinded for other clinical information. They subsequently reached consensus on a lesion by lesion basis.

The pathologist (AJHS) was unaware of the results of the PET-images. Because it is impossible to exactly match individual lesions on PET with the exact same lymph nodes as analyzed after resection or cytological aspiration, it was decided to categorized all histopathological and PET findings into relevant anatomical regions. The regions were defined as follows: superficial or deep groin, para-iliacal, obturator, popliteal, supraclavicular, axillar, mediastinal, skeleton, back, neck, arm, calf and heel. PET and histological data from these areas were correlated and sensitivity and specificity were calculated. Therefore only regions with histopathological confirmation were analyzed for accuracy.

Per anatomical region all positive lymph nodes were measured in mm and the mitotic rate of the lymph node with the highest proliferation was calculated to estimate the detection level of FLT-PET.

The results of clinical staging (pre-surgery), staging with FLT-PET (pre-surgery) and pathological staging (post-surgery) were compared.

## Results

### *FLT Distribution in patients*

Ten patients were included. Patient and primary melanoma characteristics are shown in Table 1.

Patients received a median of 400 (185-430) MBq FLT. Intense FLT uptake was observed in the skeleton, with a distribution pattern that is typical for bone marrow uptake (Figure 1). Also the liver shows avid uptake. Minor uptake is observed in intestinal structures. All other organs and tissues show low grade and homogeneous uptake. No activity is present in the brain.

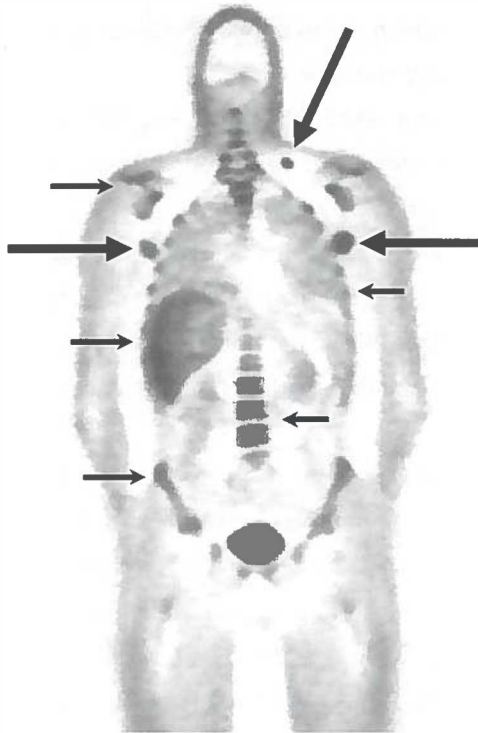
In all patients one or more abnormal lesions were found using FLT PET. Patient based sensitivity therefore was 100%.

**Table 1. Patient Characteristics**

Patient	Age	Sex	Clark Level	Breslow Thickness (mm)	Locoregional Disease
1.	48	Female	*	*	Groin
2.	39	Female	IV	1,8	Groin
3.	42	Male	IV	4,1	Axilla
4.	73	Male	IV	4,4	Groin
5.	78	Male	IV	1	Groin
6.	34	Male	**	6	Axillas
7.	40	Male	IV	1,35	Axilla
8.	29	Male	*	*	Groin
9.	40	Female	III	0,7	Axilla
10.	54	Male	**	>4	Groin

\* Unknown primary. \*\*Primary melanoma too small to assess Clark level.

**FIGURE 1.**



FLT-PET of 34 year male (Pt 6) 2 months after resection of the primary melanoma on his back. Metastases can be observed in his left and right axilla and left supraclavicular area and are indicated by large arrows. Physiological uptake can be observed in liver and one marrow e.g. in the pelvis, vertebrae, ribs, and bony structures of the shoulder; indicated by small arrows; less intense, uniform tracer uptake was present in the lungs. Uptake of the tracer in the brain was negligible and no uptake was observed in the mediastinum and myocardium.

### ***Region based analysis***

Twenty-two true positive, 3 true negative, 3 false negative and 2 false positive regions were observed, resulting in pathological proven sensitivity of 88% (Table 2). There were 3 true negative and 2 false positive lesions.

Two of the three false negative results were caused by multiple cutaneous and subcutaneous malignant lesions (satellite or primary lesions) located on the back of 2 patients, with diameters ranging from 1 to 10 mm and mitotic rate ranging from 5 to 16 per 2 mm<sup>2</sup> (Table 3). The other false negative result was caused by a micrometastasis in a lymph node in the groin.

One of the two false positive lesions was located in the groin, but no positive lymph nodes were found after resection of the groin area. The other false positive lesion was located in the heel. This was the location of the primary melanoma, which was resected in toto 4 years earlier and is still clinically negative.

The three true negative regions, which displayed very little or no FLT-uptake were one region with negative lymph nodes after resection and two resected benign skin lesions; one located on the calf and one on the arm.

At the lesion level, analysis of tumor size and mitotic rate of metastatic lymph nodes, revealed that, the smallest detected lesion, consisted of three closely adjacent lymph nodes with in each lymph node a micrometastasis (<2mm). The detected lesion, with the lowest mitotic activity that was still detected, had a mitotic rate of 9 mitoses per 2 mm<sup>2</sup>.

In two of the above mentioned true positive lesions, FLT-PET detected malignancy, which was initially missed with conventional staging techniques. In both patients this had therapeutic consequences as either dissection or radiation therapy was now indicated, but no influence on staging. These lesions were found in patient 1 and 2. In patient 1, a lesion in the fossa poplitea was indicated as malignant by FLT-PET and was confirmed on ultrasound guided aspiration cytology. The patient underwent a groin dissection and a resection of the popliteal lesion. In the supraclavicular region of patient 2, an additional lesion was detected, which was confirmed by ultrasound guided aspiration cytology. This patient received radiation therapy for locoregional control.

**Table 2. Cross table of FLT-PET regions compared with histopathological regions**

	FLT +	FLT -
Histopathology +	22	3
Histopathology -	2	3

Sensitivity=88%; specificity=60%.

***Additional lesions***

Eleven previously unknown lesions were present on FLT-PET (Table 3). These were not histopathological confirmed, but analyzed with conventional staging techniques. Five lesions were true positive when compared with CT or physical examination. Two



mediastinal and two para-aortal lesions were confirmed as metastases (>1cm); one lesion in the supraclavicular lesion was confirmed on physical examination.

Four of these 11 unknown lesions were true negative based on a completely normal CT scan or clinical follow-up. One mediastinal and one para-aortal lesion were negative on CT (<1cm). Two lesions in the head and neck area were confirmed to be clinically negative as well during clinical follow-up.

Finally, two lesions detected by FLT-PET and interpreted as malignant, could not be evaluated. The lesion in patient 2, which was interpreted as benign was located in a lumbar vertebra, which was below the level of the CT-scan. The bone scan, which was performed 2.5 months later showed multiple lesions in the spine. It can be assumed that these lesions were already present at the time of the FLT-PET. The remaining lesion in patient 5, was located in the area of popliteal lymph nodes of the involved leg next to a vascular prosthesis. However, recently this patient developed brain metastases, for which he was palliatively treated. During a follow-up of period of 3 months, this lesion remained clinical negative. Although the above mentioned two lesions were not confirmed by histopathology, it can be assumed that these two lesions were malignant, since these patients developed disseminated disease within 12 weeks.

There were four lesions, which were missed on FLT-PET without histopathological evaluation (Table 3). These four lesions were false negative on FLT-PET when compared with CT. Three of these lesions were interpreted as mediastinal lymph node metastases (>1cm) on CT and one a bone metastasis in a thoracic vertebra on CT.

**Table 3. False negative, false positive and additional FLT-PET findings**

Location	# of lesions	PA	Result	Diagnostics
deep groin	1	pos	FN	Aspiration cytology
dermal or subcutaneous metastases on the back	9	pos	FN	Histopathology
back (primary tumor)	1	pos	FN	Histology
deep groin	1	neg	FP	Histopathology
leg (heel)	1	neg	FP	Re-resection in 1998 negative and clinical negative, follow-up of 5 years
mediastinal	3	NP	FN	CT
thoracic vertebra	1	NP	FN	CT
lumbar vertebra	1	NP	NA	bone scan with multiple bone metastases (also spinal) 2.5 months after PET
fossa poplitea	1	NP	NA	Clinical negative, follow-up of 4 months
mediastinal	1	NP	TN	CT
para-aortal	1	NP	TN	CT
head and neck	2	NP	TN	Clinical negative, follow-up of 3 months
mediastinal	2	NP	TP	CT
para-aortal	2	NP	TP	CT
supraclavicular	1	NP	TP	Physical examination

FN=false negative; FP=false positive; NA=not assessable; neg=negative; NP=not performed; pos=positive; TN=true negative; TP=true positive.

### ***Effect of FLT-PET on staging***

FLT-PET detected the extent of the locoregional disease correctly in all patients (Table 4). The clinical (pre-surgery), FLT-PET and pathologic (post-surgery) staging were compared. All patients were clinically stage III. However, one patient was upstaged to stage IV both by CT and FLT-PET, as both modalities detected mediastinal metastases. Another patient was upstaged by FLT-PET as compared with the clinical pre-surgery staging, which was confirmed by CT. The detected metastases, which caused the upstaging in the second patient, were located in para-aortal (lymphatic) region.

**Table 4. Staging**

Patient	Clinical staging			PET staging			Pathological staging			
	T	N	Stage	N	M	Stage	T	N <sup>†</sup>	M	Stage
1.	*	+	III	+	0	III	*	p2b	0	IIIB
2.	2a	+	III	+	1	IV	2a	p3	1c	IV
3.	4b	+	III	+	0	III	4b	p3	0	IIIC
4.	4b	+	III	+	1	IV	4b	p3	1c	IV
5.	1a	+	III	+	0	III	1a	p3	0	IIIC
6.	4b	+	III	+	0	III	4b	p3	0	IIIC
7.	2a	+	III	+	0	III	2a	p1b	0	IIIB
8.	*	+	III	+	0	III	*	p3	0	IIIC
9.	1a	+	III	+	0	III	1a	p1b	0	IIIB
10.	4b	+	III	+	0	III	4b	p3	0	IIIC

\*Unknown primary. +=positive lymph nodes on physical or cytological examination. †All patients had loco-regional lesions visualized by FLT-PET.

## Discussion

The study shows the feasibility of FLT-PET in the visualization of locoregional metastasized melanoma, as well as metastatic disease.

In ten patients, FLT-PET was compared with the histopathological results of the locoregional lymph nodes. All available resected tissue samples and lesions on FLT-PET were categorized in anatomical regions and were compared. The sensitivity was 88% and specificity 60%, based on 3 true negative and 2 false positive lesions. Due to the low number of false positive and true negative lesions, the specificity is less reliable. FLT-PET detected all locoregional metastases. Analyzing the effect of FLT on tumor stage, 2 (20%) of patients could be upstaged. However, also CT generated this upstaging.

The detection limit for lymph node metastases was lower than for the in-transit metastases. All in-transit metastases were below the detection limit of lymph node metastases of approximately 6 mm (3 lesions with micrometastases <2mm) and below detection limit of mitotic rate 9 per 2 mm<sup>2</sup> of FLT-PET. All in-transit metastases had a diameter of 1-10 mm and a mitotic rate of 5-10 per 2 mm<sup>2</sup>. Taken the detection limit into account, sensitivity of FLT-PET increased to 90% when compared with histopathologically examined samples only. Comparing FLT with FDG, the detection limit of FDG-PET for lymph nodes with melanoma metastases also depends on tumor volume and imaging equipment and technique (11-14,27-31). A tumor volume larger than 78 mm<sup>3</sup> is needed for

a sensitivity higher than 90% or a diameter of at least 6 mm for a sensitivity higher than 83% (11,31). These FDG data are in the same range as our FLT findings.

The role of FDG-PET for detecting melanoma has been evaluated extensively over the last decade. For staging patients with stage I and II melanoma, the sentinel node biopsy will remain the method of choice (5,28). FDG-PET can be of value in stage III and IV, or for patients with recurrent melanoma (10,32). In the literature there is a large variation in sensitivity and specificity of FDG-PET for the detection of melanoma metastases. A recent review by Mijnhout et al showed a sensitivity and specificity for the detection of melanoma metastases with of FDG-PET of respectively 79%(95%CI 66-93%) and 86%(95%CI 78-95%) (13). Recent reports show comparable results (10,24,32,33). FDG-PET displays false negative findings caused by small skin metastases or primary small skin lesions of melanoma as well (32,33). The cutaneous and subcutaneous lesions, which were missed by FDG-PET had a diameter between 1 and 10 mm (33). When comparing these figures with the performance of FLT-PET, FLT-PET appears to be equally accurate as FDG-PET and has the same detection limit (32).

In this study no patient had brain or liver metastases. The detection of liver metastases by FLT-PET could be disturbed by the physiological uptake in the liver. However, brain metastases could be detected, since there is no physiological uptake of FLT in the brain and FLT-PET has been able to detect brain tumors (19,34,35).

## **Conclusion**

The results of this study indicate that FLT-PET could be a new method for staging melanoma patients with stage III and probably also for investigating the extent of stage IV disease. The question whether FLT-PET or FDG-PET performs best in the staging stage III melanoma patients remains to be answered.

## References

1. Nabi HA, Zubeldia JM. Clinical applications of (18)F-FDG in oncology. *J Nucl Med Technol.* 2002; 30: 3-9.
2. Herholz K, Rudolf J, Heiss WD. FDG transport and phosphorylation in human gliomas measured with dynamic PET. *J Neurooncol.* 1992; 12: 159-165.
3. Som P, Atkins HL, Bandyopadhyay D, et al. A fluorinated glucose analog, 2-fluoro-2-deoxy-D-glucose (F-18): nontoxic tracer for rapid tumor detection. *J Nucl Med.* 1980; 21: 670-675.
4. Wahl RL, Hutchins GD, Buchsbaum DJ, Liebert M, Grossman HB, Fisher S. 18F-2-deoxy-2-fluoro-D-glucose uptake into human tumor xenografts. Feasibility studies for cancer imaging with positron-emission tomography. *Cancer.* 1991; 67: 1544-1550.
5. Cobben DC, Koopal S, Tiebosch AT, et al. New diagnostic techniques in staging in the surgical treatment of cutaneous malignant melanoma. *Eur J Surg Oncol.* 2002; 28: 692-700.
6. Gershenwald JE, Thompson W, Mansfield PF, et al. Multi-institutional melanoma lymphatic mapping experience: the prognostic value of sentinel lymph node status in 612 stage I or II melanoma patients. *J Clin Oncol.* 1999; 17: 976-983.
7. Morton DL, Wen DR, Wong JH, et al. Technical details of intraoperative lymphatic mapping for early stage melanoma. *Arch Surg.* 1992; 127: 392-399.
8. Morton DL, Thompson JF, Essner R, et al. Validation of the accuracy of intraoperative lymphatic mapping and sentinel lymphadenectomy for early-stage melanoma: a multicenter trial. Multicenter Selective Lymphadenectomy Trial Group. *Ann Surg.* 1999; 230: 453-463.
9. Belhocine T, Pierard G, De Labrassinne M, Lahaye T, Rigo P. Staging of regional nodes in AJCC stage I and II melanoma: 18FDG PET imaging versus sentinel node detection. *Oncologist.* 2002; 7: 271-278.
10. Tyler DS, Onaitis M, Kherani A, et al. Positron emission tomography scanning in malignant melanoma. *Cancer.* 2000; 89: 1019-1025.
11. Wagner JD, Schauwecker DS, Davidson D, Wenck S, Jung SH, Hutchins G. FDG-PET sensitivity for melanoma lymph node metastases is dependent on tumor volume. *J Surg Oncol.* 2001; 77: 237-242.
12. Schwimmer J, Essner R, Patel A, et al. A review of the literature for whole-body FDG PET in the management of patients with melanoma. *Q J Nucl Med.* 2000; 44: 153-167.
13. Mijnhout GS, Hoekstra OS, van Tulder MW, et al. Systematic review of the diagnostic accuracy of (18)F-fluorodeoxyglucose positron emission tomography in melanoma patients. *Cancer.* 2001; 91: 1530-1542.
14. Belhocine T, Pierard G, De Labrassinne M, Lahaye T, Rigo P. Staging of regional nodes in AJCC stage I and II melanoma: 18FDG PET imaging versus sentinel node detection. *Oncologist.* 2002; 7: 271-278.
15. Kubota R, Yamada S, Kubota K, Ishiwata K, Tamahashi N, Ido T. Intratumoral distribution of fluorine-18-fluorodeoxyglucose in vivo: high accumulation in macrophages and granulation tissues studied by microautoradiography. *J Nucl Med.* 1992; 33: 1972-1980.
16. Yamada Y, Uchida Y, Tatsumi K, et al. Fluorine-18-fluorodeoxyglucose and carbon-11-methionine evaluation of lymphadenopathy in sarcoidosis. *J Nucl Med.* 1998; 39: 1160-1166.
17. Langen KJ, Braun U, Rota KE, et al. The influence of plasma glucose levels on fluorine-18-fluorodeoxyglucose uptake in bronchial carcinomas. *J Nucl Med.* 1993; 34: 355-359.

18. Mier W, Haberkorn U, Eisenhut M.  $[(18)F]FLT$ ; portrait of a proliferation marker. *Eur J Nucl Med.* 2002; 29: 165-169.
19. Shields AF, Grierson JR, Dohmen BM, et al. Imaging proliferation in vivo with  $[F-18]FLT$  and positron emission tomography. *Nat Med.* 1998; 4: 1334-1336.
20. Sherley JL, Kelly TJ. Regulation of human thymidine kinase during the cell cycle. *J Biol Chem.* 1988; 263: 8350-8358.
21. Machulla HJ, Blochter A, Kuntzsch M, Piert M, Wei R, Grierson JR. Simplified labeling approach for synthesizing 3'-deoxy-3'- $[^{18}F]$ fluorothymidine ( $[^{18}F]FLT$ ). *Journal of Radiochemical and Nuclear Chemistry.* 2000; 243: 843-846.
22. Schelbert HR, Hoh CK, Royal HD, et al. Procedure guideline for tumor imaging using fluorine-18-FDG. *J Nucl Med.* 1998; 39: 1302-1305.
23. Lonneux M, Borbath I, Bol A, et al. Attenuation correction in whole-body FDG oncological studies: the role of statistical reconstruction. *Eur J Nucl Med.* 1999; 26: 591-598.
24. Balch CM, Buzaid AC, Soong SJ, et al. Final version of the American Joint Committee on Cancer staging system for cutaneous melanoma. *J Clin Oncol.* 2001; 19: 3635-3648.
25. Buck AK, Schirrmeister H, Hetzel M, et al. 3-deoxy-3- $[(18)F]$ fluorothymidine-positron emission tomography for noninvasive assessment of proliferation in pulmonary nodules. *Cancer Res.* 2002; 62: 3331-3334.
26. Vesselle H, Grierson J, Muzi M, et al. In vivo validation of 3'-deoxy-3'- $[(18)F]$ fluorothymidine ( $[(18)F]FLT$ ) as a proliferation imaging tracer in humans: correlation of  $[(18)F]FLT$  uptake by positron emission tomography with Ki-67 immunohistochemistry and flow cytometry in human lung tumors. *Clin Cancer Res.* 2002; 8: 3315-3323.
27. Wagner JD, Schauwecker D, Davidson D, et al. Prospective study of fluorodeoxyglucose-positron emission tomography imaging of lymph node basins in melanoma patients undergoing sentinel node biopsy. *J Clin Oncol.* 1999; 17: 1508-1515.
28. Mijnhout GS, Hoekstra OS, Van Lingen A, et al. How morphometric analysis of metastatic load predicts the (un)usefulness of PET scanning: the case of lymph node staging in melanoma. *J Clin Pathol.* 2003; 56: 283-286.
29. Macfarlane DJ, Sondak V, Johnson T, Wahl RL. Prospective evaluation of 2- $[18F]$ -2-deoxy-D-glucose positron emission tomography in staging of regional lymph nodes in patients with cutaneous malignant melanoma. *J Clin Oncol.* 1998; 16: 1770-1776.
30. Acland KM, Healy C, Calonje E, et al. Comparison of positron emission tomography scanning and sentinel node biopsy in the detection of micrometastases of primary cutaneous malignant melanoma. *J Clin Oncol.* 2001; 19: 2674-2678.
31. Crippa F, Leutner M, Belli F, et al. Which kinds of lymph node metastases can FDG PET detect? A clinical study in melanoma. *J Nucl Med.* 2000; 41: 1491-1494.
32. Prichard RS, Hill AD, Skehan SJ, O'Higgins NJ. Positron emission tomography for staging and management of malignant melanoma. *Br J Surg.* 2002; 89: 389-396.
33. Stas M, Stroobants S, Dupont P, et al. 18-FDG PET scan in the staging of recurrent melanoma: additional value and therapeutic impact. *Melanoma Res.* 2002; 12: 479-490.
34. Dohmen BM, Shields AF, Grierson JR, et al.  $[^{18}F]FLT$ -PET in brain tumors; [abstract]. *J Nucl Med.* 2000; 41(suppl): 216P.

35. Bendaly EA, Sloan AE, Dohmen BM, et al. Use of  $^{18}\text{F}$ -FLT-PET to assess the metabolic activity of primary and metastatic brain tumors [abstract]. *Journal of Nuclear Medicine*. 2002; 43 (suppl): 111P.





## Chapter 5

### Selectivity of 3'-deoxy-3'-[<sup>18</sup>F]fluorothymidine (FLT) and 2-[<sup>18</sup>F]fluoro-2-deoxy-D-glucose (FDG) for tumor versus inflammation in a rodent model

Aren van Waarde<sup>1</sup>, David C.P.Cobben<sup>1</sup>, Albert J.H.Suurmeijer<sup>2</sup>, Bram Maas<sup>1</sup>, Willem Vaalburg<sup>1</sup>, Erik F.J. de Vries<sup>1</sup>, Pieter L. Jager<sup>1</sup>, Harald J. Hoekstra<sup>3</sup> and Philip H.Elsinga<sup>1</sup>

<sup>1</sup>PET Center, <sup>2</sup>Department of Pathology and Laboratory Medicine and <sup>3</sup>Department of Surgical Oncology (HJH), Groningen University Hospital, P.O.Box 30001, 9700 RB Groningen, The Netherlands.

*Journal of Nuclear Medicine – in press*

## Summary

Increased glucose metabolism of inflammatory tissues is the main source of false positive 2-[<sup>18</sup>F]fluoro-2-deoxy-D-glucose (FDG)-PET findings in oncology. It has been suggested that radiolabeled nucleosides could be more tumor-specific. To test this hypothesis, we compared the biodistribution of 3'-deoxy-3'-[<sup>18</sup>F]fluorothymidine (FLT) and FDG in Wistar rats, which were tumor-bearing (C6 rat glioma in the right shoulder) and also had a sterile inflammation in the left calf muscle (induced by injection of 0.1 ml turpentine). Twenty-four hours after turpentine injection, the rats received an intravenous bolus (30 MBq) of either [<sup>18</sup>F]FLT (n=5) or [<sup>18</sup>F]FDG (n=5). It proved necessary to pretreat the animals with thymidine phosphorylase (> 1000 U/kg, i.v.), before injection of FLT to reduce the serum levels of endogenous thymidine, in order to acquire satisfactory tumor uptake of radioactivity. Tumor/muscle ratios of FDG at 2 h post injection ( $13.2 \pm 3.0$ ) were higher than those of FLT ( $3.8 \pm 1.3$ ). FDG showed a high physiological uptake in brain and heart, whereas FLT was avidly taken up by bone marrow. FDG accumulated in the inflamed muscle, with  $4.8 \pm 1.2$  times higher uptake in the affected thigh than in the contralateral healthy thigh, in contrast to FLT for which this ratio was not significantly different from unity ( $1.3 \pm 0.4$ ). In FDG-PET images, tumor and inflammation were both visible, but FLT-PET showed only the tumor. Thus, the hypothesis of a higher tumor specificity of FLT was confirmed in our animal model.

## Introduction

2- $^{18}\text{F}$ Fluoro-2-deoxy-D-glucose (FDG) is currently the most widely used radiopharmaceutical in clinical oncology. This analog of glucose is trapped in tissues after phosphorylation by hexokinase, but is not a substrate for glycolysis. Although the applications of FDG-PET in tumor detection, staging and therapy evaluation are rapidly expanding, FDG uptake is not tumor-specific. Various forms of inflammatory lesions also take up FDG and are a major cause of false positive results. Histological confirmation of FDG-positive lesions is therefore required in many types of tumors.(3,6,1,2,5,4) Macrophages, which invade tumors, especially after anticancer therapy, can induce high FDG uptake as well and can complicate the interpretation of FDG-PET.(9,8,1,7) A decreased uptake of FDG is seen in hyperglycemic patients which can cause false negative results.

Another approach for tumor visualisation is the use of radiolabeled nucleosides such as  $^{11}\text{C}$ thymidine. Since  $^{11}\text{C}$ thymidine is rapidly incorporated in newly synthesized DNA, this radiopharmaceutical can be used to image cellular proliferation. Animal and *in vitro* studies have suggested that thymidine shows considerable uptake in malignant tissue but much less uptake in inflammatory cells than FDG.(11,10) Unfortunately, the imaging quality of  $^{11}\text{C}$ thymidine is relatively poor and its clinical applications are limited, owing to rapid *in vivo* degradation and the short half-life of  $^{11}\text{C}$  (20 min).(14,12,13)

However, the pyrimidine analogue 3'-deoxy-3'-fluorothymidine (FLT) can be labeled with  $^{18}\text{F}$  (half-life 109.8 min) and is resistant to metabolic breakdown.(15) FLT is transported by the same nucleoside carrier as thymidine and is also phosphorylated by the same enzyme, S-phase-specific thymidine kinase 1, which leads to intracellular trapping of radioactivity within the cytosol.(21,20,16,17,18,19) In contrast to thymidine, FLT remains in the cytosolic fraction as FLT-monophosphate and acts as a DNA chain terminator because of the 3' substitution (17). Thus, only a very small DNA incorporation of FLT has been observed in cell lines.(18)

Although inflammatory cells display a high metabolic activity and an avid uptake of FDG, they are recruited from elsewhere and do not divide at the site of inflammation. Since the mitotic activity of inflammatory cells is low, these cells can be expected to show a relatively low uptake of radiolabeled nucleosides. Thus, FLT may overcome one major drawback of FDG imaging.

To the best of our knowledge, no reports have appeared in the literature in which the selectivity of FDG and FLT for tumor and inflammation was compared. Therefore, we decided to examine the biodistribution of these radiopharmaceuticals in male Wistar rats which were tumor-bearing and also had a sterile inflammation. The inflammation was induced by injection of turpentine, which is known to result in exudation of plasma and migration of neutrophils within 24 hours.(22)

## **Materials and methods**

### ***Materials***

[<sup>18</sup>F]FLT was produced by radiofluoridation of the 2,3'-anhydro-5'-O-(4,4'-dimethoxytrityl)-thymidine precursor, with radiochemical yields of 5-10 %. [<sup>18</sup>F]FDG was produced by the Hamacher method (nucleophilic fluorination reaction followed by deprotection). The specific radioactivities of [<sup>18</sup>F]FLT and [<sup>18</sup>F]FDG were always > 10 (usually 50-100) TBq/mmol. Thymidine phosphorylase (from the bacterium *Escherichia coli*) was obtained from Sigma (St.Louis, MO, USA). Matrigel<sup>®</sup> Basement Membrane Matrix was purchased from BD Biosciences (Bedford, MA, USA). Turpentine came from a local paint shop.

### ***Animal model***

The experiments were performed by licensed investigators in accordance with the Law on Animal Experiments of The Netherlands. Male Wistar rats (200-240 g body weight) were obtained from Harlan (Lelystad, The Netherlands). After one week of acclimation, C6 glioma cells ( $2 \times 10^6$ , in a 1:1 v/v mixture of Matrigel<sup>®</sup> and Dulbecco's Minimal Essential Medium containing 5% fetal calf serum) were subcutaneously injected on the right shoulder. Matrigel<sup>®</sup> was included to avoid migration of tumor cells to other sites than the place of injection. Ten days later, 0.1 ml of turpentine was intramuscularly injected into the thigh of the left hindleg. After an additional 24 hours, the radiopharmaceutical (either FDG or FLT) was intravenously administered (tail vein).

### ***Phosphorylase pretreatment***

In order to reduce the serum levels of endogenous thymidine, five rats were pretreated with thymidine phosphorylase (1000-1500 U/kg body weight), 45 min before

injection of the radiopharmaceutical FLT. The enzyme was administered by intravenous infusion via a tail vein. As phosphorylase is supplied in potassium phosphate buffer, a very slow rate of infusion was used (less than 50  $\mu$ l per minute, total volume 0.6-1.0 ml) to avoid myocardial arrest. Plasma thymidine was measured using reversed-phase HPLC (24,23).

### ***Biodistribution experiments***

Twenty-four hours after the turpentine injection, the rats were anesthetized using (S)-ketamine (Ketanest<sup>R</sup>, 50 mg/kg i.p.) and medetomidine (Domitor<sup>R</sup>, 0.3 mg/kg i.p.). Animals were kept under anesthesia for the rest of the experiment. A bolus of either [<sup>18</sup>F]FLT or [<sup>18</sup>F]FDG (0.3 ml containing 30 MBq) was administered by intravenous injection into a lateral tail vein. The rats were sacrificed 120 min after radiotracer injection by extirpation of the heart (under general ketamine/ medetomidine anesthesia). Blood was collected and normal tissues (brain, fat, bone, heart, intestines, kidney, liver, lung, skeletal muscle, pancreas, spleen, submandibular gland and urinary bladder) were excised. Urine was collected and plasma plus a red cell fraction were obtained from blood centrifugation (5 min at 1000 g). The complete tumor was excised and carefully separated from muscle and skin. Inflamed muscle was recognisable by its pale color and could generally be distinguished from the surrounding darker tissue. A relatively small sample including the inflamed region ( $0.71 \pm 0.32$  grams) was excised from the affected thigh. All samples were weighed, and the radioactivity was measured using a LKB-Wallac Compugamma<sup>R</sup> CS 1282 counter (LKB, Bromma, Sweden, Wallac Oy, Turku, Finland), applying a decay correction. The results were expressed as dimensionless standard uptake values (dpm measured per g of tissue/dpm injected per g of body weight). Tissue/plasma and tumor/muscle concentration ratios of radioactivity were also calculated.

### ***Histological examination of inflamed muscle and C6 tumors***

Excised tumors and the inflamed parts of the thigh muscle were fixed in formalin and embedded in paraffin. Five  $\mu$ m-sections were stained with hematoxylin and eosin.

### ***PET imaging***

Ketamine/medetomidine-anesthetized rats were placed into a positron camera (Siemens ECAT 962/HR+, FWHM is 4.5 mm) and received a bolus injection of either

[<sup>18</sup>F]FLT or [<sup>18</sup>F]FDG (30 MBq) via a tail vein. Data was acquired from 90-150 min. A zoom factor of 1.5 was applied during reconstruction (by filter-back projection) and the matrix size was 128 x 128.

### ***Statistical analysis***

Statistical analysis was performed using the software package Statistix (NH Analytical Software, Roseville MN, USA). Differences between the various groups (FLT, FLT with phosphorylase pretreatment, FDG) were tested for statistical significance using the two-sided Student t-test for independent samples. P-values < 0.05 were considered significant.

## **Results**

### ***Development of tumor and inflammation***

The growth rate of C6 tumors in Wistar rats proved to be variable. Tumor mass at radiotracer injection was  $1.61 \pm 0.89$  grams (mean  $\pm$  SD, range 0.41 to 2.97 grams). Turpentine injection resulted in visible swelling of the inflamed thigh after 24 hours, although behavior of the rats during this period was normal. Body weight of the animals during the biodistribution experiments was  $325 \pm 27$  grams.

### ***FLT uptake in untreated rats***

In initial experiments on three rats, the radiopharmaceutical FLT was administered directly to the animals without any pretreatment. To our surprise, the nucleoside was not accumulated in any organ above plasma levels with the exception of bone marrow, small intestine, kidney and urinary bladder (Table 1). Even the C6 tumors did not accumulate radioactivity (Table 2). High serum levels of endogenous thymidine may have saturated tissue nucleoside transporters or thymidine kinase 1, and have blocked uptake or trapping of FLT. Drs A.F.Shields (Karmanos Cancer Institute, Detroit, MI), P.S.Conti and J.Bading (University of Southern California, Los Angeles) suggested to infuse thymidine phosphorylase before injection of FLT to circumvent this problem. The next five rats were pretreated in this way; the radiolabeled nucleoside was administered 45 min after the start of enzyme infusion. Data of untreated animals were compared to those in the thymidine phosphorylase-pretreated group.

**Table 1. Standard Uptake Values at 120 min post injection**

Tissue	FLT Untreated (n=3)	FLT + phosphorylase (n=5)	FDG (n=5)	Effect phosphorylase on FLT uptake	FLT + phosphorylase vs. FDG
Cerebellum	0.06 ± 0.01	0.04 ± 0.02	1.23 ± 0.29	NS	< 0.001
Cortex	0.05 ± 0.01	0.04 ± 0.02	1.86 ± 0.45	NS	< 0.001
Rest brain	0.06 ± 0.01	0.04 ± 0.02	1.45 ± 0.33	NS	< 0.001
Adipose tissue	0.14 ± 0.16	0.03 ± 0.02	0.09 ± 0.04	NS	< 0.05
Urinary bladder	0.74 ± 0.49	1.57 ± 0.68	1.65 ± 0.92	NS	NS
Bone	0.19 ± 0.03	1.18 ± 0.67	0.35 ± 0.11	0.06	0.09
Bone marrow	1.04 ± 0.54	6.67 ± 2.53	1.55 ± 0.41	< 0.02	< 0.05
Heart	0.46 ± 0.20	0.26 ± 0.15	5.84 ± 3.29	NS	< 0.02
Large intestine	0.54 ± 0.25	0.55 ± 0.16	1.37 ± 0.32	NS	0.001
Small intestine	1.08 ± 0.45	1.28 ± 0.58	1.10 ± 0.23	NS	NS
Kidney	2.28 ± 0.69	1.19 ± 0.49	1.89 ± 0.43	0.06	< 0.05
Liver	0.61 ± 0.28	0.39 ± 0.20	0.51 ± 0.11	NS	NS
Lung	0.46 ± 0.16	0.34 ± 0.19	1.15 ± 0.26	NS	0.0005
Muscle	0.42 ± 0.15	0.29 ± 0.09	0.18 ± 0.06	NS	0.05
Pancreas	0.41 ± 0.21	0.26 ± 0.12	0.32 ± 0.05	NS	NS
Plasma	0.58 ± 0.25	0.31 ± 0.15	0.43 ± 0.17	NS	NS
Red blood cells	0.55 ± 0.21	0.31 ± 0.15	0.31 ± 0.09	NS	NS
Spleen	0.56 ± 0.20	1.16 ± 0.63	1.64 ± 0.42	NS	NS
Submandibular gland	0.31 ± 0.11	0.34 ± 0.17	1.18 ± 0.30	NS	< 0.001
C6 tumor	0.55 ± 0.06	1.14 ± 0.62	2.34 ± 0.72	NS	< 0.05
Inflammation	0.51 ± 0.18	0.37 ± 0.16	0.82 ± 0.14	NS	< 0.002
Urine	12.6 ± 2.0	16.3 ± 12.4	9.0 ± 2.0	NS	NS

NB The bone sample contained marrow, thus bone uptake does not reflect defluorination. NS=not significant.

### **FLT uptake after pretreatment**

Pretreatment of animals with thymidine phosphorylase (i.v., 45 min before administration of the radiotracer) did not affect tissue/plasma ratios of FLT in brain, adipose tissue, urinary bladder, heart, kidney, liver, lung, normal and inflamed skeletal muscle, pancreas and red blood cells. However, infusion of the enzyme increased the accumulation of FLT in bone, bone marrow and the C6 tumor (Table 1 and 2). Plasma levels of radioactivity tended to be decreased after phosphorylase infusion. Thus, tissue/plasma ratios of radioactivity were significantly increased in bone, bone marrow, intestines, tumor, spleen and submandibular gland (values not shown in Table 1). Tumor/muscle ratios of radioactivity were also significantly increased after phosphorylase treatment (Table 2). Plasma levels of thymidine were measured in a parallel experiment on a single rat and were found to decrease from 0.15 µg/ml to undetectable levels after phosphorylase infusion.

**Table 2. Tissue/plasma and tissue/muscle ratios besides selectivity index (tumor vs. inflammation)**

Parameter	FLT	FLT +	FDG	Effect	FLT +
	untreated	phosphorylase			phosphorylase
	(n=3)	(n=5)	(n=5)		vs. FDG
Tumor/plasma	1.0 ± 0.4	3.8 ± 1.4	6.1 ± 2.7	< 0.05	NS
Tumor/muscle	1.4 ± 0.4	3.8 ± 1.3	13.2 ± 3.0	0.05	0.001
Inflammation/ plasma	0.9 ± 0.1	1.2 ± 0.3	2.1 ± 0.8	NS	< 0.05
Inflammation/ muscle	1.2 ± 0.0	1.3 ± 0.4	4.8 ± 1.2	NS	0.0002
Selectivity index*	1.8 ± 1.7	> 10.6**	3.5 ± 1.2		

\*Defined as (tumor uptake – muscle uptake)/(inflammation uptake – muscle uptake), i.e. tumor/inflammation ratio corrected for background. \*\*Standard deviation cannot be given since in some animals, tracer uptake in inflamed and healthy contra lateral muscles was equal.

### **Biodistribution of FDG and FLT**

The next five animals received FDG rather than FLT, in order to compare the biodistribution of both radiopharmaceuticals. The glucose analogue FDG showed physiological uptake in heart and brain. FDG showed higher uptake than FLT in C6 tumors, inflamed muscle, brain, adipose tissue, kidney, large intestine, lung, and submandibular gland (Table 1). In contrast, FLT accumulated more in bone, bone marrow and healthy muscle than FDG (Table 1).



### ***Selectivity of FDG and FLT***

FLT was not accumulated in inflammatory tissue (tissue/plasma and tissue/muscle ratios were not significantly different from unity). However, FDG accumulation in inflamed thigh muscle was 4.8-fold higher ( $p = 0.0002$ ) than in the non-inflamed contralateral thigh (Table 2). The selectivity index (tumor/inflammatory tissue ratio corrected for the uptake in healthy muscle) was  $> 10.6$  for FLT and 3.5 for FDG (Table 2).

Tumor/plasma ratios of FLT and FDG were not significantly different, but tumor/muscle ratios of FDG were significantly higher ( $p = 0.001$ ) than those of FLT (Table 2).

### ***Histology of inflamed muscle and C6 tumors***

Histological examination of the muscle specimens excised 24 hours after turpentine injection showed an acute inflammatory reaction. Massive infiltration of neutrophils was seen in and between partially necrotic muscle fibers, the picture of an acute myositis (Fig.1). In the border of the inflammatory infiltrate, macrophages and few fibroblasts could be discerned.

Histological examination of the excised C6 tumors showed the picture of a malignant mesenchymal tumor (Figure 2). Spindled tumor cells with pleomorphic, hyperchromatic nuclei were arranged in short bundles. Many mitoses were found (range 25-40 per 2 mm<sup>2</sup>). Small areas of tumor necrosis were seen, comprising less than 10 percent of the total tumor volume.

**Figure 1.**

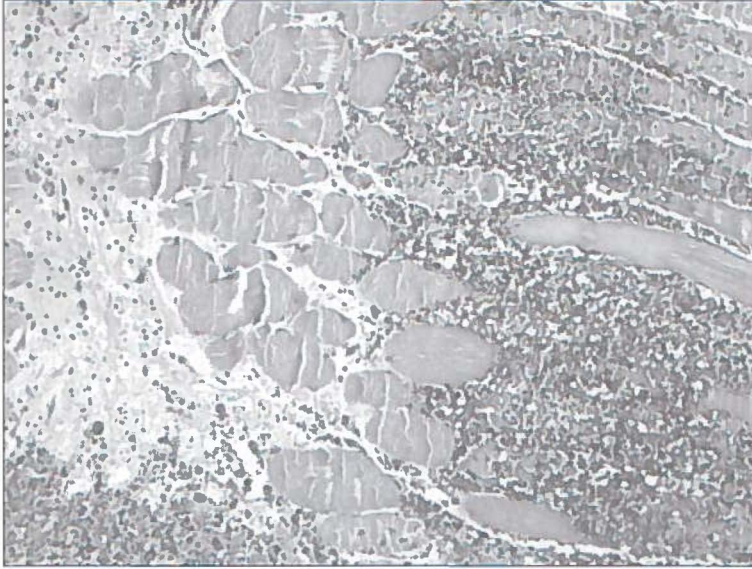


Figure 1. Microscopic image of a specimen of inflamed rat muscle, 24 hours after injection of turpentine.

**Figure 2.**

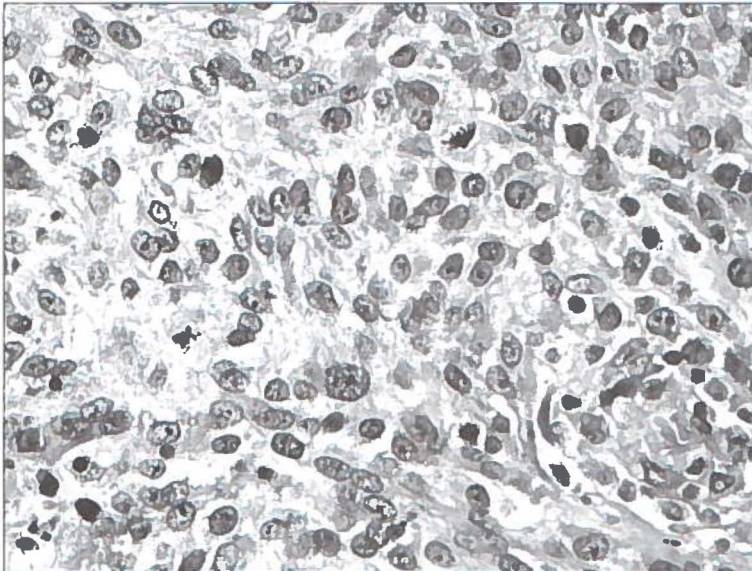


Figure 2. Microscopic image of a specimen of rat tumor, 11 days after inoculation of C6 cells. Histological examination of the excised C6 tumors showed the picture of a malignant mesenchymal tumor. Spindled tumor cells with pleomorphic, hyperchromatic nuclei were arranged in short bundles. Many mitoses were found (range 25-40 per  $2\text{ mm}^2$ ). Small areas of tumor necrosis were seen, comprising less than 10 percent of the total tumor volume.

### **PET images**

PET images of tumor- and inflammation-bearing rats, made with the two tracers, are shown in Figure 3. The head of the animals is at the right hand side of the picture, and the rats are seen from below. Both FLT and FDG clearly visualized the C6 tumor in the right shoulder. FDG showed high, physiological uptake in the brain, in contrast to FLT. The inflammation in the left hindleg was visualized with FDG, but not with FLT.

**Figure 3**

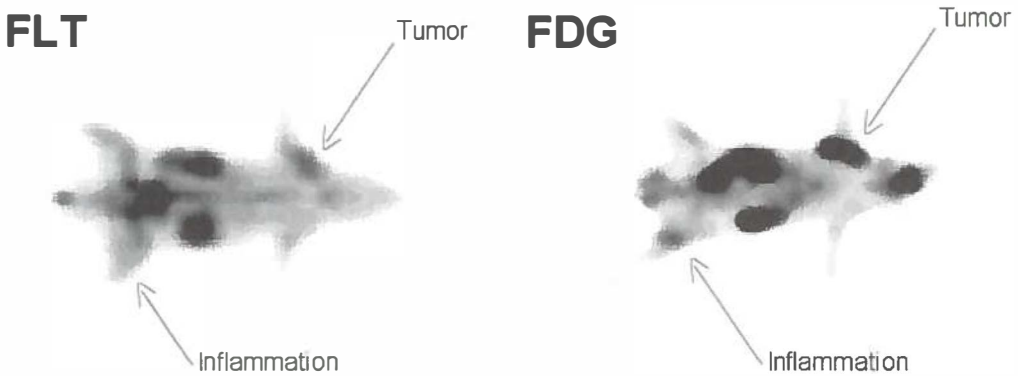


Figure 3. PET images of rats made with FLT and FDG. Note that FLT visualizes only the tumor, whereas both tumor and inflammation are visible after injection of FDG.

### **Discussion**

This study confirms that the standard uptake value of FLT in inflammatory tissue is lower than that of FDG (see Table 1 and Fig.3). Although the tumor uptake of FLT is also considerably lower than that of FDG (Table 1), the selectivity of FLT for tumor vs. inflammation is nevertheless higher than that of glucose analogue: 10.6- vs. 3.5-fold at 120 min post injection, when the data are corrected for background (Table 2). Thus, the hypothesis of a higher tumor specificity of FLT was confirmed in our animal model. Apparently radiolabeled nucleosides have similar advantages as radiolabeled amino acids regarding tumor specificity.<sup>23,24</sup>

Standard uptake values of FDG in C6 tumors were 2-fold higher than those of FLT. Tumor/muscle ratios of FDG ( $13.2 \pm 3.0$ ) were clearly superior to those of FLT ( $3.8 \pm 1.3$ ). These results are in accordance with clinical data from FDG and FLT-PET scans, where

colorectal cancers have been found to display a twofold higher uptake (SUV) of FDG than of FLT.<sup>25</sup>

However, FDG showed relatively poor selectivity for tumor versus inflammatory tissue. The inflamed thigh was clearly visualized in a PET image (Fig.3). Tissue uptake of FDG in inflamed muscle was 4.8-fold greater than in the healthy contralateral leg, and the selectivity index of FDG for tumor vs. inflammation was 3.5 (Table 2). Since only part of the volume of the inflamed muscle samples consisted of neutrophils and macrophages, FDG uptake in these inflammatory cells may have been > 10-fold greater than in normal muscle cells.

FLT showed better tumor selectivity than FDG in our model. The inflamed thigh showed similar tracer uptake as the healthy contralateral thigh in a PET image (Fig.3). Biodistribution studies indicated that FLT accumulation in inflamed muscle was not significantly different from that in non-inflamed tissue of the contralateral thigh (ratio  $1.3 \pm 0.4$ , see Table 2). The selectivity index of FLT for tumor vs. inflammation was 10.6 or greater (Table 2).

In Wistar rats, the glucose analogue showed a biodistribution as expected on the basis of clinical FDG-PET scans, i.e. high and physiological uptake in brain and heart, besides renal excretion and accumulation in the urine (Table 1). In contrast to FDG, FLT mainly accumulated in bone marrow (Table 1). Low levels of radioactivity in the brain are probably due to the fact that FLT does not cross the intact blood-brain barrier.

The data presented in the Tables indicate that endogenous thymidine can have a strong effect on the *in vivo* uptake of FLT. Low tissue uptake of FLT in untreated rats is probably a consequence of high levels of endogenous thymidine in rodent serum<sup>26</sup>, since previous infusion of thymidine phosphorylase significantly increased uptake of the radiolabeled nucleoside in target organs (Table 1). Thymidine may compete with FLT for the active site of nucleoside carriers in cell membranes<sup>27</sup> and also for the active site of the trapping enzyme, thymidine kinase 1 (TK1). Affinity of human TK1 for thymidine has been reported to be 4-fold higher ( $0.5 \mu\text{M}$ ) than the affinity for FLT ( $2.1 \mu\text{M}$ )<sup>21</sup>

Apparently, substantial plasma concentrations of endogenous thymidine can result in suppression of FLT uptake in most tissues (Table 1). In contrast to rats, humans have much (9-16 fold) lower levels of serum thymidine ( $0.01\text{-}0.02$  vs.  $0.15\text{-}0.27 \mu\text{g/ml}$ ).<sup>26</sup> Therefore, FLT-PET scans of cancer patients show adequate image contrast.<sup>19,20,25,28,29</sup>

After infusion of a thymidine-degrading enzyme, physiological accumulation of FLT above plasma levels was observed in C6 tumors, bone, bone marrow, large and small intestine and spleen (Table 1). Many of these organs contain rapidly dividing tissue (malignant cells in the tumor, bone marrow in the skeleton, mucosa in the intestines). Thus, in pre-treated rats, FLT behaved as a tracer of cellular proliferation. This finding is in accordance with reports from the literature which suggest that there is a significant correlation between standardized uptake values of FLT and proliferative activity of various lesions.<sup>28,30,31</sup> *In vitro* studies have shown that FLT uptake is related to thymidine kinase-1 activity and the percentage of cells in S-phase.<sup>16,17</sup> FDG was accumulated in the same rapidly dividing tissues as FLT (Table 2) and showed even higher standard uptake values in tumor and large intestine.

## **Conclusion**

In our animal model, FLT visualized only the tumor, whereas FDG delineated both tumor and inflammation. Based on these animal data, FLT scans of oncological patients can be expected to have more false negatives (because of lower tumor uptake) and less false positives (because of negligible accumulation in granulocytes) than whole-body FDG scans.

## References

1. Lorenzen, J., de Wit, M., Buchert, R., Igel, B., and Bohuslavizki, K. H. Granulationsgewebe: Pitfall in der Therapiekontrolle mit F-18-FDG-PET nach Chemotherapie. *Nuklearmedizin*, 38: 333-336, 1999.
2. Shreve, P. D., Anzai, Y., and Wahl, R. L. Pitfalls in oncologic diagnosis with FDG PET imaging: physiologic and benign variants. *Radiographics*, 19: 61-77, 1999.
3. Strauss, L. G. Fluorine-18 deoxyglucose and false-positive results: a major problem in the diagnostics of oncological patients. *Eur.J.Nucl.Med.*, 23: 1409-1415, 1996.
4. Zhuang, H., Cunnane, M. E., Ghesani, N. V., Mozley, P. D., and Alavi, A. Chest tube insertion as a potential source of false-positive FDG-positron emission tomographic results. *Clin.Nucl.Med.*, 27: 285-286, 2002.
5. Kerrou, K., Montravers, F., Grahek, D., Younsi, N., Perniceni, T., Godeberge, P., Canuel, C., De Gramont, A., and Talbot, J. N. [<sup>18</sup>F]-FDG uptake in soft tissue dermatome prior to herpes zoster eruption: an unusual pitfall. *Ann.Nucl.Med.*, 15: 455-458, 2001.
6. Shreve, P. D. Focal fluorine-18 fluorodeoxyglucose accumulation in inflammatory pancreatic disease. *Eur.J.Nucl.Med.*, 25: 259-264, 1998.
7. Kaim, A. H., Weber, B., Kurrer, M. O., Gottschalk, J., von Schulthess, G. K., and Buck, A. Autoradiographic quantification of <sup>18</sup>F-FDG uptake in experimental soft-tissue abscesses in rats. *Radiology*, 223: 446-451, 2002.
8. Kubota, R., Kubota, K., Yamada, S., Tada, M., Ido, T., and Tamahashi, N. Microautoradiographic study for the differentiation of intratumoral macrophages, granulation tissues and cancer cells by the dynamics of fluorine-18-fluorodeoxyglucose uptake. *J.Nucl.Med.*, 35: 104-112, 1994.
9. Kubota, R., Yamada, S., Kubota, K., Ishiwata, K., Tamahashi, N., and Ido, T. Intratumoral distribution of fluorine-18-fluorodeoxyglucose in vivo: high accumulation in macrophages and granulation tissues studied by microautoradiography. *J.Nucl.Med.*, 33: 1972-1980, 1992.
10. Sugawara, Y., Gutowski, T. D., Fisher, S. J., Brown, R. S., and Wahl, R. L. Uptake of positron emission tomography tracers in experimental bacterial infections: a comparative biodistribution study of radiolabeled FDG, thymidine, L-methionine, <sup>67</sup>Ga-citrate, and <sup>125</sup>I-HSA. *Eur J Nucl Med*, 26: 333-341, 1999.
11. Wahl, R. L. and Fisher, S. J. A comparison of FDG, L-methionine and thymidine accumulation into experimental infections and reactive lymph nodes. *J.Nucl.Med.* 34, 104P. 1993.
12. Mankoff, D. A., Shields, A. F., Link, J. M., Graham, M. M., Muzi, M., Peterson, L. M., Eary, J. F., and Krohn, K. A. Kinetic analysis of 2-[<sup>11</sup>C]thymidine PET imaging studies: validation studies. *J.Nucl.Med.*, 40: 614-624, 1999.
13. Krohn, K. A., Mankoff, D. A., and Eary, J. F. Imaging cellular proliferation as a measure of response to therapy. *J.Clin.Pharmacol., Suppl*: 96S-103S, 2001.
14. Mankoff, D. A., Shields, A. F., Graham, M. M., Link, J. M., Eary, J. F., and Krohn, K. A. Kinetic analysis of 2-[carbon-11]thymidine PET imaging studies: compartmental model and mathematical analysis. *J.Nucl.Med.*, 39: 1043-1055, 1998.
15. Shields, A. F., Grierson, J. R., Kozawa, S. M., and Zheng, M. Development of labeled thymidine analogs for imaging tumor proliferation. *Nucl.Med.Biol.*, 23: 17-22, 1996.
16. Rasey, J. S., Grierson, J. R., Wiens, L. W., Kolb, P. D., and Schwartz, J. L. Validation of FLT uptake as a measure of thymidine kinase-1 activity in A549 carcinoma cells. *J.Nucl.Med.*, 43: 1210-1217, 2002.

17. Toyohara, J., Waki, A., Takamatsu, S., Yonekura, Y., Magata, Y., and Fujibayashi, Y. Basis of FLT as a cell proliferation marker: comparative uptake studies with [<sup>3</sup>H]thymidine and [<sup>3</sup>H]arabinothymidine, and cell-analysis in 22 asynchronously growing tumor cell lines. *Nucl.Med.Biol.*, 29: 281-287, 2002.
18. Seitz, U., Wagner, M., Neumaier, B., Wawra, E., Glatting, G., Leder, G., Schmid, R. M., and Reske, S. N. Evaluation of pyrimidine metabolising enzymes and in vitro uptake of 3'- [<sup>18</sup>F]fluoro-3'-deoxythymidine ([<sup>18</sup>F]FLT) in pancreatic cancer cell lines. *Eur.J Nucl.Med.Mol.Imaging*, 29: 1174-1181, 2002.
19. Wagner, M., Seitz, U., Buck, A., Neumaier, B., Schultheiss, S., Bangerter, M., Bommer, M., Leithauser, F., Wawra, E., Munzert, G., and Reske, S. N. 3'-[<sup>18</sup>F]fluoro-3'-deoxythymidine ([<sup>18</sup>F]-FLT) as positron emission tomography tracer for imaging proliferation in a murine B-Cell lymphoma model and in the human disease. *Cancer Res.*, 63: 2681-2687, 2003.
20. Shields, A. F., Grierson, J. R., Dohmen, B. M., Machulla, H. J., Stayanoff, J. C., Lawhorn, C. J., Obradovich, J. E., Muzik, O., and Mangner, T. J. Imaging proliferation in vivo with [F-18]FLT and positron emission tomography. *Nat.Med.*, 4: 1334-1336, 1998.
21. Munch-Petersen, B., Cloos, L., Tyrsted, G., and Eriksson, S. Diverging substrate specificity of pure human thymidine kinases 1 and 2 against antiviral dideoxynucleosides. *J.Biol Chem.*, 266: 9032-9038, 1991.
22. Yamada, S., Kubota, K., Kubota, R., Ido, T., and Tamahashi, N. High accumulation of fluorine-18-fluorodeoxyglucose in turpentine-induced inflammatory tissue. *J.Nucl.Med.*, 36: 1301-1306, 1995.
23. Hustinx, R., Lemaire, C., Jerusalem, G., Moreau, P., Cataldo, D., Duysinx, B., Aerts, J., Fassotte, M. F., Foidart, J., and Luxen, A. Whole-body tumor imaging using PET and 2-<sup>18</sup>F-fluoro-L-tyrosine: preliminary evaluation and comparison with <sup>18</sup>F-FDG. *J.Nucl.Med.*, 44: 533-539, 2003.
24. Jager, P. L., Franssen, E. J., Kool, W., Szabo, B. G., Hoekstra, H. J., Groen, H. J., de Vries, E. G. E., van Imhoff, G. W., Vaalburg, W., and Piers, D. A. Feasibility of tumor imaging using L-3-[iodine-123]-iodo-alpha-methyl-tyrosine in extracranial tumors. *J.Nucl.Med.*, 39: 1736-1743, 1998.
25. Francis, D. L., Visvikis, D., Costa, D. C., Arulampalam, T. H., Townsend, C., Luthra, S. K., Taylor, I., and Eil, P. J. Potential impact of [<sup>18</sup>F]3'-deoxy-3'-fluorothymidine versus [<sup>18</sup>F]fluoro-2-deoxy-d-glucose in positron emission tomography for colorectal cancer. *Eur.J Nucl.Med.Mol.Imaging*, 2003.
26. Nottebrock, H. and Then, R. Thymidine concentrations in serum and urine of different animal species and man. *Biochem.Pharmacol.*, 26: 2175-2179, 1977.
27. Kong, X. B., Zhu, Q. Y., Vidal, P. M., Watanabe, K. A., Polsky, B., Armstrong, D., Ostrander, M., Lang, S. A., Jr., Muchmore, E., and Chou, T. C. Comparisons of anti-human immunodeficiency virus activities, cellular transport, and plasma and intracellular pharmacokinetics of 3'-fluoro-3'-deoxythymidine and 3'-azido-3'-deoxythymidine. *Antimicrob.Agents Chemother.*, 36: 808-818, 1992.
28. Buck, A. K., Schirrmester, H., Hetzel, M., Von Der, H. M., Halter, G., Glatting, G., Mattfeldt, T., Liewald, F., Reske, S. N., and Neumaier, B. 3'-deoxy-3'-[<sup>18</sup>F]fluorothymidine-positron emission tomography for noninvasive assessment of proliferation in pulmonary nodules. *Cancer Res.*, 62: 3331-3334, 2002.
29. Vesselle, H., Grierson, J., Muzi, M., Pugsley, J. M., Schmidt, R. A., Rabinowitz, P., Peterson, L. M., Vallieres, E., and Wood, D. E. In Vivo Validation of 3'-deoxy-3'-[<sup>18</sup>F]fluorothymidine ([<sup>18</sup>F]FLT) as a Proliferation Imaging Tracer in Humans: Correlation of [<sup>18</sup>F]FLT Uptake by Positron Emission Tomography with Ki-67 Immunohistochemistry and Flow Cytometry in Human Lung Tumors. *Clin.Cancer Res.*, 8: 3315-3323, 2002.
30. Barthel, H., Cleij, M. C., Collingridge, D. R., Hutchinson, O. C., Osman, S., He, Q., Luthra, S. K., Brady, F., Price, P. M., and Aboagye, E. 3'-deoxy-3'-[<sup>18</sup>F]Fluorothymidine as a new marker for

monitoring tumor response to antiproliferative therapy *in vivo* with positron emission tomography. *Cancer Res.*, 63: 3791-3798, 2003.

31. Dittmann, H., Dohmen, B. M., Kehlbach, R., Bartusek, G., Pritzkow, M., Sarbia, M., and Bares, R. Early changes in [<sup>18</sup>F]FLT uptake after chemotherapy: an experimental study. *Eur.J Nucl.Med.Mol.Imaging*, 29: 1462-1469, 2002.



## Chapter 6

### Detection and grading of soft tissue sarcomas of the extremities with $^{18}\text{F}$ - $^3$ -fluoro- $^3$ -deoxy-L-thymidine

D.C.P. Cobben<sup>1,2</sup>, P.H. Elsinga<sup>1</sup>, A.J.H. Suurmeijer<sup>3</sup>, W. Vaalburg<sup>1</sup>, B. Maas<sup>1</sup>, P.L. Jager<sup>1</sup>,  
H.J. Hoekstra<sup>2</sup>

PET center<sup>1</sup>, Department of Surgical Oncology<sup>2</sup>, Department of Pathology and Laboratory  
Medicine<sup>3</sup>, Groningen University Hospital, Groningen, The Netherlands.

*Clinical Cancer Research 2004; 10: 1685-90*

## Summary

**Purpose** The aim of the study is to investigate the feasibility of  $^{18}\text{F}$ -3'-fluoro-3'-deoxy-L-thymidine positron emission tomography (FLT-PET) for the detection and grading of soft tissue sarcoma (STS).

**Experimental design** Nineteen patients with 20 soft tissue sarcomas of the extremities were scanned, using attenuation corrected whole-body FLT-PET. Standardized uptake values (SUVs) and tumor/non-tumor ratios (TNTs) were compared with histopathological parameters using French and Japanese grading systems.

**Results** Mean SUV, max SUV and TNT could differentiate between low grade (grade 1; n=6) STS and high grade (grade 2 and 3; n=14) STS according to the French grading system ( $p=0.001$ ). Mean SUV, max SUV and TNT correlated with mitotic score, MIB-1 score, the French and Japanese grading system ( $p=0.550-0.747$ ).

**Conclusions** FLT-PET is able to visualize STS and differentiate between low grade and high grade STS. The uptake of FLT correlates with the proliferation of STS.

## Introduction

Soft-tissue sarcomas (STS) form a heterogeneous group of rare malignancies, which arise from mesenchymal soft tissues and account for approximately 1% of all cancers. In the United States, 8300 new cases are diagnosed each year and in the Netherlands about 400.<sup>1,2</sup> At first presentation, 13% of the patients with STS have metastases. The lung is the most common metastatic site, followed by bone, liver, and brain. Less common sites are regional lymph nodes, retroperitoneum and soft tissues.<sup>3,4</sup> After treatment of the primary tumor, approximately 40% of the patients will develop recurrences either locally or distantly.

The presence or absence of metastases and the malignancy grade of the tumor will dictate the treatment. Grading is frequently performed according to the French grading system.<sup>5</sup> In this grading system, points are scored for histological grade, tumor differentiation and amount of necrosis and number of mitotic figures. Recently, a Japanese grading system, using the MIB-1 score instead of the mitotic score, has been introduced, which correlates stronger with the prognosis than the French grading system.<sup>6,7</sup>

Optimal management of STS depends on the anatomical site, local growth pattern, tumor size and grade and accurate staging of the disease, when first diagnosed. The site, growth pattern and size of the primary tumor are best determined by magnetic resonance imaging (MRI) or spiral computed tomography (CT). However, the clinical and radiological differentiation between benign soft tissue masses and soft tissue sarcomas, is difficult.<sup>8</sup> Information regarding distant metastases is obtained primarily by chest radiography or a CT scan of the lungs, while bone-scintigraphy is of limited value.<sup>8,9</sup> Distant metastases to the lungs are ruled out by CT. Physical examination, CT, MRI or ultrasonography are best used for the detection of local recurrences. However, after surgery and radiation therapy, physical examination and interpretation of the diagnostic images remains difficult.<sup>8</sup>

Therefore, the need for non-invasive detection, staging and grading of a soft tissue tumor mass, has increased. During the last decade the value of positron emission tomography (PET) in STS with several tracers, especially <sup>18</sup>F-fluoro-2'-deoxy-D-glucose (FDG), has been investigated.<sup>10-16</sup> However, the current potential of FDG-PET in the detection and/or grading is still unknown.<sup>10,11,15,17-32</sup>

Several years ago <sup>18</sup>F-fluoro-3'-deoxy-3'-L-fluorothymidine (FLT) was introduced as PET tracer.<sup>33</sup> This tracer has theoretical advantages over the currently used FDG, since no

uptake in inflammatory cells is anticipated. The aim of this study is to investigate the feasibility of FLT-PET for the detection and grading of soft tissue sarcoma (STS).

### **Patients and methods**

This prospective study, approved by Medical Ethics Committee of the Groningen University Hospital, consisted of 19 consecutive patients with a soft tissue sarcoma of the extremity. All patients were treated at the Groningen University Hospital and gave written informed consent. For inclusion, the liver and kidney functions and hematological parameters (Hb, Ht, erythrocytes, thrombocytes, leukocytes and white cell count) should be within normal limits. Pregnant patients or patients with psychiatric disorders were excluded from the study.

Synthesis of FLT was performed according to the method of Machulla et al.<sup>34</sup> FLT was produced by fluorination with [<sup>18</sup>F]fluoride of the 4,4'-dimethoxytrityl protected anhydrothymidine, followed by a deprotection step and purification by HPLC. FLT was produced with a radiochemical purity of >95% and specific activity of >10 TBq/mmol. The radiochemical yield was  $5.6 \pm 2.8\%$  (decay corrected).

Nineteen patients were examined in the period of February 2002 until July 2003, using an ECAT EXACT HR+ (Siemens/CTI Inc., Knoxville, TN). Prior to PET imaging, patients were instructed to fast for at least 6 hours in order to keep the study comparable with studies performed with FDG.<sup>35</sup> They were also instructed to drink one liter of water prior to imaging to stimulate FLT excretion from the renal calyces and stimulate subsequent voiding. For injection of FLT, a venous cannula was inserted in the forearm of the patient.

Patients received a median of 400 (115-430) MBq FLT. Sixty minutes after injection, the region of the tumor was imaged in emission-transmission-transmission-emission mode. After scanning the tumor region, a non attenuation-corrected whole-body scan was performed from crown to femur for 5 minutes per bed position. Data from multiple bed positions were iteratively reconstructed (ordered subset expectation maximization).<sup>36</sup>

Histological typing of the tumors of all patients was performed on haematoxylin and eosin (HE) stained sections according to the WHO classification.<sup>37</sup> Immunophenotype was determined in poorly differentiated tumors. Tumors were graded using both the French and Japanese grading system.<sup>5-7</sup>

The number of mitotic figures was counted per 2 mm<sup>2</sup> in HE stained slides, after selecting the most cellular areas with the highest mitotic rate. Proliferating cells were detected with immunohistochemistry, using monoclonal antibody MIB-1 and antigen retrieval, as described earlier.<sup>12</sup> Monoclonal antibody MIB-1 recognizes the protein Ki-67 in all phases of the cell cycle with the exception of G<sub>0</sub>.

The MIB-1 score was estimated by counting the percentage of MIB-1 positive cell nuclei per 1,000 tumor cells in the region of the tumor with the greatest density of staining, which in most instances corresponds to areas with the highest mitotic activity.

## **Data analysis**

### ***Region of interest (ROI)***

Qualitative and quantitative evaluation of the PET scans was performed by analyzing the hypermetabolic zones on transaxial sections. The slice with the highest uptake was selected for ROI analysis.

### ***Standardized uptake value (SUV)***

After selecting the plane with the maximum SUV, a ROI was drawn manually. ROIs were placed at the 70% contour of the maximal SUV in the tumor. The same ROI was applied in the contralateral leg or arm. The mean SUV of the tumor was divided by SUV of the background region to produce the tumor/non-tumor ratio (TNT). In patients 3 and 13 it was not possible to let the ROI-tool calculate a mean SUV from 70% of the maximal SUV in the non-tumor region, because the calculated ROI was below the background uptake of FLT (Table 1). Therefore the highest mean of the manually drawn ROI, with the highest SUV, was used. TNTs and SUVs were compared with histopathological parameters.

The pathologist (AJHS) was unaware of the results of the PET-images. The images were analyzed independently by a clinical investigator (DCPC) unaware of histological typing and grading of the tumors. After calculating the SUVs and TNTs of the PET lesions, the PET data were correlated with the histopathological findings.

### ***Whole body images***

Whole body images were scored for presence/absence of lesions outside the location of the primary tumor, blinded for other clinical information. Lesions were

interpreted visually as malignant, if the FLT uptake in the lesion was higher than the surrounding tissue.

### ***Statistical analysis***

Kruskall Wallis non-parametric testing was used to see if the groups, as defined by the French or Japanese grading system, differed. Dunnett's T3 post-hoc multiple comparisons test was performed for variance analysis between the different groups, as defined by the French or Japanese grading system, for mean SUV, max SUV and TNT. Mann-Whitney testing was used to compare the mean SUV, max SUV and TNT between the French or Japanese grading system. Spearman's correlation coefficient was used to correlate mean SUV, max SUV and TNT, with mitotic score, MIB-1 score and the French or Japanese grading system. Two-tailed P-values <0.05 were considered significant.

## **Results**

### ***Patients***

Nineteen patients with a median age of 58 (27-75) years, 7 women and 12 men, were included in this study (Table 1). Eighteen patients had one STS and one patient had two STS. Patient characteristics are presented in Table 1. Eighteen patients had a biopsy prior to the FLT-PET and one patient had a FLT-PET prior to the biopsy. A total of 17 incision biopsies and 2 true cut biopsies were performed.

### ***Primary tumors***

Twenty tumors in a total of 19 patients were clearly visible with high contrast and were interpreted as malignant. Figure 1 is an example of a FLT-PET whole body image (Pt 16). The sensitivity for detecting malignant lesions was 100%. The Kruskal-Wallis variance analysis showed significant different variance in mean SUV, max SUV and TNT between the groups, defined by the French or Japanese grading system.

The French and Japanese grading system were compared with mean SUV, max SUV and TNT. Mean SUV, max SUV and TNT could differentiate between grade 1 STS and grade 3 STS and between low grade and high grade STS (Tables 2A and 2B).

Mean SUV, max SUV and TNT were able to differentiate between low grade STS and high grade STS according to the French and Japanese grading system. Figure 2A is an

example of a FLT-PET of a low grade STS (Pt 6) and Figure 2B of a high grade STS (Pt 13).

**Table 1. Patient characteristics mean SUV, TNT, mitotic score, MIB-1 score and grading**

Pt	Sex	Age	Diagnosis	Max Diameter (cm)	Location	SUV Tumor	SUV Non-tumor	TNT	MS <sup>5</sup>	FTG <sup>5</sup>	MIB-1 Score <sup>6,7</sup>	JTG <sup>6,7</sup>
1	M	55	Well differentiated liposarcoma	17	leg	0.2	0.1	2.4	1	1	1	1
2	M	55	Myxoid liposarcoma	10	leg	1.1	0.5	2.1	1	1	1	1
3	M	62	Myxoid liposarcoma	11	leg	1.5	0.6	2.4	1	1	1	1
4	M	71	Recurrent MFH	2	leg	1.0	0.6	1.7	1	1	1	1
5	F	61	Well differentiated liposarcoma	30	leg	0.4	0.7	0.6	1	1	1	1
6	F	73	Well differentiated liposarcoma	22	leg	0.9	0.6	1.5	1	1	1	1
7	M	27	Epitheloid sarcoma	7	leg	1.4	0.6	2.3	1	2	2	2
8	M	28	Synoviasarcoma	12	leg	0.8	0.4	2.1	1	2	2	2
9	M	33	Myxofibrosarcoma	17	leg	3.4	0.6	5.4	2	2	2	2
10	M	70	Pleiomorphic MFH	10	leg	3.7	0.6	5.9	2	2	2	2
11	F	71	Leiomyosarcoma (recurrence)	7	arm	2.1	0.6	3.4	2	2	2	2
12	F	75	Myxofibrosarcoma	14	leg	3.5	0.6	6.4	1	2	1	1
13	M	52	Pleiomorphic MFH	20	Leg	2.8	0.4	7.0	2	3	2	3
			Pleiomorphic MFH (recurrence in opposite leg)	2	Leg	2.3	0.3	7.1	2	3	2	3
14	M	53	Pleiomorphic liposarcoma	28	leg	2.2	0.6	3.4	3	3	3	3
15	M	70	Myxofibrosarcoma	10	leg	2.3	0.5	4.7	2	3	3	3
16	M	71	Pleiomorphic leiomyosarcoma	20	leg	4.9	0.7	6.6	2	3	3	3
17	F	47	Pleiomorphic leiomyosarcoma	11	arm	4.8	0.9	5.3	3	3	3	3
18	F	56	Extraskelatal osteosarcoma	6	leg	2.8	0.3	9.3	3	3	3	3
19	F	58	Pleiomorphic sarcoma NOS	5	leg	3.7	1.5	2.5	3	3	3	3

FTG=French tumor grade; JTG=Japanese Tumor Grade; MFH=malignant fibrous histiocytoma; MS=mitotic score; NOS=not otherwise specified; Pt=patient.

**Figure 1.**

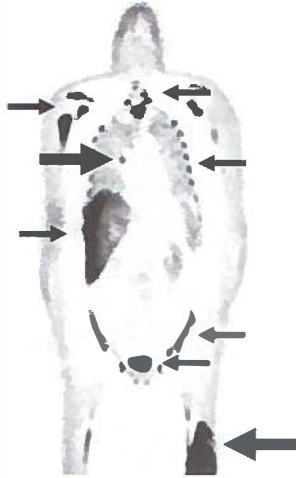


Figure 1 demonstrates a whole body image of patient 16. Physiological uptake of FLT can be seen in the bone marrow of the pelvis, ribs, vertebrae and in the bones of the shoulder, in the liver and bladder (small arrows). The STS can be seen in the left upper leg and a lung metastasis in the mediastinum (large arrows).

**Table 2A. Mean SUV, Max SUV and TNT in the French or Japanese grading system**

<b>French Grading System<sup>5</sup></b>	<b>Grade 1* (n=6)</b>	<b>Grade 2* (n=6)</b>	<b>Grade 3* (n=8)</b>	<b>Low grade<sup>#</sup> vs High grade</b>
Mean SUV	0.9 (0.2-1.5)	2.8 (0.8-3.7)	2.8 (2.2-4.9)	0.001
Max SUV	1.2 (0.3-1.7)	3.4 (1.0-5.2)	3.3 (2.8-6.7)	0.001
TNT	1.9 (0.6-2.4)	4.4 (2.1-6.4)	6.0 (2.5-9.3)	0.001
<b>Japanese Grading System<sup>6,7</sup></b>	<b>Grade 1* (n=7)</b>	<b>Grade 2* (n=5)</b>	<b>Grade 3* (n=8)</b>	<b>Low grade<sup>#</sup> vs High grade</b>
Mean SUV	1.0 (0.2-3.5)	2.1 (0.8-3.7)	2.8 (2.2-4.9)	0.011
Max SUV	1.3 (0.3-5.2)	2.8 (1.0-4.7)	3.3 (2.8-6.7)	0.014
TNT	2.1 (0.6-6.4)	3.4 (2.1-5.9)	6.0 (2.5-9.3)	0.008

\*Values expressed as medians (range); <sup>#</sup>statistic difference between medians (P values); Low grade=grade 1; High grade=grade 2+3.



**Table 2B. P values of Dunnett T3 comparisons for mean SUV, max SUV and TNT in the French or Japanese grading system**

<b>French Grading System<sup>5</sup></b>	<b>Grade 1 vs Grade 2</b>	<b>Grade 1 vs Grade 3</b>	<b>Grade 2 vs Grade 3</b>
Mean SUV	0.056	0.001	0.594
Max SUV	0.066	0.002	0.660
TNT	0.063	0.003	0.468
<b>Japanese Grading System<sup>6,7</sup></b>	<b>Grade 1 vs Grade 2</b>	<b>Grade 1 vs Grade 3</b>	<b>Grade 2 vs Grade 3</b>
Mean SUV	0.385	0.011	0.473
Max SUV	0.536	0.032	0.409
TNT	0.503	0.022	0.286

**Figure 2A. MRI and FLT-PET images of a patient with low grade STS**

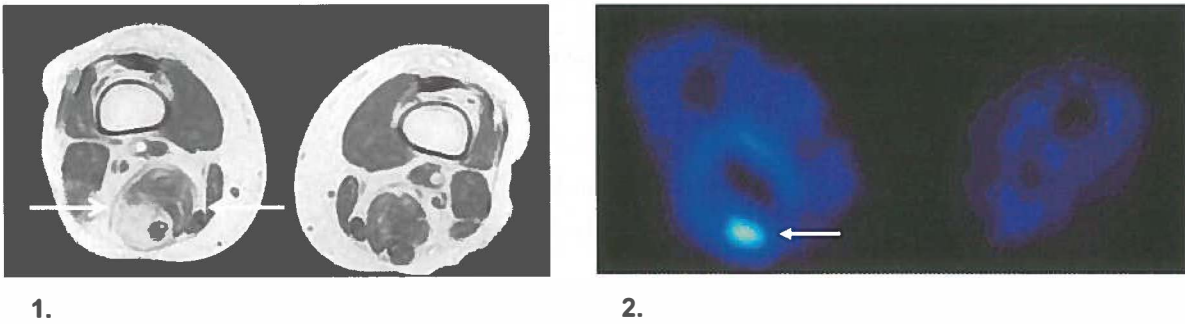


**Figure 2B. MRI and FLT-PET images of a patient with high grade STS**

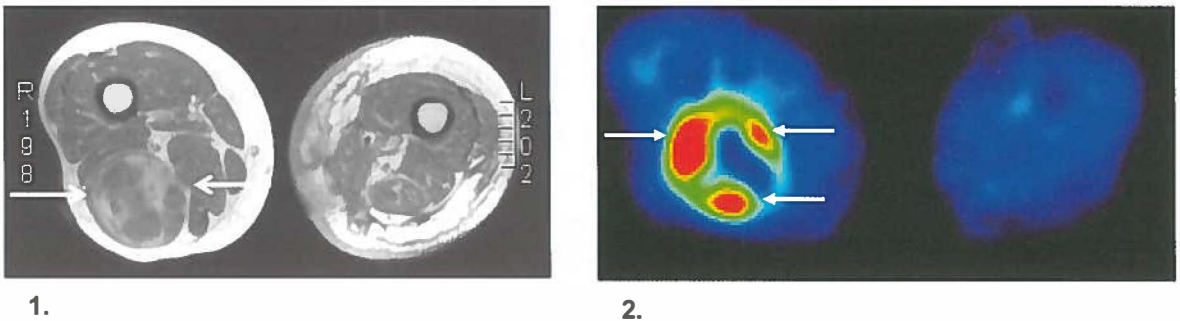


Figure 2A shows the MRI (1) and FLT-PET (2) images of a low grade STS (Pt 6) and Figure 2B of a high grade STS (Pt 13). The MRI images of both patients demonstrate a heterogeneous tumor. However, the FLT uptake in the high grade STS is higher (indicated as red) than in the low grade STS (indicated as blue).

All correlations between mean SUV, max SUV, TNT, mitotic score, MIB-1 score and the French and Japanese grading system were significant (Table 2B). The correlation coefficients varied from 0.550 to 0.747 with all p values <0.05. The strongest correlation was found between TNT and the French grading system.

**Table 3. Spearman's correlations ( $\rho$ ) between grade, Mean SUV, TNT, mitotic score and MIB-1 score**

	Mitotic Score <sup>5</sup>	MIB-1 Score <sup>6,7</sup>	French Grading System <sup>5</sup>	Japanese Grading System <sup>6,7</sup>
Mean SUV	0.721 <sup>#</sup>	0.652 <sup>#</sup>	0.724 <sup>#</sup>	0.647 <sup>#</sup>
Max SUV	0.668 <sup>#</sup>	0.610 <sup>#</sup>	0.723 <sup>#</sup>	0.627 <sup>#</sup>
TNT	0.646 <sup>#</sup>	0.550 <sup>*</sup>	0.747 <sup>#</sup>	0.668 <sup>#</sup>

<sup>#</sup>p<0.005; <sup>\*</sup>p<0.05.

### ***Additional findings with whole body FLT-PET***

In four patients single or multiple lesions were seen or missed on the whole body FLT-PET. In two patients the lesions detected on FLT-PET were malignant. In patient 13, FLT-PET detected, besides a new primary STS in the right thigh, a 1.5 cm small local recurrence of a sarcoma in the left thigh, which was previously treated with surgery and radiation therapy. In patient 16, FLT-PET detected lung metastases, which were confirmed on CT as well.

In three patients the lesions seen on FLT-PET were not malignant according to pathological examination or follow-up. In patient 10, the lesions on FLT-PET in the groin and supraclavicular region were negative on physical examination and follow-up. In patient 13, the lesion on FLT-PET in the groin was histologically negative after lymph node dissection. In patient 14, the lesions on FLT-PET in the groin were indicated as lymph nodes with follicular hyperplasia after lymph node dissection.

In one patient a metastatic lymph node was missed on FLT-PET. In patient 7, a axillary lymph node dissection was performed. In the lymph node dissection, one lymph node contained two metastases with both a diameter of 5 mm with 11 mitotic figures per 2mm<sup>2</sup>. This metastatic lymph node was not detected on whole-body FLT-PET.

## Discussion

The results of this study revealed that FLT-PET is able to visualize STS and recurrent STS and has the clinical potential to distinguish between low (grade 1) and high grade (grade 2 and 3) STS.

FLT uptake appeared to be related to proliferation and tumor grade. Mean SUV, max SUV and TNT correlated with mitotic score, MIB-1 score and the French and Japanese grading of STS. No difference between the French and Japanese grading system was found based on the correlations.

In the French grading system of STS, all three parameters (level of histological differentiation, amount of necrosis and mitotic index) are independent predictors of metastasis.<sup>38</sup> It has been demonstrated that when using the MIB-1 score instead of the mitotic score in the French grading system, the grading of soft tissue sarcoma improved. This modified Japanese grading system proved to be the most significant predictor of overall survival.<sup>6,7</sup> Therefore, a PET-tracer that would reflect proliferation, could have the potential to visualize grading of STS. For this purpose <sup>18</sup>F-fluoro-3'-deoxy-3'-L-fluorothymidine (FLT) was developed.<sup>33,39</sup> This pyrimidine analog, is phosphorylated by the enzyme thymidine kinase 1 (TK<sub>1</sub>), which leads to intracellular trapping.<sup>33</sup> During DNA synthesis, TK<sub>1</sub> concentration increases almost tenfold and is, therefore, an accurate reflection of cellular proliferation.<sup>40</sup>

Most previous studies for detecting sarcomas have been performed with <sup>18</sup>F-fluoro-2'-deoxy-D-glucose-PET (FDG-PET) and have recently been critically reviewed in two meta-analyses.<sup>31,32</sup> The sensitivity of FDG-PET for detecting primary and recurrent sarcomas varies from 88 to 92% and specificity varies from 73 to 87%.<sup>31,32</sup> FDG-PET can be useful in tumor grading, but is, with the exception of a study of Eary et al, not able to differentiate between benign lesions and low grade sarcoma.<sup>16,17,31,32</sup> The accuracy for the differentiation is influenced by technical limitations, time between injection and scanning, false negative and false positive findings.<sup>18,21,22,26,29</sup> The SUV for FDG-PET for low grade (grade 1) STS varied between 1.6 and 2.6, as compared to 0.2 and 1.5 for FLT-PET; the SUV for FDG-PET for high grade STS (grade 2 and 3) varied between 8.0 and 9.4 as compared to 0.8 and 4.9 for FLT-PET.<sup>23,29</sup> Despite the lower sensitivity of FDG-PET than FLT-PET, the uptake of FDG was higher than FLT. In a comparative study with FLT-PET, the correlation between FDG SUV and proliferation of the STS should be investigated.

In conclusion, FLT-PET is able to visualize and differentiate high grade from low grade STS. The uptake of FLT correlates with the proliferation of soft tissue sarcomas.

## References

1. Jemal, A., Murray, T., Samuels, A., Ghafoor, A., Ward, E., and Thun, M. J. Cancer statistics, 2003. *CA Cancer J Clin.*, 53: 5-26, 2003.
2. Visser, O., Coebergh, J. W. W., van Dijck, J. A. A. M., and Siesling, S. Incidence of cancer in the Netherlands 1998. Utrecht: Vereniging van Integrale Kankercentra: 2002.
3. Gustafson, P. Soft tissue sarcoma. Epidemiology and prognosis in 508 patients. *Acta Orthop.Scand.Suppl.*, 259: 1-31, 1994.
4. Nijhuis, P. H., Schaapveld, M., Otter, R., Molenaar, W. M., van der Graaf, W. T., and Hoekstra, H. J. Epidemiological aspects of soft tissue sarcomas (STS)—consequences for the design of clinical STS trials. *Eur.J Cancer*, 35: 1705-1710, 1999.
5. Guillou, L., Coindre, J. M., Bonichon, F., Nguyen, B. B., Terrier, P., Collin, F., Vilain, M. O., Mandard, A. M., Le, D., V, Leroux, A., Jacquemier, J., Duplay, H., Sastre-Garau, X., and Costa, J. Comparative study of the National Cancer Institute and French Federation of Cancer Centers Sarcoma Group grading systems in a population of 410 adult patients with soft tissue sarcoma. *J Clin.Oncol.*, 15: 350-362, 1997.
6. Hasegawa, T., Yamamoto, S., Nojima, T., Hirose, T., Nikaido, T., Yamashiro, K., and Matsuno, Y. Validity and reproducibility of histologic diagnosis and grading for adult soft-tissue sarcomas. *Hum.Pathol.*, 33: 111-115, 2002.
7. Hasegawa, T., Yokoyama, R., Lee, Y. H., Shimoda, T., Beppu, Y., and Hirohashi, S. Prognostic relevance of a histological grading system using MIB-1 for adult soft-tissue sarcoma. *Oncology*, 58: 66-74, 2000.
8. Ham, S. J., van der Graaf, W. T., Pras, E., Molenaar, W. M., van den, B. E., and Hoekstra, H. J. Soft tissue sarcoma of the extremities. A multimodality diagnostic and therapeutic approach. *Cancer Treat.Rev.*, 24: 373-391, 1998.
9. Jager, P. L., Hoekstra, H. J., Leeuw, J., Der Graaf, W. T., de Vries, E. G., and Piers, D. A. Routine bone scintigraphy in primary staging of soft tissue sarcoma; Is it worthwhile? *Cancer*, 89: 1726-1731, 2000.
10. van Ginkel, R. J., Hoekstra, H. J., Pruijm, J., Nieweg, O. E., Molenaar, W. M., Paans, A. M., Willemsen, A. T., Vaalburg, W., and Koops, H. S. FDG-PET to evaluate response to hyperthermic isolated limb perfusion for locally advanced soft-tissue sarcoma. *J Nucl.Med.*, 37: 984-990, 1996.
11. Kole, A. C., Nieweg, O. E., van Ginkel, R. J., Pruijm, J., Hoekstra, H. J., Paans, A. M., Vaalburg, W., and Koops, H. S. Detection of local recurrence of soft-tissue sarcoma with positron emission tomography using [<sup>18</sup>F]fluorodeoxyglucose. *Ann.Surg.Oncol.*, 4: 57-63, 1997.
12. Plaat, B., Kole, A., Mastik, M., Hoekstra, H., Molenaar, W., and Vaalburg, W. Protein synthesis rate measured with L-[<sup>11</sup>C]tyrosine positron emission tomography correlates with mitotic activity and MIB-1 antibody- detected proliferation in human soft tissue sarcomas. *Eur.J Nucl.Med.*, 26: 328-332, 1999.
13. Kole, A. C., Plaat, B. E., Hoekstra, H. J., Vaalburg, W., and Molenaar, W. M. FDG and L-[<sup>11</sup>C]-tyrosine imaging of soft-tissue tumors before and after therapy. *J Nucl.Med.*, 40: 381-386, 1999.
14. van Ginkel, R. J., Kole, A. C., Nieweg, O. E., Molenaar, W. M., Pruijm, J., Koops, H. S., Vaalburg, W., and Hoekstra, H. J. L-[<sup>11</sup>C]-tyrosine PET to evaluate response to hyperthermic isolated limb perfusion for locally advanced soft-tissue sarcoma and skin cancer. *J Nucl.Med.*, 40: 262-267, 1999.
15. Schwarzbach, M., Willeke, F., Dimitrakopoulou-Strauss, A., Strauss, L. G., Zhang, Y. M., Mechttersheimer, G., Hinz, U., Lehnert, T., and Herfarth, C. Functional imaging and detection of local recurrence in soft tissue sarcomas by positron emission tomography. *Anticancer Res.*, 19: 1343-1349, 1999.

16. Reske, S. N. and Kotzerke, J. FDG-PET for clinical use. Results of the 3rd German Interdisciplinary Consensus Conference, "Onko-PET III", 21 July and 19 September 2000. *Eur.J Nucl.Med.*, 28: 1707-1723, 2001.
17. Eary, J. F., Conrad, E. U., Bruckner, J. D., Folpe, A., Hunt, K. J., Mankoff, D. A., and Howlett, A. T. Quantitative [<sup>18</sup>F]fluorodeoxyglucose positron emission tomography in pretreatment and grading of sarcoma. *Clin.Cancer Res.*, 4: 1215-1220, 1998.
18. Schulte, M., Brecht-Krauss, D., Heymer, B., Guhlmann, A., Hartwig, E., Sarkar, M. R., Diederichs, C. G., Schultheiss, M., Kotzerke, J., and Reske, S. N. Fluorodeoxyglucose positron emission tomography of soft tissue tumours: is a non-invasive determination of biological activity possible? *Eur.J Nucl.Med.*, 26: 599-605, 1999.
19. Schwarzbach, M. H., Dimitrakopoulou-Strauss, A., Willeke, F., Hinz, U., Strauss, L. G., Zhang, Y. M., Mechtersheimer, G., Attigah, N., Lehnert, T., and Herfarth, C. Clinical value of [<sup>18</sup>F]] fluorodeoxyglucose positron emission tomography imaging in soft tissue sarcomas. *Ann.Surg.*, 231: 380-386, 2000.
20. Garcia, R., Kim, E. E., Wong, F. C., Korkmaz, M., Wong, W. H., Yang, D. J., and Podoloff, D. A. Comparison of fluorine-18-FDG PET and technetium-99m-MIBI SPECT in evaluation of musculoskeletal sarcomas. *J Nucl.Med.*, 37: 1476-1479, 1996.
21. Nieweg, O. E., Pruim, J., van Ginkel, R. J., Hoekstra, H. J., Paans, A. M., Molenaar, W. M., Schraffordt Koops, H. S., and Vaalburg, W. Fluorine-18-fluorodeoxyglucose PET imaging of soft-tissue sarcoma. *J Nucl.Med.*, 37: 257-261, 1996.
22. Dimitrakopoulou-Strauss, A., Strauss, L. G., Schwarzbach, M., Burger, C., Heichel, T., Willeke, F., Mechtersheimer, G., and Lehnert, T. Dynamic PET 18F-FDG studies in patients with primary and recurrent soft- tissue sarcomas: impact on diagnosis and correlation with grading. *J Nucl.Med.*, 42: 713-720, 2001.
23. Lodge, M. A., Lucas, J. D., Marsden, P. K., Cronin, B. F., O'Doherty, M. J., and Smith, M. A. A PET study of 18FDG uptake in soft tissue masses. *Eur.J Nucl.Med.*, 26: 22-30, 1999.
24. Schwarzbach, M. H., Dimitrakopoulou-Strauss, A., Mechtersheimer, G., Hinz, U., Willeke, F., Cardona, S., Attigah, N., Strauss, L. G., Herfarth, C., and Lehnert, T. Assessment of soft tissue lesions suspicious for liposarcoma by F18- deoxyglucose (FDG) positron emission tomography (PET). *Anticancer Res.*, 21: 3609-3614, 2001.
25. Folpe, A. L., Lyles, R. H., Sprouse, J. T., Conrad, E. U., III, and Eary, J. F. (F-18) fluorodeoxyglucose positron emission tomography as a predictor of pathologic grade and other prognostic variables in bone and soft tissue sarcoma. *Clin.Cancer Res.*, 6: 1279-1287, 2000.
26. Lucas, J. D., O'Doherty, M. J., Wong, J. C., Bingham, J. B., McKee, P. H., Fletcher, C. D., and Smith, M. A. Evaluation of fluorodeoxyglucose positron emission tomography in the management of soft-tissue sarcomas. *J Bone Joint Surg.Br.*, 80: 441-447, 1998.
27. Delbeke, D., Martin, W. H., Sandler, M. P., Chapman, W. C., Wright, J. K., Jr., and Pinson, C. W. Evaluation of benign vs malignant hepatic lesions with positron emission tomography. *Arch.Surg.*, 133: 510-515, 1998.
28. Watanabe, H., Shinozaki, T., Yanagawa, T., Aoki, J., Tokunaga, M., Inoue, T., Endo, K., Mohara, S., Sano, K., and Takagishi, K. Glucose metabolic analysis of musculoskeletal tumours using 18fluorine- FDG PET as an aid to preoperative planning. *J Bone Joint Surg.Br.*, 82: 760-767, 2000.
29. Lucas, J. D., O'Doherty, M. J., Cronin, B. F., Marsden, P. K., Lodge, M. A., McKee, P. H., and Smith, M. A. Prospective evaluation of soft tissue masses and sarcomas using fluorodeoxyglucose positron emission tomography. *Br.J Surg.*, 86: 550-556, 1999.
30. Haberkorn, U. [The role of diagnostic PET in treatment planning before tumor surgery]. *Chirurg*, 72: 1010-1019, 2001.

31. Ioannidis, J. P. and Lau, J. 18F-FDG PET for the diagnosis and grading of soft-tissue sarcoma: a meta-analysis. *J.Nucl.Med.*, 44: 717-724, 2003.
32. Bastiaannet, E., Groen, H., Jager, P. L., Cobben, D. C. P., van der Graaf, W. T. A., Vaalburg, W., and Hoekstra, H. J. The value of FDG-PET in the detection, grading and response to therapy of soft tissue and bone sarcomas; a systematic review and meta-analysis. *Cancer Treat.Rev.*, 30:83-101, 2004.
33. Shields, A. F., Grierson, J. R., Dohmen, B. M., Machulla, H. J., Stayanoff, J. C., Lawhorn-Crews, J. M., Obradovich, J. E., Muzik, O., and Mangner, T. J. Imaging proliferation in vivo with [F-18]FLT and positron emission tomography. *Nat.Med.*, 4: 1334-1336, 1998.
34. Machulla, H. J., Blochter, A., Kuntzsch, M., Piert, M., Wei, R., and Grierson, J. R. Simplified labeling approach for synthesizing 3'-deoxy-3'-[<sup>18</sup>F]fluorothymidine ([<sup>18</sup>F]FLT). *Journal of Radiochemical and Nuclear Chemistry*, 243: 843-846, 2000.
35. Schelbert, H. R., Hoh, C. K., Royal, H. D., Brown, M., Dahlbom, M. N., Dehdashti, F., and Wahl, R. L. Procedure guideline for tumor imaging using fluorine-18-FDG. *J.Nucl.Med.*, 39: 1302-1305, 1998.
36. Lonneux, M., Borbath, I., Bol, A., Coppens, A., Sibomana, M., Bausart, R., Defrise, M., Pauwels, S., and Michel, C. Attenuation correction in whole-body FDG oncological studies: the role of statistical reconstruction. *Eur.J.Nucl.Med.*, 26: 591-598, 1999.
37. Fletcher, C. D. M., Unni, K., and Mertens, F. WHO classification of tumours. Pathology and genetics of tumours of soft tissue and bone. Lyon: IARC Press, 2002.
38. Coindre, J. M., Terrier, P., Guillou, L., Le, D., V, Collin, F., Ranchere, D., Sastre, X., Vilain, M. O., Bonichon, F., and N'Guyen, B. B. Predictive value of grade for metastasis development in the main histologic types of adult soft tissue sarcomas: a study of 1240 patients from the French Federation of Cancer Centers Sarcoma Group. *Cancer*, 91: 1914-1926, 2001.
39. Mier, W., Haberkorn, U., and Eisenhut, M. [(18)F]FLT; portrait of a proliferation marker. *Eur.J.Nucl.Med.*, 29: 165-169, 2002.
40. Sherley, J. L. and Kelly, T. J. Regulation of human thymidine kinase during the cell cycle. *J.Biol.Chem.*, 263: 8350-8358, 1988.





## Chapter 7

### **<sup>18</sup>F-FLT-PET for the visualization of laryngeal cancer: comparison with <sup>18</sup>F-FDG-PET**

David C.P. Cobben<sup>1,2</sup>, Bernard F.A.M. van der Laan<sup>3</sup>, Bram Maas<sup>1</sup>, Willem Vaalburg<sup>1</sup>,  
Albert J.H. Suurmeijer<sup>4</sup>, Harald J. Hoekstra<sup>2</sup>, Pieter L. Jager<sup>1</sup>, Philip H. Elsinga<sup>1</sup>

PET-center<sup>1</sup>, Departments of Surgical Oncology<sup>2</sup>, Otorhinolaryngology-Head and Neck  
Surgery<sup>3</sup> and Pathology and Laboratory Medicine<sup>4</sup> and Groningen University Hospital,  
Groningen, The Netherlands.

*Journal of Nuclear Medicine 2004; 45: 226-231*

## Summary

**Rationale:** In this study the feasibility of  $^{18}\text{F}$ -3'-fluoro-3'-deoxy-L-thymidine positron emission tomography (FLT-PET) for detecting laryngeal cancer was investigated and compared with FDG-PET.

**Methods:** Eleven patients with (or strongly suspected with) recurrent laryngeal cancer and 10 patients with histologically proven primary laryngeal cancer underwent one attenuation corrected FLT-PET, 60 minutes after injection of a median of 213 (175-400)MBq FLT, and one attenuation corrected FDG-PET, 90 minutes after injection of a median of 340 (165-650)MBq FDG. All patients were staged by endoscopy and CT according to the UICC TNM staging system. All patients underwent a biopsy of the laryngeal area after the PET-scans. Lesions on FDG-PET, and FLT-PET were compared with histopathological results. Mean SUV, max SUV and tumor/to non-tumor ratio (TNT) were calculated for FLT and FDG. Wilcoxon non-parametric testing was used for comparison of FDG with FLT uptake. Spearman's correlation coefficient was used to correlate mean SUV, max SUV and TNT of FDG-PET and FLT-PET. Two-tailed P-values <0.05 were considered significant.

**Results:** FDG-PET as well as FLT-PET detected laryngeal cancer correctly in 15 out of 17 patients. One lesion was judged as positive on FDG-PET, which turned out as normal tissue. Two lesions were judged as positive on FLT-PET, which turned out as inflammation in one lesion and normal tissue in the other lesion. Max SUV was 3.3 (1.9-8.5) for FDG and 1.6 (1.0-5.7) for FLT ( $p < 0.001$ ). Mean SUV was 2.7 (1.5-6.5) for FDG and 1.2 (0.8-3.8) for FLT ( $p < 0.001$ ). TNT was 1.9 (1.3-4.7) for FDG and 1.5 (1.1-3.5) for FLT ( $p < 0.05$ ).

**Conclusion:** The number of laryngeal cancers detected with FLT-PET and FDG-PET was equal. In laryngeal cancer the uptake of FDG is higher than FLT.

## Introduction

The current standard for staging of laryngeal cancer is direct laryngoscopy complemented with histological biopsy and computed tomography (CT) or magnetic resonance imaging (MRI) (1,2). The detection of tumors and metastatic lymph nodes by CT and MRI is solely dependent on changes in tissue structure and size of lymph nodes (2). Therefore, primary or recurrent tumors that do not distort tissue structures and non-enlarged metastatic nodes can be missed. In addition, tissue changes caused by radiation therapy can complicate interpretation of CT and MRI images as well. Despite the fact that a biopsy is the gold standard, locating the possible site of a recurrence for biopsy is still very difficult, since most recurrent head and neck cancers are located in the submucosa (1). Furthermore, the ENT-surgeon will be reluctant to obtain multiple blind biopsies, since biopsies could initiate or aggravate radionecrosis (2).

Positron emission tomography (PET), using 2'-<sup>18</sup>F-fluoro-2'-deoxy-D-glucose (FDG), is accepted as a powerful non-invasive metabolic imaging method for the diagnosis and staging of cancer (3-5). FDG-PET has been introduced as a non-invasive diagnostic tool in head and neck cancer, where it is especially accurate for the detection of cancer and provides prognostic information (6-8). However, experience with FDG-PET applied solely in patients with laryngeal cancer is limited. FDG-PET in patients with suspected recurrent laryngeal cancer has proven to be valuable to distinguish between benign and malignant tissue changes after radiation therapy (9-11). Even less data on FDG-PET is available in patients with untreated primary laryngeal cancer (9,12).

Since FDG is also metabolized in non-tumor tissue, false positive results can occur (13-15). These are the results of FDG uptake in inflammatory, reactive tissue or supraclavicular fat. In addition muscle uptake of FDG may interfere with FDG-PET interpretation. Furthermore, the time interval between radiation therapy and FDG-PET is essential for accurate diagnosis (1,9,16) .

Recently, <sup>18</sup>F-3'-fluoro-3'-deoxy-L-thymidine (FLT) has been introduced as a PET-tracer by Shields and Grierson, which might not have these drawbacks (17,18). This pyrimidine analog, is phosphorylated by the enzyme thymidine kinase 1 (TK<sub>1</sub>), which leads to intracellular trapping (18). During DNA synthesis, TK<sub>1</sub> activity increases almost tenfold and is thus an accurate reflection of cellular proliferation (19). FLT uptake is probably related to TK<sub>1</sub> activity and therefore also related to proliferation. The aim of this study was to investigate the feasibility of FLT-PET for detection of primary and recurrent laryngeal

cancer in comparison with FDG-PET. A second aim was to investigate possible differences in uptake of FLT and FDG in malignant and normal tissue.

## **Materials and methods**

### ***Patients***

This prospective study consisted of 21 consecutive patients: 11 patients with suspected recurrent laryngeal cancer and 10 patients with primary laryngeal cancer, after informed consent was obtained. Patients were included from September 2001 until March 2003.

The 11 patients with suspicion of recurrent laryngeal cancer had initially been treated for a laryngeal squamous cell carcinoma with radiation therapy. These patients were suspected to have recurrent disease, because they developed increased hoarseness, edema, pain in the larynx or referred pain. All patients with suspected recurrent laryngeal cancer underwent a diagnostic laryngoscopy for a biopsy. The 10 patients with primary laryngeal squamous cell carcinoma were candidates for radiation therapy. All patients had been clinically staged according to the UICC TNM classification (20).

All patients underwent a physical examination of the head and neck, chest X-ray, endoscopic examination under general anesthesia, biopsies of suspected areas and a spiral CT of the neck. For inclusion, liver and kidney functions and hematological parameters (Hb, Ht, erythrocytes, thrombocytes, leukocytes and white cell count) had to be within normal limits. Pregnant patients and patients with psychiatric disorders were excluded. All screened patients could be included in the study. The medical ethics committee of the Groningen University Hospital approved the study protocol.

### ***Tracer synthesis***

Synthesis of FLT was performed according to the method of Machulla et al (21). FLT was produced by [<sup>18</sup>F]fluorination of the 4,4'-dimethoxytrityl protected anhydrothymidine, followed by a deprotection step. After purification by reversed phase HPLC, the product was made isotonic and passed through a 0.22 µm filter. FLT was produced with a radiochemical purity of >95% and specific activity of >10 TBq/mmol. The radiochemical yield was 7.5 ± 5.1% (EOB).

Synthesis of FDG was performed according to the method of Hamacher et al by an automated synthesis module (22). The radiochemical yield was  $65.9 \pm 7.1\%$  (EOB).

### ***PET scanning***

All studies were performed using an ECAT EXACT HR+ (Siemens/CTI Inc., Knoxville, TN). Prior to PET imaging, patients were instructed to fast for at least 6 hours. They were also instructed to drink one liter of water prior to imaging to stimulate FLT and FDG excretion from the renal calyces and subsequent voiding.

For injection of the radiopharmaceuticals, a venous cannula was inserted in the forearm of the patient. The interval between the FDG-PET and FLT-PET was maximal 16 days. All patients were scanned 4 positions from the nose down in emission-transmission-transmission-emission mode, with 3 and 5 minutes per bed position for transmission and emission scanning, respectively. Twenty-one patients with a median age of 65 (50-81) years, 20 men and 1 woman, were included in this study (Table 1). Patients received a median of 340 (165-650)MBq FDG and a median of 213 (175-400)MBq FLT. Patients were scanned sixty minutes after FLT and 90 minutes after FDG injection. Previous experience with FLT, indicated that the tumor over non-tumor ratios were constant from 60 minutes post-injection of the tracer. PET images were iteratively reconstructed (ordered subset expectation maximization) (23).

### ***Pathological evaluation***

Biopsies of the laryngeal area and surgical specimens of total laryngectomies were examined on haematoxylin and eosin (H and E) stained sections. The pathologist (AJHS) was unaware of the results of the PET images. In patients, in whom a total laryngectomy was performed, the maximum tumor diameter was obtained (Table 1). In the remaining patients only biopsies were performed and used for histological investigation.

### ***Data analysis***

FLT-PET and FDG-PET images were analyzed for uptake in malignant lesions and normal anatomical structures. An experienced PET-physician (DCPC) evaluated the images only aware of the location of the primary or suspected lesion, but blinded for other clinical information.

Table 1. Patient characteristics

	Pt	Sex	Age	TNM PLC	Treatment PLC	Tx-interval Before PET-scan	MDT (mm)	FDG	FLT	Pathology	FDG	FDG	FDG	FLT	FLT	FLT
											Max SUV Tumor	Mean SUV Tumor	TNT	Max SUV Tumor	Mean SUV Tumor	TNT
Suspected recurrence group	1	F	52	T2N0	RTX	6 months	NA	-	+	Inflammation	NA	NA	NA	1.4	1.1	1.1
	2	M	64	T1N0	RTX	9 years	NA	-	-	No abnormalities	NA	NA	NA	NA	NA	NA
	3	M	56	T3N2c	Follow-up <sup>#</sup>	3 months	1,8	+	+	RLC	3.2	2.8	1.5	1.2	1,1	1.2
	4	M	70	T1a/CISN0	CO2 laser	6 years	NA*	+	+	RLC	1.9	1.5	1.5	1.5	1.2	1.5
	5	M	65	T2N0	RTX	9 months	18	+	+	RLC	3.0	2.3	1.5	1.3	1.1	1.4
	6	M	50	T2N0	RTX	10 months	15	+	+	RLC	8.5	6.5	4.1	2.9	1.9	3.2
	7	M	58	T1N0	RTX	1.5 months	40	+	+	RLC	3.7	2.9	2.4	1.5	1.3	1.4
	8	M	66	T4N0	RTX	3 months	20	+	+	RLC	3.3	2.6	1.4	1.9	1.4	1.4
	9	M	56	T3N1	RTX	16 months	17	+	+	RLC	2.9	2.2	1.4	1.0	0.8	1.1
	10	M	65	T1aN0	CO2 laser	13 months	NA	+	+	No abnormalities	1.9	1.6	1.3	1.5	1.2	1.1
	11	M	55	T2N0	RTX	5 months	NA	-	-	Inflammation	NA	NA	NA	NA	NA	NA
Primary laryngeal cancer group	12	M	79	T2N0	RTX	NA	NA*	+	+	PLC	2.5	1.8	1.3	1.7	1.2	1.7
	13	M	72	T3-4N0	RTX	NA	NA*	+	+	PLC	5.8	4.4	3.1	5.7	3.8	3.5
	14	M	66	T1aN0	RTX	NA	NA*	-	-	PLC	NA	NA	NA	NA	NA	NA
	15	M	55	T2N0	RTX	NA	NA*	+	+	PLC	6.2	4.8	2.8	3.2	2.0	2.2
	16	M	65	T4N0	RTX	NA	NA*	+	+	PLC	5.8	4.4	2.3	3.7	2.6	2.2
	17	M	79	T4N0	RTX	NA	NA*	+	+	PLC	3.2	2.5	2.8	2.3	1.9	1.9
	18	M	64	T1aN0	RTX	NA	NA*	+	+	PLC	2.1	1.6	1.3	1.2	0.9	1.5
	19	M	72	T1bN0	RTX	NA	NA*	-	-	PLC	NA	NA	NA	NA	NA	NA
	20	M	53	T2N0	RTX	NA	NA*	+	+	PLC	3.8	2.8	4.7	1.6	1.2	2.0
	21	M	81	T2bN0	RTX	NA	NA*	+	+	PLC	4.6	3.5	2.9	1.6	1.1	1.6

CIS=carcinoma in situ; MDT=maximum diameter of the tumor; NA=Not applicable; NP=not performed; PLC=primary laryngeal cancer; RLC=recurrent laryngeal cancer; Tx-interval= time interval between therapy of primary laryngeal cancer and PET-scan; \* =only biopsies performed; #follow-up instead of RTX, because of primary treatment of lung cancer; -=negative; +=positive.

FLT-PET and FDG-PET images were first visually interpreted. Presence of a hypermetabolic lesion was judged as positive, absence of a hypermetabolic lesion as negative. After visual interpretation both the FLT-PET and FDG-PET images were analyzed randomly for hypo- and hypermetabolic lesions and sagittal sections. The slice with the highest uptake was selected for ROI analysis. After selecting the plane with the maximum SUV, a ROI was drawn manually. ROIs were placed at the 70% contour of the maximal SUV in the tumor when possible. In other cases ROIs were drawn manually. The same ROI method was applied on the same slice in normal laryngeal tissue above or below the tumor site, to calculate the background SUV. The mean SUV of the tumor was divided by the mean SUV of the background region to produce the tumor/non-tumor ratio (TNT). TNTs and SUVs of FLT-PET and FDG-PET were compared. Images were displayed on a SUN workstation. ROI calculation was performed Clinical Applications Programming Package version 5 (CAPP5, CTI, Knoxville (TN), USA).

### ***Statistical analysis***

The results of the visually interpreted PET images were compared with the histological data, which was used as standard. Wilcoxon signed rank test was used to compare mean SUV, max SUV and TNT between FDG-PET and FLT-PET. Spearman's correlation coefficient was used to correlate mean SUV, max SUV and TNT of FDG-PET and FLT-PET. Two-tailed P-values <0.05 were considered significant.

## **Results**

### ***Patients***

Fifteen patients underwent a biopsy of the laryngeal area after the PET-scans in the Groningen University Hospital. However, patients 7, 8, 11, 12, 15 and 20 underwent a biopsy in a referring hospital. These biopsies were performed at 7 months, 17, 11, 27, 42 and 21 days prior to the PET-scans, respectively.

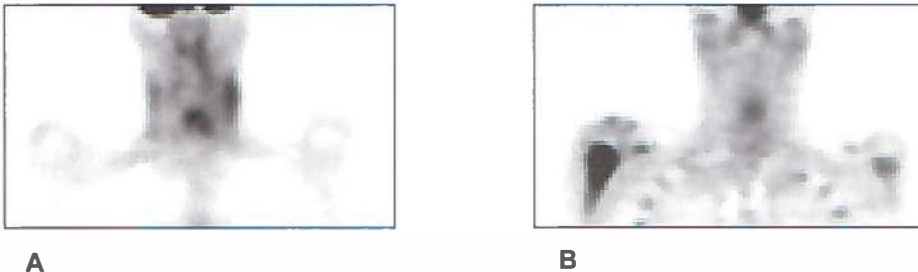
### ***Visualization of laryngeal cancer***

In patients 2, 11, 14 and 19 no uptake of FLT or FDG could be observed and therefore no SUV could be calculated. Histopathological investigation showed no

malignancy in patients 2 and 11. However, in patients 14 and 19 histopathological investigation showed two recurrent laryngeal cancers.

FDG-PET and FLT-PET detected 15 out of 17 laryngeal cancers. One lesion (Patient 10) was judged as positive on FDG-PET, which was normal tissue. FLT-PET and FDG-PET missed two T1 tumors of patient 14 and 19. Two lesions (Patients 3 and 10) were judged as positive FLT-PET on, which was inflammation in one lesion and normal tissue in the other lesion. Figure 1 demonstrates a FDG and FLT-PET image of a patient with primary laryngeal cancer.

**Figure 1. FLT-PET and FDG-PET image of primary laryngeal cancer**



Coronal FDG-PET (A) and FLT-PET (B) image of patient 3, diagnosed with primary laryngeal cancer. With both imaging modalities, uptake of the tracer in the laryngeal region can be observed. Max FDG SUV was 3.2 and max FLT SUV was 1.2. Physiological FDG uptake can be seen in the muscles of the neck and physiological FLT uptake can be observed in the bone marrow of the ribs and bones of the shoulder.

**Comparison between FDG and FLT uptake**

The uptake of FDG, was significantly higher than FLT, when expressed in mean SUV, max SUV and TNT (Table 2). The correlations between mean SUV, max SUV, TNT, of FDG and FLT, varied between 0.613 and 0.705, and were significant ( $p < 0.05$ ).

**Table 2. Wilcoxon non-parametric test**

	Max SUV	Mean SUV	TNT
FDG-PET	3.3 (1.9-8.5) <sup>#</sup>	2.7 (1.5-6.5) <sup>#</sup>	1.9 (1.3-4.7) <sup>*</sup>
FLT-PET	1.6 (1.0-5.7)	1.2 (0.8-3.8)	1.5 (1.1-3.5)

SUV expressed as median (min-max); <sup>#</sup> $p < 0.001$ ; <sup>\*</sup> $p < 0.05$ .



## Discussion

This study was conducted in 21 patients and shows that both FDG-PET and FLT-PET detected 15 out of 17 laryngeal cancers. The lesions of four patients, suspicious for laryngeal cancer turned out to be normal or inflammatory laryngeal tissue. FDG-PET detected one of those lesions as positive and FLT-PET detected two of those lesion as positive. The uptake of FDG, mean SUV of 2.7 (1.5-6.5), in laryngeal cancer was significantly higher than FLT, mean SUV of 1.2 (0.8-3.8).

Although little data are available, the limited FDG-PET data of this study, concerning the sensitivity, are in the same range as the FDG-PET data in the literature. Sensitivity for the detection of laryngeal cancer ranged between 80% and 97% (9,11,12,16,24,25), specificity ranged from 61% to 82% (10,11,16). The specificity, obtained in this study, which was 100% (3/3) for FDG-PET, is less reliable and not comparable with the literature, due to the low number of false positive and true negative lesions.

False positive results with FDG-PET can occur, since FDG is also trapped in normal tissue. Secretion of FDG in normal mucosa and saliva and pooling of saliva in the larynx may cause increased uptake in the laryngeal area (13). Increased uptake is also found in salivary glands, tonsil tissue, muscle tissue of the larynx and the neck, benign laryngeal papilloma and the base of the tongue (15). Moreover, wound healing after biopsies prior to the FDG-PET, local inflammation such as osteomyelitis, cellulitis or a polyp may cause increased local FDG uptake (9,10,13,26). Furthermore, the time interval between radiation therapy and the FDG-PET is essential for accurate diagnosis (9,10,16,27).

As an alternative for FDG, potentially more specific tracers have been developed, which take part in other metabolic processes. Several amino acids, imaging protein synthesis, have been developed as tracers. Most of these studies have been performed with L-[methyl-<sup>11</sup>C]-methionine (MET). The disadvantage of MET is substantial accumulation of non-protein related metabolites in tumor tissue (28). L-[1-<sup>11</sup>C]-tyrosine (TYR) has also been used to detect tumors and determine protein metabolism. In laryngeal and hypopharyngeal cancer TYR was able to detect all primary tumors and there was a correlation between protein synthesis rate and SUV (29-31). However, the disadvantage of this tracer is the low tumor uptake and accumulation in salivary glands, which could impair the detection of metastatic lymph nodes in head and neck cancer (28,29). In 1998 Shields et al developed FLT, a pyrimidine analogue, which indirectly

measures DNA-synthesis through the DNA salvage pathway (18). Recent articles about FLT-PET focussed on the detection of colorectal and lung cancer and their metastases (32,33). A correlation was found between the SUV and proliferation in single pulmonary nodules (32,34,35).

Despite these promising properties of FLT, FLT-PET hardly detected a recurrent laryngeal tumor (patient 3), which displayed avid uptake of FDG. The tumor was a 1.8 mm large poorly differentiated tumor surrounded with ulcers. This could explain the low FLT uptake and avid FDG uptake in the surrounding inflammation tissue. FLT-PET and FDG-PET missed two T1 tumors, which were detected on CT. The size of these tumors could be below the detection level of PET and a partial volume effect could be involved. In the literature FDG-PET misses T1 to T4 laryngeal tumors as well. However, no (histological) explanation is given for these false negative findings (11,24,25). Unfortunately, it is impossible to obtain the size of a primary laryngeal cancer. This is because diagnosis and extent of the tumor are obtained by a laryngoscopically guided biopsy and CT, since almost all T<sub>1</sub>-T<sub>3</sub> tumors are treated with radiation therapy. The size of the biopsy obtained from the tumor, is often too small to accurately assess the Ki-67 data for the correlation with FLT-uptake. In contrast, reliable Ki-67 data is possible in patients with a T<sub>4</sub> tumor, who undergo a total laryngectomy and are not palliatively treated with radiation therapy. In these patients the tumor can be fully histologically examined. However, a T<sub>4</sub> tumor often causes acute respiratory distress, urging an acute laryngectomy, making a PET-scan unethical and impossible.

Malignant tissue displayed a significant higher uptake of FDG as compared to FLT. The mean FDG SUV in the literature for patients with primary or recurrent laryngeal cancer ranges from 4.6 to 10.7 (9,12,13). These values are higher than the max FDG SUV of 3.3 (range 1.9-8.5) and mean SUV 2.7 (range 1.5-6.5) in this study. No literature is available on FLT-PET for detecting laryngeal cancer. However, in patients with colorectal cancer and lung cancer the SUV of FDG-PET and FLT-PET were compared. The mean FLT-PET SUV in colorectal cancer was 4.2 as compared with a mean FDG-PET SUV of 8.7; the FLT SUV in lung cancer ranged between 1.2 and 3.1 and FDG-PET SUV from 1.7 to 8.9 (32,33). Although these articles discuss different types of malignancies, they also report significantly lower uptake of FLT as compared to FDG, just as was found for the detection of laryngeal cancer in this study. The lower level of uptake probably raises the detection limit.

The correlation between FDG and FLT uptake was not very strong. The SUV is the net result of several uptake processes. The availability of the tracer in the blood pool, non-specific uptake, perfusion of the tumor, membrane transport, metabolic processes in which the tracer is involved and (ir)reversible trapping of the tracer flow over the membrane are factors which can influence the SUV. It is our impression that both FLT and FDG are taken up by the malignant cells, but that the demand for glucose is larger than for thymidine. The phosphorylation rate in vitro is about 30% of the phosphorylation rate of serum thymidine by thymidine kinase 1, which could be one explanation for a low FLT uptake in the tumor (36,37).

The number of patients in this study is too small to draw conclusions about the accuracy of FDG-PET and FLT-PET for detecting laryngeal cancer in general and for detecting primary or recurrent laryngeal cancer specifically. Larger groups of patients are needed with at least two observers to calculate the inter-observer agreement, which would reflect clinical reality more accurately.

Future aspects for FDG-PET and FLT-PET for laryngeal cancer are only partly clear. The role for FDG-PET in the future for detecting laryngeal cancer seems to be in the differentiation between non-tumor and tumor tissue in patients suspected of recurrent laryngeal cancer (1,9-11,13). It is reasonable to delay biopsy on a negative FDG-PET and prevent unnecessary biopsies, which could initiate or aggravate radionecrosis (1,10,11). Imaging with PET lacks of anatomical detail, but could be overcome by a PET-CT. Too little data are available for the detection of untreated primary laryngeal cancer, which has not been treated with radiation therapy (9,24,25). Further research is needed to investigate if FDG-PET is an adequate tracer for the detection of primary laryngeal cancer. Because of the low uptake of FLT in laryngeal FLT-PET seems less adequate for the detection of laryngeal cancer (11).

The number of laryngeal cancers detected with FLT-PET and FDG-PET was equal. The uptake of FDG in laryngeal cancer is higher than FLT.

## References

1. Schechter NR, Gillenwater AM, Byers RM, et al. Can positron emission tomography improve the quality of care for head- and-neck cancer patients? *Int J Radiat Oncol Biol Phys.* 2001; 51: 4-9.
2. Zinreich SJ. Imaging in laryngeal cancer: computed tomography, magnetic resonance imaging, positron emission tomography. *Otolaryngol Clin North Am.* 2002; 35: 971-91.
3. Hustinx R, Benard F, Alavi A. Whole-body FDG-PET imaging in the management of patients with cancer. *Semin Nucl Med.* 2002; 32: 35-46.
4. Bomanji JB, Costa DC, Ell PJ. Clinical role of positron emission tomography in oncology. *Lancet Oncol.* 2001; 2: 157-64.
5. Gambhir SS, Czernin J, Schwimmer J, Silverman DH, Coleman RE, Phelps ME. A tabulated summary of the FDG PET literature. *J Nucl Med.* 2001; 42: 1-93S.
6. Wong RJ, Lin DT, Schoder H, et al. Diagnostic and prognostic value of [(18)F]fluorodeoxyglucose positron emission tomography for recurrent head and neck squamous cell carcinoma. *J Clin Oncol.* 2002; 20: 4199-208.
7. Allal AS, Dulguerov P, Allaoua M, et al. Standardized uptake value of 2-[(18)F] fluoro-2-deoxy-D-glucose in predicting outcome in head and neck carcinomas treated by radiotherapy with or without chemotherapy. *J Clin Oncol.* 2002; 20: 1398-404.
8. Halfpenny W, Hain SF, Biassoni L, Maisey MN, Sherman JA, McGurk M. FDG-PET. A possible prognostic factor in head and neck cancer. *Br J Cancer.* 2002; 86: 512-6.
9. McGuirt WF, Greven KM, Keyes JW, Jr., et al. Positron emission tomography in the evaluation of laryngeal carcinoma. *Ann Otol Rhinol Laryngol.* 1995; 104: 274-8.
10. Terhaard CH, Bongers V, van Rijk PP, Hordijk GJ. F-18-fluoro-deoxy-glucose positron-emission tomography scanning in detection of local recurrence after radiotherapy for laryngeal/ pharyngeal cancer. *Head Neck.* 2001; 23: 933-41.
11. Greven KM, Williams DW, III, Keyes JW, Jr., McGuirt WF, Watson NE, Jr., Case LD. Can positron emission tomography distinguish tumor recurrence from irradiation sequelae in patients treated for larynx cancer? *Cancer J Sci Am.* 1997; 3: 353-7.
12. Lowe VJ, Kim H, Boyd JH, Eisenbeis JF, Dunphy FR, Fletcher JW. Primary and recurrent early stage laryngeal cancer: preliminary results of 2-[fluorine 18]fluoro-2-deoxy-D-glucose PET imaging. *Radiology.* 1999; 212: 799-802.
13. Greven KM, Williams DW, III, Keyes JW, Jr., et al. Distinguishing tumor recurrence from irradiation sequelae with positron emission tomography in patients treated for larynx cancer. *Int J Radiat Oncol Biol Phys.* 1994; 29: 841-5.
14. Cohade C, Osman M, Pannu HK, Wahl RL. Uptake in supraclavicular area fat ("USA-Fat"): description on 18F-FDG PET/CT. *J Nucl Med.* 2003; 44: 170-6.
15. Stokkel MP, Bongers V, Hordijk GJ, van Rijk PP. FDG positron emission tomography in head and neck cancer: pitfall or pathology? *Clin Nucl Med.* 1999; 24: 950-4.
16. Lonneux M, Lawson G, Ide C, Bausart R, Remacle M, Pauwels S. Positron emission tomography with fluorodeoxyglucose for suspected head and neck tumor recurrence in the symptomatic patient. *Laryngoscope.* 2000; 110: 1493-7.
17. Mier W, Haberkorn U, Eisenhut M. [(18)F]FLT; portrait of a proliferation marker. *Eur J Nucl Med.* 2002; 29: 165-9.

18. Shields AF, Grierson JR, Dohmen BM, et al. Imaging proliferation in vivo with [F-18]FLT and positron emission tomography. *Nat Med.* 1998; 4: 1334-6.
19. Sherley JL, Kelly TJ. Regulation of human thymidine kinase during the cell cycle. *J Biol Chem.* 1988; 263: 8350-8.
20. Sobin L, Wittekind C. TNM Classification of Malignant Tumours. (6 edn). New York: John Wiley & Sons, 2002.
21. Machulla HJ, Blochter A, Kuntzsch M, Piert M, Wei R, Grierson JR. Simplified labeling approach for synthesizing 3'-deoxy-3'-[<sup>18</sup>F]fluorothymidine ([<sup>18</sup>F]FLT). *Journal of Radiochemical and Nuclear Chemistry.* 2000; 243: 843-6.
22. Hamacher K, Coenen HH, Stocklin G. Efficient stereospecific synthesis of no-carrier-added 2-[<sup>18</sup>F]-fluoro-2-deoxy-D-glucose using aminopolyether supported nucleophilic substitution. *J Nucl Med.* 1986; 27: 235-8.
23. Lonnew M, Borbath I, Bol A, et al. Attenuation correction in whole-body FDG oncological studies: the role of statistical reconstruction. *Eur J Nucl Med.* 1999; 26: 591-8.
24. Henze M, Mohammed A, Mier W, et al. Pretreatment evaluation of carcinomas of the hypopharynx and larynx with 18F-fluorodeoxyglucose, 123I-alpha-methyl-L-tyrosine and 99mTc-hexakis-2-methoxyisobutylisonitrile. *Eur J Nucl Med Mol Imaging.* 2002; 29: 324-30.
25. Kim HJ, Boyd J, Dunphy F, Lowe V. F-18 FDG PET scan after radiotherapy for early-stage larynx cancer. *Clin Nucl Med.* 1998; 23: 750-2.
26. Sugawara Y, Braun DK, Kison PV, Russo JE, Zasadny KR, Wahl RL. Rapid detection of human infections with fluorine-18 fluorodeoxyglucose and positron emission tomography: preliminary results. *Eur J Nucl Med.* 1998; 25: 1238-43.
27. Bataini JP, Jaulerry C, Brunin F, Ponvert D, Ghossein NA. Significance and therapeutic implications of tumor regression following radiotherapy in patients treated for squamous cell carcinoma of the oropharynx and pharyngolarynx. *Head Neck.* 1990; 12: 41-9.
28. Jager PL, Vaalburg W, Pruim J, de Vries EG, Langen KJ, Piers DA. Radiolabeled amino acids: basic aspects and clinical applications in oncology. *J Nucl Med.* 2001; 42: 432-45.
29. de Boer JR, van der Laan BF, Pruim J, et al. Carbon-11 tyrosine PET for visualization and protein synthesis rate assessment of laryngeal and hypopharyngeal carcinomas. *Eur J Nucl Med Mol Imaging.* 2002; 29: 1182-7.
30. de Boer JR, Pruim J, Burlage F, et al. Therapy evaluation of laryngeal carcinomas by tyrosine-pet. *Head Neck.* 2003; in press.
31. de Boer JR, Pruim J, van der Laan BF, Que TH, Willemsen AT, Albers FW, Vaalburg W. L-1-11C-tyrosine PET in patients with laryngeal carcinomas: comparison of standardized uptake value and protein synthesis rate. *J Nucl Med.* 2003; 44: 341-6.
32. Francis DL, Visvikis D, Costa DC, et al. Potential impact of [(18F)3'-deoxy-3'-fluorothymidine versus [(18F)fluoro-2-deoxy- d-glucose in positron emission tomography for colorectal cancer. *Eur J Nucl Med Mol Imaging.* 2003; 30: 988-994.
33. Yap C, Vranjesevic D, Cameron R, Czernin J. F18-Fluorine-thymidine; a new molecular probe for PET imaging of cancer [abstract]. *Ann Surg Oncol.* 2003; 10: S38.
34. Buck AK, Schirrmeyer H, Hetzel M, et al. 3-deoxy-3-[(18F)fluorothymidine-positron emission tomography for noninvasive assessment of proliferation in pulmonary nodules. *Cancer Res.* 2002; 62: 3331-4.

35. Vesselle H, Grierson J, Muzi M, et al. In Vivo Validation of 3'deoxy-3'-[(18)F]fluorothymidine ([18F]FLT) as a Proliferation Imaging Tracer in Humans: Correlation of [18F]FLT Uptake by Positron Emission Tomography with Ki-67 Immunohistochemistry and Flow Cytometry in Human Lung Tumors. *Clin Cancer Res.* 2002; 8: 3315-23.
36. Toyohara J, Waki A, Takamatsu S, Yonekura Y, Magata Y, Fujibayashi Y. Basis of FLT as a cell proliferation marker: comparative uptake studies with [3H]thymidine and [3H]arabinothymidine, and cell-analysis in 22 asynchronously growing tumor cell lines. *Nucl Med Biol.* 2002; 29: 281-7.
37. Munch-Petersen B, Cloos L, Tyrsted G, Eriksson S. Diverging substrate specificity of pure human thymidine kinases 1 and 2 against antiviral dideoxynucleosides. *J Biol Chem.* 1991; 266: 9032-8.

## Chapter 8

### **Is $^{18}\text{F}$ -3'-fluoro-3'-deoxy-L-thymidine useful for staging and restaging of patients with non-small cell lung cancer?**

D.C.P. Cobben<sup>1,2</sup>, P.H. Elsinga<sup>1</sup>, H.J. Hoekstra<sup>2</sup>, A.J.H. Suurmeijer<sup>3</sup>, W. Vaalburg<sup>1</sup>, B. Maas<sup>1</sup>, P.L. Jager<sup>1</sup>, H.M.J. Groen<sup>4</sup>.

<sup>1</sup>PET-center, <sup>2</sup>Department of Surgical Oncology, <sup>3</sup>Department of Pathology and Laboratory Medicine, <sup>4</sup>Department of Pulmonary Diseases, Groningen University Hospital, P.O. Box 30.001, 9700 RB Groningen, the Netherlands.

*Submitted*

## Summary

**Rationale:** To compare  $^{18}\text{F}$ -3'-fluoro-3'-deoxy-L-thymidine positron emission tomography (FLT-PET) with clinical TNM staging, including FDG-PET, in patients with NSCLC.

**Methods:** Patients with NSCLC underwent a whole-body FDG-PET and whole-body FLT-PET, using a median of 360 MBq FDG (160-500) and 210 MBq FLT (130-420). FDG-PET was performed 1.5 hours post-FDG injection, FLT-PET 1 hour post-FLT-PET injection. Two independent viewers categorized all lesions independently on localization and intensity of tracer uptake. All FDG-PET and FLT-PET lesions were compared. Staging with FLT-PET was compared with clinical TNM-staging, based on history, physical examination, bronchoscopy, CT and FDG-PET. From eight patients SUVs were calculated. Maximal SUV (max SUV) and mean SUV were calculated.

**Results:** 16 patients with stage IB-IV NSCLC and one patient with strong suspicion of NSCLC were investigated. In 8 patients without pretreatment, on a lesion-by-lesion basis sensitivity was 80% and in the 9 patients with pretreatment before FLT-PET this number was 27%, using FDG-PET as the reference standard. As compared with clinical TNM staging, FLT-PET staged 8 of 17 patients correctly. In the group with previous therapy 5 out of 9 patients were staged correctly and in the group without pretreatment 3 out of 8 patients were staged correctly with FLT as compared to the TNM staging system. Max SUV of FLT-PET, 2.7 (0.8-4.5) was significantly lower than FDG-PET, 8.0 (3.7-18.8) (n=8; P=0.012). Mean SUV of FLT-PET, 2.7 (1.4-3.3) was significantly lower than FDG-PET, 6.2 (2.8-13.9) (n=6; P=0.027).

**Conclusion:** FLT-PET is not useful for staging and restaging patients with NSCLC.



## **Introduction**

Positron emission tomography (PET), using 2-<sup>18</sup>F-fluoro-2-deoxy-D-glucose (FDG), has been accepted as a non-invasive metabolic imaging method for the staging of lung cancer.(1) FDG-uptake reflects glucose consumption.(2) However, FDG is not a selective tracer, since it also accumulates in inflammatory cells. Macrophages invade tumors and appear in inflammatory lesions, causing false positive FDG-PET results.(3-5) Another problem is a decreased uptake during hyperglycemia.(6) Furthermore, FDG-PET lacks sensitivity for imaging brain metastases, since it is avidly taken up by the brain.

In the search for more specific PET-tracers, <sup>18</sup>F-fluoro-3'-deoxy-3'-L-fluorothymidine (FLT) has been developed by Shields and Grierson. FLT may not have these drawbacks.(7,8) This pyrimidine analog, is phosphorylated by the enzyme thymidine kinase 1 (TK<sub>1</sub>), which leads to intracellular trapping.(8) TK<sub>1</sub> concentration increases almost tenfold during DNA synthesis and FLT uptake may therefore accurately reflect cellular proliferation.(9)

Little data are available on the clinical comparison of FLT with FDG for staging and restaging of NSCLC.(10-12) The aim of the study was to compare <sup>18</sup>F-3'-fluoro-3'-deoxy-L-thymidine positron emission tomography (FLT-PET) with clinical TNM staging in patients with NSCLC, including FDG-PET.

## **Materials and methods**

### ***Patients***

In this prospective study, patients with histological and/or cytological confirmed NSCLC, who attended the outpatient department for various treatments, were included. All patients were staged according to the TNM staging system prior to FLT-PET scanning.(13) Clinical TNM staging was based on patient history, physical examination, bronchoscopy, chest X-ray, CT and FDG-PET. All patients were or would be included in chemo-/radiotherapy protocols at time of the inclusion. Organ functions such as liver, kidney and bone marrow should be within normal limits. Pregnant patients and patients with psychiatric disorders were excluded. The Medical Ethics Committee of the Groningen University Hospital approved the study protocol. All patients gave written informed consent.

### ***Tracer synthesis***

Synthesis of FLT was performed according to the method of Machulla et al.(14) FLT was produced by [<sup>18</sup>F]fluorination of the 4,4'-dimethoxytrityl protected anhydrothymidine, followed by a deprotection step. After purification by reversed phase HPLC, the product was made isotonic and passed through a 0.22 µm filter. FLT was produced with a radiochemical purity of >95% and specific activity of >10 TBq/mmol. Synthesis of FDG was performed according to the method of Hamacher et al by an automated synthesis module.(15)

### ***PET-scanning***

All FLT-PET scans were attenuation corrected and performed on an ECAT EXACT HR+ (Siemens/CTI Inc., Knoxville, TN). Nine FDG-PET scans were attenuation corrected on an ECAT EXACT HR+ (Siemens/CTI Inc., Knoxville, TN). The remaining eight FDG-PET scans were non-attenuation corrected, of which four were scanned on an ECAT EXACT HR+ and four on an ECAT 951/31. It is our experience that the difference between both cameras and the use of attenuation and non-attenuation technique for FDG-PET is negligible for staging of patients with NSCLC. Since FLT was the experimental tracer and our experience with FLT in lung cancer was limited, we used only attenuation-corrected images made with the EXACT HR+ camera. Prior to PET imaging, patients were instructed to fast for at least 6 hours. They also were instructed to drink one liter of water prior to imaging to stimulate FLT and FDG excretion from the renal calyces. For injection of the radiopharmaceuticals, a venous cannula was inserted in the forearm of the patient. From this cannula, a 2 ml blood sample was taken to measure serum glucose level before each FDG-PET scan. The median interval (range) between FDG-PET and FLT-PET was 3 (1-63) days. Patients were injected with a median (range) of 360 (160-500) MBq FDG and 210 (130-420) MBq FLT. Ninety minutes post-FDG injection and sixty minutes post-FLT injection, interleaved attenuation-corrected whole-body scanning was performed from crown to femur with 3 and 5 minutes per bed position for transmission and emission scanning, respectively. Data from multiple bed positions were iteratively reconstructed (ordered subset expectation maximization) into attenuated and non-attenuated FLT and FDG whole-body PET images.(16)

## **Data Analysis**

Two experienced PET-physicians evaluated the FLT-PET images independently and were unaware of patients' clinical information, including FDG-PET. The observers ranked the intensity of each lesion. The intensity was ranked as 0 (not visible), 1 (slight increase in uptake), 2 (moderate increase in uptake) and 3 (strong increase in uptake) as compared with the background uptake in the lungs. The observers reached consensus on a lesion-by-lesion basis according to the same intensity scale for differently scored lesions. Thereafter, lesions ranked as 0 or 1, were grouped as 'hypo/normometabolic' lesions and lesions that were ranked as 2 or 3 were grouped as 'hypermetabolic' lesions.

To compare the staging properties of FLT-PET with the clinical TNM system, the presence or absence of pulmonary, mediastinal and distant hypermetabolic lesions, were used. The mediastinal lesions were assigned according to the Mountain and Dresler classification of regional lymph nodes.(17) The exact location of N1 and N2 lesions is difficult to assess on PET and therefore these lesions were read in conjunction with CT, after all PET-scans had been evaluated. Lesions outside the mediastinum were described according to their anatomical locations.

After analysis of the lesions and the staging properties, SUV calculation was performed on the attenuation corrected FDG-PET and FLT-PET scans. The visually most hypermetabolic lesion on FLT-PET of each patient was compared with the corresponding lesion on FDG-PET on sagittal sections. The slice with the highest uptake was selected for ROI analysis. After selecting the plane with the maximum SUV, a ROI was drawn manually. ROIs were placed at the 70% contour of the maximal SUV in the tumor when possible. In other cases ROIs were drawn manually. SUVs of FLT-PET and FDG-PET were compared. Images were displayed on a SUN workstation. ROI calculation was performed Clinical Applications Programming Package version 5 (CAPP5, CTI, Knoxville (TN), USA).

## **Statistical Analysis**

The degree of inter-observer agreement, for detection of FLT-PET and FDG-PET lesions, was quantified with kappa ( $\kappa$ ) statistics. For analyses regarding the intensity of each lesion, the values from the consensus readings were used. Sensitivity was calculated on lesion level, using the number of pulmonary, mediastinal and distant hypermetabolic lesions. Sensitivity is expressed as mean with a 95% coincidence interval (CI). Staging

properties of FLT-PET based on the presence or absence of pulmonary, N1 or N2 lesions, or distant hypermetabolic lesions, were compared with the clinical TNM staging system. Wilcoxon signed rank test was used to compare max SUV and mean SUV, between FDG-PET and FLT-PET. Two-tailed P-values <0.05 were considered significant.

## **Results**

### ***Patients***

From January 2002 until March 2003 seventeen consecutive patients were included in this study. Their characteristics are shown in Table 1. Nine patients were included for primary staging and eight patients were included for restaging. Seven of the restaged patients completed therapy before the PET-scans. Patient 3 was scanned during chemotherapy, because of clinical progression. All patients had histological confirmed tumors, with the exception of patient 17, who had no malignancy.

**Table 1. Patient characteristics and detectability of hypermetabolic lesions on FLT-PET as compared with standard FDG-PET**

	Pt	Age	Sex	Histology	TNM	Stage	Previous therapy	Time interval between treatment and PET	Consensus FDG				Consensus FLT			
									TL	N1	N2	D	TL	N1	N2	D
Patients with pretreatment	1.	57	F	AC	T2N2-3M1	IV	Cisplatin and Gemcitabine	27 months	4	1	4	2	1	1	2	2*
	2.	56	F	AC	T2N3M1	IV	Docetaxel	14 months	1	0	1	3*	2	0	0	3*
	3.	64	F	AC	T4N0M1	IV	Cisplatin and Gemcitabine and second line Paclitaxel and Docetaxel	Just before 3rd cycle of Docetaxel	2	0	0	1	1	0	0	0
	4.	58	M	SCC	T4N1M1	IV	Epirubicin and Gemcitabine	9 months	1	1	0	1	1	0	0	0
	5.	62	M	LCUC	T4N2M0	IIIB	Cisplatin and Gemcitabine	17 months	1	0	0	0	1	0	0	0
	6.	54	F	AC	T4N2M1	IV	Cisplatin and Gemcitabine and second line Docetaxel and Irinotecan	1 month	4	0	1	11*	2	0	1	2
	7.	45	M	SCC	T1N0M1	IV	Radiotherapy on abdomen (in 1983), mediastinum (in 1983) and head and neck and supraclavicular region (in 2000)	20 months	0	0	0	2	0	0	0	1
	8.	61	M	SCC	T2N2M1	IV	Radiotherapy on recurrent tumor	2 months	1	0	1	1*	0	0	0	1
	9.	53	M	AC	TxN2/3M1	IV	Radiotherapy on acetabulum	1 week	5	0	1	30*	0	0	0	0
Patients without pretreatment	10.	57	M	SCC	T2N0M0	IB	None	NA	1	0	0	0	1	0	0	0
	11.	70	M	SCC	T2N2M0	IIIA	None	NA	1	0	1	0	0	1	1	0
	12.	67	M	SCC	T4N0M1	IV	None	NA	1	0	0	1*	1	0	0	1*
	13.	73	M	SCC	T4N2M0	IIIB	None	NA	1	0	0	0	1	0	0	1
	14.	74	M	SCC	T4N2M0	IIIB	None	NA	0	0	3	0	0	0	3	1
	15.	65	M	LCUC	T4N2M1	IV	None	NA	1	1	1	1*	1	0	0	0
	16.	43	F	AC	T4N2M1	IV	None	NA	2	0	3	2	1	1	2	0
	17.	52	M	NM	NM		None	NA	0	0	0	0	0	0	0	0
<b>Total</b>									26	3	16	55	13	3	9	12

\*including pulmonary lesions located outside the lobe with the primary tumor. AC= adenocarcinoma; D=distant hypermetabolic lesion(s); LCUC= large cell undifferentiated carcinoma; N= lesion(s) at N1 and/or N2 location; N1=lesion(s) located at N1 node location; N2= lesion(s) located at N2 node location; NA=not plicable; NM=no malignancy; SCC= squamous cell carcinoma; TL= lesion(s) in lung(s).

### **Accuracy of FLT-PET**

FLT-PET demonstrated easily interpretable images (Figure 1). Most prominent physiological uptake of the tracer was observed in liver, bone marrow, intestines and bladder. Negligible and uniform tracer uptake was present in the lungs. No uptake of the tracer was observed in the brain, mediastinum and myocardium.

**Figure 1. FDG and FLT uptake in patient with post-obstructive pneumonia**

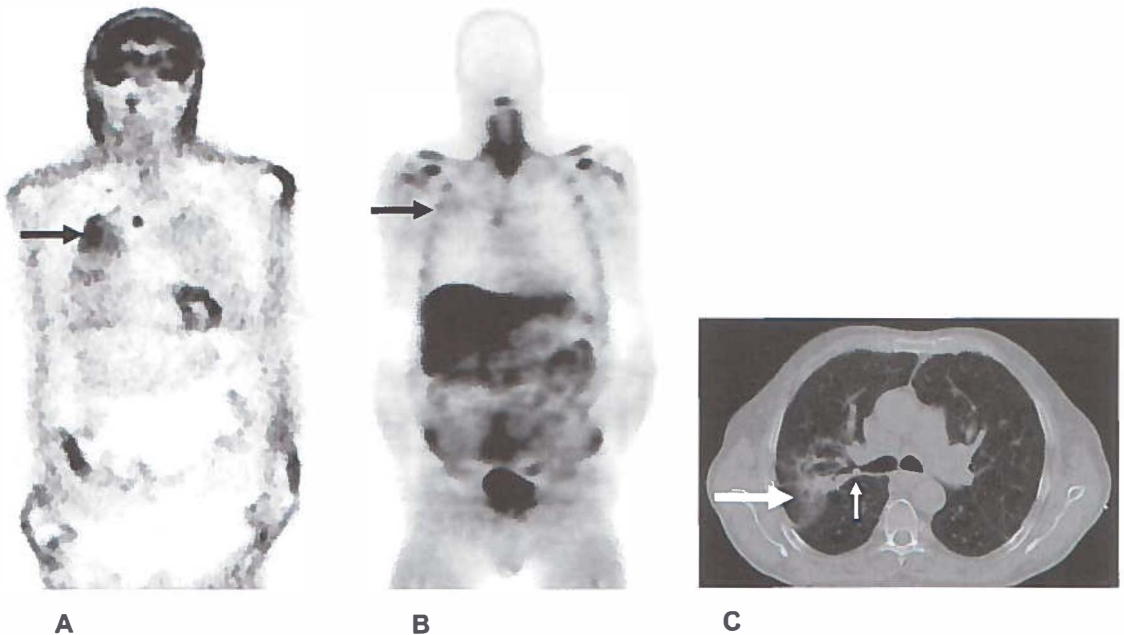


Figure 1. Coronal FDG-PET (A), FLT-PET (B) and CT image (C) of patient 11, diagnosed with squamous cell carcinoma in the right upper bronchus (small white arrow) and distally with suspected post-obstruction pneumonia (large white arrow) on CT. Avid uptake of FDG can be seen in a pre-tracheal lesion and the primary tumor, located in an area of elevated uptake, probably post-obstructive pneumonia (black arrow). Less avid uptake of FLT can be seen in the area of the tumor and little FLT uptake can be seen in the suspected infected area (black arrow). In the bone marrow of the ribs, shoulder bones, liver and intestine, there is physiological FLT uptake.

The inter-observer agreement for the detection of lesions (kappa) was 0.51 (SE=0.06) for FLT-PET and 0.55 (SE=0.06) for FDG-PET.

Overall sensitivity of FLT-PET for the detection of all hypermetabolic lesions was 37% (95% CI., 29-45%) as compared with those lesions on FDG-PET (Table 2). Sensitivity of FLT-PET for the detection of pulmonary, mediastinal (expressed as N1 and N2 lesions) and distant hypermetabolic lesions was respectively 50% (95% CI., 34-66%), 100%, 56%

(95% CI., 37-75%) and 21% (95% CI., 12-30%), using FDG-PET as the reference standard. Sensitivity was calculated on a lesion-by-lesion basis for FLT-PET using FDG-PET as the reference standard. In 8 patients without pretreatment sensitivity was 80% (95% CI., 67-93%), in 9 patients with pretreatment sensitivity was 27% (95% CI., 3-51%).

FLT-PET staged 8 of 17 patients correctly compared with clinical TNM staging (Table 1). In 8 patients without pretreatment, FLT-PET staged 3 patients correctly and 5 in 9 patients with pretreatment, compared with the clinical TNM staging.

The uptake of FDG was significantly higher than FLT, when expressed in max SUV and mean SUV (Table 2).

**Table 2. Maximum and Mean SUV and Wilcoxon non-parametric test**

Pt	lesion	FLT	FLT	FDG	FDG
		Max SUV Tumor	Mean SUV Tumor	Max SUV Tumor	Mean SUV Tumor
1.	N	4.5	3.3	9.9	6.9
2.	P	3.0	2.4	9.2	7.3
3.	P	1.6	NA	6.7	5.4
4.	P	3.9	3.1	18.8	13.9
10.	P	3.1	2.9	10.0	7.8
13.	P	0.8	NA	5.4	4.4
14.	N	2.4	1.9	5.1	3.7
16.	P	1.8	1.4	3.7	2.8
		Max SUV (n=8)		Mean SUV (n=6)	
FLT-PET		2.7 (0.8-4.5) <sup>#</sup>		2.7 (1.4-3.3) <sup>*</sup>	
FDG-PET		8.0 (3.7-18.8) <sup>#</sup>		6.2 (2.8-13.9) <sup>*</sup>	

<sup>#</sup>P=0.012; <sup>\*</sup>P=0.027; N=mediastinal lesion; NA=not assessable; P=pulmonary lesion; SUV expressed as median (min-max).

### **Additional FLT-PET findings**

In patient 11, CT showed a T1 tumor suspicious for malignancy in the right upper lobe. On both FDG-PET and FLT-PET mediastinal hypermetabolic lesions were detected (Figure 1). On FDG-PET and CT the primary tumor was located within an area, suspicious for post-obstructive inflammation. On FDG-PET this area showed diffuse FDG uptake. In contrast, on FLT-PET this inflammation was not visible, as would be expected. Patient 9 was treated with radiation therapy on the acetabulum. The field of radiation therapy and the remnant of the metastasis showed up with slightly decreased FLT activity. This lesion was ranked as hypometabolic lesion, because the observers were blinded to the clinical

history of the patient (Figure 2). On FDG-PET this area showed up as a hypermetabolic lesion, bearing in mind that this could be caused by locally increased uptake of inflammatory tissue (Figure 2). Patient 4 demonstrated a photopenic defect in the liver, which corresponds with the photopenic defect in the hypermetabolic lesion on FDG-PET in the liver (Figure 3). Vital tumor tissue in the margin cannot be discriminated from the surrounding tissue because of the high physiological FLT uptake in the liver. This lesion was suspicious for a liver metastasis seen on CT.

**Figure 2. FDG-PET versus FLT-PET for pulmonary malignancy**

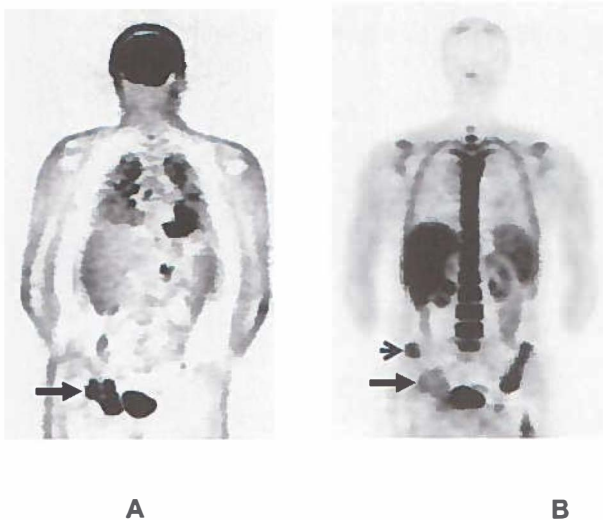


Figure 2. Coronal FDG-PET (A) and FLT-PET (B) image of patient 9, with multiple lesions in both lungs on FDG-PET and no lesions on FLT-PET. The metastasis in the right acetabulum, which had been irradiated 1 week earlier, is very prominent on FDG-PET (large arrow), but less intense on FLT-PET (large arrow). In addition, the irradiated bone marrow, cranial of the tumor, has become metabolically inactive, visible as less intense FLT uptake as compared to the non-irradiated bone marrow (small arrow).



**Figure 3. FDG-PET versus FLT-PET for liver metastasis**

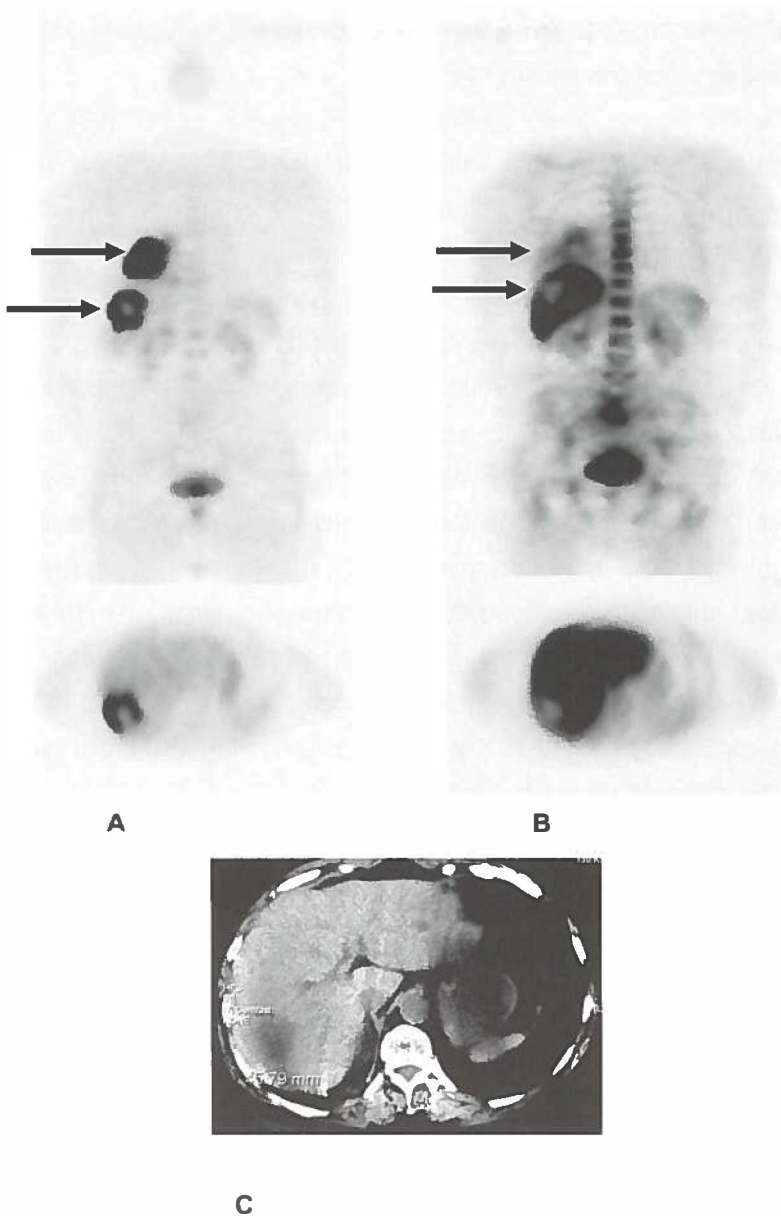


Figure 3. Coronal and transaxial FDG-PET (A), FLT-PET (B) and CT (C) images of patient 4, diagnosed with a large tumor in the right lower lung and a large metastasis in the liver on CT (large arrows). FDG-PET showed avid uptake in the lung tumor and liver metastasis (large arrows), while FLT uptake was slightly less in the pulmonary lesion and almost absent in the liver metastasis.

## Discussion

Despite the potential of FLT for imaging proliferation of cancer, our results indicate that FLT is inferior to FDG for staging NSCLC. This is consistent with two recently published abstracts and one article.(10-12)

This article focuses solely on the staging properties of FLT-PET in patients with NSCLC. Sensitivity of mediastinal and distant hypermetabolic lesions was low, which resulted to incorrect staging in 9 of 17 patients (5 in the group with pretreatment and 4 in the group without pretreatment). Most visible FLT lesions were categorized as less intense lesions than the comparable lesions on FDG-PET. Other studies confirm that FLT-PET is not an accurate tracer for staging patients with NSCLC.(10-12)

FLT uptake is related to cellular proliferation, while FDG uptake is related to increased glucose metabolism. Since most cancer cells are metabolically active, but fewer cells are proliferating, a higher net uptake of FDG than FLT in the tumor can be expected. Besides tumor cells, usually many inflammation cells are present in malignant lesions, resulting in a higher FDG uptake compared to FLT.(3) Moreover, it is known that the FLT phosphorylation rate in vitro is about 30% of the phosphorylation rate of serum thymidine by thymidine kinase 1. This could explain the low FLT uptake in the tumor.(18,19) In this study, in a small and heterogeneous group of patients, the max SUV of FLT ranged from 0.8 to 4.5 as compared to 3.7 to 18.8 for FDG. Vesselle et al also found low FLT uptake, with max SUVs ranging from 0.9 to 6.9 (20); Buck et al found max SUVs ranging from 1.3 to 10.4.(12) Lesions with a low SUV can increase the risk for misinterpretation and thus influence the accuracy of staging with FLT-PET.

Other mechanisms could explain the low sensitivity of FLT-PET for the detection of NSCLC lesions. One explanation for the low sensitivity of FLT-PET in this study could be that nine patients had received chemotherapy and/or radiation therapy prior to the PET-scans. The effects of chemotherapy on FLT uptake have been studied in vitro and in vivo in animals. This was performed in esophageal cells, 24 and 72 hours with four different types of chemotherapy and in mice with a fibrosarcoma 24 and 48 hours after 5-FU.(21,22) These studies showed that the increase or decrease of FLT uptake in the tumor after chemotherapy depends on the type of chemotherapy. However, no clinical data are available to explain the (decreased) uptake of FLT in NSCLC patients with progression after first and second line chemotherapy. Next to this, in the 8 patients, who did not receive previous therapy, the results for staging were also poor, which is in

concordance with the preliminary results of Yap et al, who found a poor sensitivity for FLT-PET in untreated NSCLC patients as well.(10) On one hand, a decrease of FLT after therapy could be a major advantage for FLT-PET compared to FDG-PET and should not per se be interpreted as a lack of sensitivity. On the other hand, the group of pretreated patients showed clinical progression, indicating lower sensitivity of FLT-PET. The ideal situation would be to obtain pathological confirmation of the lesions, to correlate the cellular activity with FLT uptake.

## **Conclusion**

Our study indicates that not only the pulmonary lesions, but also mediastinal and distant metastatic lesions are not well identified by FLT-PET. Therefore, staging with FLT-PET in patients with NSCLC is not recommended.

## References

- (1) Pieterman RM, van Putten JW, Meuzelaar JJ, Mooyaart EL, Vaalburg W, Koeter GH et al. Preoperative staging of non-small-cell lung cancer with positron- emission tomography. *N Engl J Med.* 2000;343:254-261.
- (2) Herholz K, Rudolf J, Heiss WD. FDG transport and phosphorylation in human gliomas measured with dynamic PET. *J Neurooncol.* 1992;12:159-165.
- (3) Kubota R, Yamada S, Kubota K, Ishiwata K, Tamahashi N, Ido T. Intratumoral distribution of fluorine-18-fluorodeoxyglucose in vivo: high accumulation in macrophages and granulation tissues studied by microautoradiography. *J Nucl Med.* 1992;33:1972-1980.
- (4) Yamada Y, Uchida Y, Tatsumi K, Yamaguchi T, Kimura H, Kitahara H et al. Fluorine-18-fluorodeoxyglucose and carbon-11-methionine evaluation of lymphadenopathy in sarcoidosis. *J Nucl Med.* 1998; 39:1160-1166.
- (5) Strauss LG. Fluorine-18 deoxyglucose and false-positive results: a major problem in the diagnostics of oncological patients. *Eur J Nucl Med.* 1996; 23:1409-1415.
- (6) Langen KJ, Braun U, Rota KE, Herzog H, Kuwert T, Nebeling B et al. The influence of plasma glucose levels on fluorine-18- fluorodeoxyglucose uptake in bronchial carcinomas. *J Nucl Med.* 1993;34:355-359.
- (7) Mier W, Haberkorn U, Eisenhut M. [(18)F]FLT; portrait of a proliferation marker. *Eur J Nucl Med.* 2002;29:165-169.
- (8) Shields AF, Grierson JR, Dohmen BM, Machulla HJ, Stayanoff JC, Lawhorn-Crews JM et al. Imaging proliferation in vivo with [F-18]FLT and positron emission tomography. *Nat Med.* 1998;4:1334-1336.
- (9) Sherley JL, Kelly TJ. Regulation of human thymidine kinase during the cell cycle. *J Biol Chem.* 1988;263:8350-8358.
- (10) Yap CS, Schiepers C, Quon A, Silverman DH, Satyamurthy N, Phelps ME et al. A comparison between [F-18]Fluorodeoxyglucose (FDG) and [F-18] 3'-deoxy-3'-fluorothymidine (FLT) uptake in solitary pulmonary nodules and lung cancer [abstract]. *J Nucl Med.* 2003;44(suppl):123P.
- (11) Buck AK, Hetzel M, Schirrmester H, Halter G, Glatting G, Juenling FD et al. [18F]FLT and [18F]FDG-PET for assessment of pulmonary nodules [abstract]. *Eur J Nucl Med.* 2003;29(suppl):S121.
- (12) Buck AK, Halter G, Schirrmester H, Kotzerke J, Wurziger I, Glatting G et al. Imaging Proliferation in Lung Tumors with PET: (18)F-FLT Versus (18)F-FDG. *J Nucl Med.* 2003;44:1426-1431.
- (13) Sobin L, Wittekind C. TNM Classification of Malignant Tumours. 6 ed. New York: John Wiley & Sons, 2002.
- (14) Machulla HJ, Blochler A, Kuntzsch M, Piert M, Wei R, Grierson JR. Simplified labeling approach for synthesizing 3'-deoxy-3'-[<sup>18</sup>F]fluorothymidine ([<sup>18</sup>F]FLT). *Journal of Radiochemical and Nuclear Chemistry.* 2000;243:843-846.
- (15) Hamacher K, Coenen HH, Stocklin G. Efficient stereospecific synthesis of no-carrier-added 2-[18F]-fluoro-2- deoxy-D-glucose using aminopolyether supported nucleophilic substitution. *J Nucl Med.* 1986;27:235-238.
- (16) Lonneux M, Borbath I, Bol A, Coppens A, Sibomana M, Bausart R et al. Attenuation correction in whole-body FDG oncological studies: the role of statistical reconstruction. *Eur J Nucl Med.* 1999;26:591-598.

- (17) Mountain CF, Dresler CM. Regional lymph node classification for lung cancer staging. *Chest*. 1997;111:1718-1723.
- (18) Munch-Petersen B, Cloos L, Tyrsted G, Eriksson S. Diverging substrate specificity of pure human thymidine kinases 1 and 2 against antiviral dideoxynucleosides. *J Biol Chem*. 1991;266:9032-9038.
- (19) Toyohara J, Waki A, Takamatsu S, Yonekura Y, Magata Y, Fujibayashi Y. Basis of FLT as a cell proliferation marker: comparative uptake studies with [3H]thymidine and [3H]arabinothymidine, and cell-analysis in 22 asynchronously growing tumor cell lines. *Nucl Med Biol*. 2002;29:281-287.
- (20) Vesselle H, Grierson J, Muzi M, Pugsley JM, Schmidt RA, Rabinowitz P et al. In vivo validation of 3'-deoxy-3'-[(18)F]fluorothymidine ([18F]FLT) as a proliferation imaging tracer in humans: correlation of [18F]FLT uptake by positron emission tomography with Ki-67 immunohistochemistry and flow cytometry in human lung tumors. *Clin Cancer Res*. 2002;8:3315-3323.
- (21) Dittmann H, Dohmen BM, Kehlbach R, Bartusek G, Pritzkow M, Sarbia M et al. Early changes in [18F]FLT uptake after chemotherapy: an experimental study. *Eur J Nucl Med Mol Imaging*. 2002;29:1462-1469.
- (22) Barthel H, Cleij MC, Collingridge DR, Hutchinson OC, Osman S, He Q et al. 3'-deoxy-3'-[18F]Fluorothymidine as a new marker for monitoring tumor response to antiproliferative therapy *in vivo* with positron emission tomography. *Cancer Res*. 2003;63:3791-3798.

# **Chapter 9**

## **Summary**

In this thesis the applicability of 2-[<sup>18</sup>F]-fluoro-2-deoxy-D-glucose positron emission tomography (FDG-PET) and [<sup>18</sup>F]-3-fluoro-3-deoxy-L-thymidine PET (FLT-PET) in solid tumors was explored. FDG-PET has become an important diagnostic tool in clinical oncology with many proven indications. One indication, which is being explored, is FDG-PET for the staging of melanoma patients. The sentinel lymph node (SLN) procedures might become a standard of care for staging melanoma patients with stage I and II disease, but results of a prospective trial are still pending. Since the diagnostics in oncology for staging melanoma patients, e.g. FDG-PET, SLN procedure and histopathological staining techniques, have improved in the last decade, a review of the literature was performed to gain more insight in these techniques. The value of FDG-PET for staging melanoma patients with clinical negative regional lymph nodes is limited. A comparison of FDG-PET with the SLN procedure in these patients could be of value and was therefore performed. Because FDG is not a tumor specific tracer, several potentially more specific tracers are under investigation. FLT is one of those tracers, which could be more tumor specific and less sensitive for inflammation than FDG, since it measures cell proliferation. Since melanomas have a high proliferation activity, a feasibility study was performed to stage patients with metastatic melanoma with FLT-PET. The results of this study were encouraging. Therefore FLT-PET was compared with FDG-PET in a tumor-inflammation rat model. To further explore the applicability, FLT-PET was used to correlate FLT uptake with proliferation activity in soft tissue sarcomas (STS). Next to this FLT-PET was compared with FDG-PET in two solid tumors, in which FDG-PET is performed frequently in clinical TNM staging. These tumors were non-small cell lung cancer (NSCLC) and primary and recurrent laryngeal carcinoma.

In the **introduction**, staging of cancer patients, positron emission tomography (PET), PET tracer basics, PET indications in oncology and the background of <sup>18</sup>F-fluoro-3'-deoxy-3'-L-fluorothymidine (FLT), are described.

FDG-PET, SLN biopsy and new pathological markers for the detection of metastatic melanoma are reviewed in **chapter 2**. The current histopathological techniques have improved and are able to detect up to 1 tumor cell in 10<sup>5</sup> cells. Therefore, the SLN biopsy is superior to FDG-PET for detecting micrometastasis, especially in patients with stage I and II melanoma. Although the SLN concept is improving the staging of melanoma patients, at this moment the clinical application is still under investigation. FDG-PET might

be superior to conventional imaging, such as ultrasound, MRI and CT, in the staging of patients with stage III and IV melanoma.

In **chapter 3**, the value of FDG-PET for the detection of lymphatic melanoma metastases, is compared with the SLN biopsy. Fifty-five patients with primary cutaneous melanoma,  $\geq 1.0$  mm Breslow thickness and no palpable regional lymph nodes, underwent a FDG-PET before SLN biopsy. SLN biopsy identified 13 patients (23%) with regional lymph node metastases. FDG-PET identified only 2 of these 13 patients. The lesions detected with FDG-PET were regional metastases of 7 mm and 8 mm in diameter. In addition, FDG-PET suggested incorrectly a regional lymph node metastasis in five patients. FDG-PET should not be considered for staging of patients with stage I and II melanoma, since SLN also reveals regional metastases, which are too small to be detected by FDG-PET.

The value of FLT-PET for staging patients with clinical stage III melanoma, is described in **chapter 4**. Ten patients underwent a whole-body FLT-PET. All PET lesions and histopathological lesions were categorized into anatomical regions and compared with each other. The sensitivity was 88% and the specificity was 60% (3/5), comparable with the results for FDG-PET. FLT-PET could therefore be used as a diagnostic method for staging patients with stage III melanoma. However, large studies are required, in which FLT-PET is compared with FDG-PET, before a final conclusion can be drawn.

The theoretical advantage of FLT, no uptake in inflammatory cells, was investigated in a tumor-inflammation-rat model and compared with FDG (**chapter 5**). Twelve rats with a C6-glioma tumor in one leg and a turpentine induced acute inflammation in the opposite leg, were studied with FDG-PET (n=6) and FLT-PET (n=6). Uptake of both tracers in several tissues, including the C6 tumor, inflammatory tissue and muscle, were compared. The tumor/muscle ratio of FLT was 3.3, which was fourfold lower than the FDG. The inflammation/muscle ratio of FLT uptake was only 1.2 as opposed to 4.6 for FDG. PET images confirmed that the inflammation was visualized with FDG, but not with FLT. The tumor was visible with both tracers. Thus, the hypothesis that FLT is a more tumor-selective tracer than FDG, was confirmed in this experimental rat model.

The application of FLT-PET for the detection and grading of soft tissue sarcomas (STS) in the extremities of nineteen patients is described in **chapter 6**. The measure for FLT uptake, standardized uptake value (SUV), was compared with proliferation markers of the tumor. These proliferation markers are the mitotic score and the MIB-1 score. The



survival and metastatic potential of a sarcoma is related to malignancy grade, which is largely based on proliferation scores. FLT-PET was able to visualize and differentiate high grade from low grade STS according to two clinical grading systems. The SUV correlated well with the proliferation of STS, expressed as mitotic score and MIB-1 score.

The value of FDG-PET and FLT-PET for the detection of primary and recurrent laryngeal carcinoma, compared histopathology, was studied in 21 patients and described in **chapter 7**. FDG-PET and FLT-PET detected 15 out of 17 laryngeal cancers correctly. FLT-PET was false positive in two cases and FDG-PET in one case. The SUV and TNT were lower for FLT than for FDG. The uptake of FDG is higher than FLT in laryngeal cancers.

FDG-PET is the current standard for staging patients with NSCLC. FDG-PET even surpasses CT for the staging of NSCLC in the mediastinum. In **chapter 8** the value of FLT-PET for staging and restaging of patients with non-small cell lung cancer in seventeen patients is described and compared with clinical TNM staging, including FDG-PET. On a lesion-by-lesion basis, the overall sensitivity of FLT-PET was 37% as compared to FDG-PET. Especially pulmonary lesions and distant metastatic lesions were missed with FLT-PET. Only 5 of the 17 patients were staged correctly with FLT-PET compared to the clinical TNM-staging system, including FDG-PET. It may be concluded that FLT-PET is therefore inadequate for staging and restaging of patients with NSCLC.

### **Overall conclusions and future perspectives**

This thesis describes the evaluation of 2-[<sup>18</sup>F]fluoro-2-deoxy-D-glucose-PET (FDG-PET) and [<sup>18</sup>F]-3-fluoro-3-deoxy-L-thymidine PET (FLT-PET) in solid tumors. Over the last decade the number of indications for FDG-PET has increased, and many new indications are under investigation. FDG-PET, which is superior to conventional imaging (ultrasound, MRI and CT), might be useful for staging patients with stage III and IV melanoma. Large patient studies are being conducted to investigate the value of FDG-PET for staging patients with stage III, IV and recurrent melanoma and the value of SLN biopsy for staging patients with stage I and II melanoma. The data obtained thus far confirm the value of FDG-PET and the SLN biopsy in patients with metastatic melanoma. This has resulted in implementing the SLN biopsy as a staging procedure for patients with metastatic melanoma and including the outcome of the sentinel node in the latest TNM-staging system for melanoma. The final results on the value of FDG-PET for staging melanoma

patients with palpable lymph nodes are pending, before it might become a standard diagnostic tool.

Although FDG-PET is superior to many conventional diagnostic techniques, it has drawbacks as well. Especially physiological uptake in the brain, heart, urinary system, inflammatory tissues and muscle can make the interpretation of the lesions difficult or cause false positive lesions. Therefore, new and more specific tracers are under investigation. One of those tracers is FLT.

What role can FLT-PET play in clinical oncology? FLT-PET is able to detect solid tumors and distinguish between tumor and inflammation in an animal model and some clinical studies. The study to measure the selectivity of FLT, was only performed in one specific (acute) inflammation model. Therefore, to investigate the claim that FLT is not taken up in inflammatory cells, more research with FLT-PET is required in different inflammation models (e.g. in lymph nodes of rats or canines), in patients with different inflammatory diseases (e.g. sarcoidosis, ulcerative colitis, Crohn's disease, etc) and in patients with proven metastatic lymph nodes.

Since FLT uptake is lower than FDG uptake in most investigated cancers, the role of FLT-PET in clinical oncology will be limited to cancers with a high proliferative activity. These forms of cancer, like oesophageal cancer, high grade soft tissue sarcomas and B-cell lymphomas, are currently under investigation. Preliminary reports on FLT-PET for the detection of lymphoma and oesophageal cancer, are promising. Both tumor types expressed a SUV of five on FDG-PET and on FLT-PET. FLT could also become a promising tracer for brain tumors, because low physiological uptake can be seen in the brain, whereas brain tumors have a high proliferation rate. When FDG-PET, CT or MRI scans are unable to differentiate between irradiation induced fibrosis and suspected recurrent tumor, FLT-PET can be a complementary diagnostic tool, before performing a biopsy.

Because FLT uptake reflects DNA synthesis, it can become a challenging tracer for therapy evaluation. The scarce data available on FLT-PET for the evaluation of chemotherapy indicates that FLT uptake is dependent on the dosage and the type of chemotherapeutic agent. FLT uptake in the tumor can either increase or decrease after chemotherapy, because these agents interfere with DNA synthesis. More research is needed on the uptake mechanisms of FLT in relation to the different chemotherapeutic agents to understand what changes in FLT uptake during and after therapy evaluation

mean for the treatment efficacy. The preliminary results of high grade STS for the therapy evaluation of isolated limb perfusion is promising as well. Since these tumors express a high initial FLT uptake, these tumors are likely to be valuable to investigate therapy evaluation.

FLT has disadvantages as well. Thus far, relatively low radiochemical yields, make it impossible to prepare multi-patient doses. However several reports have appeared, describing optimized production methods. Only a fraction of malignant cells in a tumor is in the late G<sub>1</sub> or S-phase, resulting in FLT uptake in a fraction of the cells. In contrast, the majority of malignant cells in a tumor is metabolically active, as well as the inflammatory cells surrounding the tumor. Therefore, a high FDG uptake can be expected in tumors. This may be an important reason why the FLT uptake is lower than the FDG uptake in tumors. Moreover, the phosphorylation rate of FLT is 30% of the phosphorylation rate of thymidine, which may result in decreased intracellular trapping. When FLT uptake is below the visual threshold, tumors are easily missed with FLT-PET. Because FLT is metabolized in the liver and physiologically taken up in bone marrow, it is not an accurate tracer for the detection of liver malignancies, liver metastases and bone metastases. False positive lymph nodes in patients with laryngeal cancer and in a sarcoma patient were found. False-positive FLT-PET findings of lymph nodes and high FLT uptake in the hilar regions of a sarcoidosis patient, were also mentioned by the group of Shields et al.

In conclusion, future research with FLT-PET should focus on the selective detection of highly proliferative cancers and its therapy evaluation. For these indications and the staging of cancer, FLT-PET could become a valuable complementary diagnostic tool.



# **Chapter 10**

## **Samenvatting**

Positron emissie tomografie (PET) is een 'in vivo imaging' techniek die in toenemende mate wordt toegepast bij de diagnostiek en stadiëring bij patiënten met kwaadaardige tumoren. Dit proefschrift beschrijft de toepasbaarheid van 2-[<sup>18</sup>F]-fluoro-2-deoxy-D-glucose PET (FDG-PET) en [<sup>18</sup>F]-'3-fluoro-'3-deoxy-L-thymidine PET (FLT-PET) bij diverse solide tumoren, zoals het melanoom, weke-delen tumoren, larynx carcinoom en niet-kleincellig longcarcinoom. Daarnaast wordt een experimenteel tumor-ontstekingsmodel in de rat beschreven. De specifieke eigenschappen van de beide tracers met betrekking tot de differentiatie tumor versus ontsteking werden in dit model onderzocht.

In de **inleiding** wordt allereerst ingegaan op de stadiëring van patiënten met kanker. Daarnaast wordt de techniek van PET, de diverse PET-tracers en de huidige indicaties van PET in de oncologie beschreven. Ten slotte worden de achtergrond en de diverse aspecten van de nieuwe PET-tracer [<sup>18</sup>F]-'3-fluoro-'3-deoxy-L-thymidine (FLT) belicht.

Voor het stadiëren van patiënten met een melanoom zijn de laatste jaren diverse technieken beschikbaar gekomen, zoals PET, de schildwachtklier (SWK) biopsie en nieuwe pathologische markers. In **hoofdstuk 2** wordt een overzicht gegeven van de huidige toepassingsmogelijkheden van deze technieken bij de behandeling van het melanoom.

In **hoofdstuk 3** wordt de waarde van FDG-PET voor de detectie van lymfkliermetastasen bij het klinisch niet-regionaal-gemetastaseerde melanoom vergeleken met de SWK biopsie. Vijfenvijftig patiënten met een primair melanoom, Breslow dikte van  $\geq 1.0$  mm zonder palpabele lymfklieren, ondergingen een FDG-PET voorafgaand aan de SWK biopsie. Met de SWK biopsie werden bij 13 patiënten (23%) regionale lymfkliermetastasen aangetoond. Daarentegen identificeerde FDG-PET lymfkliermetastasen bij slechts 2 van deze 13 patiënten. De laesies die gedetecteerd werden met FDG-PET bestonden uit regionale lymfkliermetastasen met een diameter van respectievelijk 7 en 8 mm. FDG-PET detecteerde bij 5 patiënten onterecht lymfkliermetastasen. Voor het stadiëren van patiënten met een klinisch stadium I en II melanoom is de SWK procedure beter dan FDG-PET. Er is daarom geen plaats voor FDG-PET in de diagnostiek van patiënten met een klinisch stadium I en II melanoom.

De waarde van FLT-PET voor de stadiëring van patiënten met klinisch stadium III melanoom wordt beschreven in **hoofdstuk 4**. Tien patiënten ondergingen een whole-body

FLT-PET. Alle laesies op FLT-PET en histopathologische laesies werden ingedeeld in anatomische regio's en met elkaar vergeleken. De sensitiviteit was 88% en de specificiteit 60%. Dit is vergelijkbaar met de resultaten uit de literatuur voor FDG-PET bij de stadiëring van stadium III melanoom. FLT-PET zou daarom gebruikt kunnen worden bij het stadiëren van patiënten met stadium III melanoom. Welke tracer de uiteindelijke voorkeur heeft bij de stadiëring van stadium III melanomen, zal in een vergelijkend onderzoek met een groter aantal patiënten onderzocht moeten worden.

Het theoretische voordeel van FLT ten opzichte van FDG is, dat FLT wel in tumorcellen, maar niet in ontstekingscellen zou worden opgenomen. Teneinde dit te onderzoeken werd een experimenteel tumor-ontstekingsmodel in de rat gebruikt. In **hoofdstuk 5** wordt een experimentele studie met dit model beschreven waarin FLT wordt vergeleken met FDG. Twaalf ratten met een C6-glioom in een voorpoot en een door terpentijn geïnduceerde acute ontsteking in een achterpoot, werden onderzocht met FDG-PET (n=6) en FLT-PET (n=6). De opname van beide tracers in verschillende weefsels werd bepaald. De tumor/spier ratio voor FLT was 3.3, welke vier keer lager was dan de ratio van FDG. De ontsteking/spier ratio van FLT was 1.2 in tegenstelling tot 4.6 voor FDG. De PET-afbeeldingen bevestigden dat de ontsteking werd gedetecteerd met FDG, maar niet met FLT. De tumor was detecteerbaar met beide tracers. De hypothese dat FLT een meer tumorspecifieke tracer is dan FDG werd in dit model bevestigd.

De toepassing van FLT-PET voor de detectie en gradering van weke-delen sarcomen (WDS) in de extremiteiten van negentien patiënten wordt beschreven in **hoofdstuk 6**. De mate van FLT-opname, uitgedrukt in standardized uptake value (SUV), werd vergeleken met afgeleiden van de delingsactiviteit van de tumor, zoals de mitotische score en de MIB-1 score. Met FLT-PET konden alle sarcomen worden afgebeeld en kon het onderscheid gemaakt worden tussen hoog- en laaggradige WDS. De SUV correleerde met de proliferatiegraad van WDS, uitgedrukt als mitotische score en MIB-1 score. Hoewel FLT-PET kan differentiëren tussen hoog- en laaggradige sarcomen, zal de plaats van FLT-PET in de diagnostiek en behandeling van weke-delen tumoren nog nader moeten worden onderzocht.

In **hoofdstuk 7** wordt het gebruik van FDG-PET en FLT-PET voor de detectie van primair en recidief larynxcarcinoom beschreven. Bij 21 patiënten werd de waarde van beide tracers onderzocht en werden de resultaten vergeleken met de huidige klinische standaard, de combinatie van CT en pathologie. FDG-PET en FLT-PET detecteerden 15

van 17 larynxcarcinomen correct. FLT-PET was vals-positief in 2 gevallen en FDG-PET in 1 geval. De SUV en tumor/non-tumor ratio waren lager voor FLT dan voor FDG. FLT-PET en FDG-PET waren even nauwkeurig voor de detectie van larynxcarcinomen, echter de opname van FLT in de tumoren was lager dan FDG.

Bij de stadiëring van patiënten met een niet-kleincellig longcarcinoom (NSCLC) is FDG-PET een standaardonderzoek. In **hoofdstuk 8** wordt de toepasbaarheid van FLT-PET voor het stadiëren en restadiëren van patiënten met NSCLC beschreven. Zeventien patiënten met een NSCLC ondergingen een FDG-PET en een FLT-PET en werd de klinische TNM-stadiëring van beide onderzoekstechnieken bestudeerd. Op basis van gedetecteerde laesies, was de sensitiviteit van FLT-PET slechts 37%, ten op zichte van FDG-PET. Door FLT werden vooral laesies in de longen en op afstand niet gedetecteerd. Slechts 5 van de 17 patiënten werden correct gestadieerd met FLT-PET, vergeleken met de klinische TNM-stadiëring. FLT-PET is daarom een inadequate methode om patiënten met NSCLC te stadiëren en te restadiëren.

### **Conclusies en toekomstperspectieven**

Dit proefschrift beschrijft de toepassingsmogelijkheden van FDG-PET en FLT-PET bij melanomen, weke-delen sarcomen, primair en recidief larynxcarcinomen, en niet-kleincellige longcarcinomen. Het experimentele onderzoek heeft aangetoond dat FLT-PET inderdaad meer tumor specifiek is dan FDG-PET.

Gedurende het laatste decennium is een aantal indicaties voor FDG-PET gedefinieerd, zoals het diagnostiseren van solitaire laesies in de longen, stadiëren van longkanker, therapie evaluatie van lymfomen en herstadiëren van recidief coloncarcinomen. In de naaste toekomst zullen waarschijnlijk ook nieuwe indicaties gedefinieerd worden. Zo heeft een whole-body FDG-PET de potentie om ongeveer 25% van de patiënten met een stadium III melanoom te 'upstagen'. De vraag is nu, hoe kan een patiënt met een stadium III melanoom het best gestadieerd worden? Hiertoe worden momenteel 'whole body FDG-PET' en 'whole-body spiraal-CT' bij het stadium III melanoom prospectief met elkaar vergeleken. De waarde van FDG-PET bij stadium IV melanoom is vooral gelegen in het vaststellen van de uitgebreidheid van de metastasering, ten einde de meest optimale kankerbehandeling te kunnen vaststellen. De SWK procedure is tot nu toe een stadiërende ingreep bij het stadium I en II melanoom en is inmiddels opgenomen in de gereviseerde TNM-classificatie. Of deze verbeterde



stadiëring van de regionale lymfklierstations en de daarbij horende therapeutische lymfklierdissectie ook zal lijden tot een verbeterde overleving wordt momenteel onderzocht.

Een beperking van de toepasbaarheid van FDG-PET is gelegen in de fysiologische opname van FDG in de hersenen, hart, urinewegen, spierweefsel en ontstekingsweefsel waardoor de interpretatie van de gevonden afwijkingen met FDG-PET bemoeilijkt kan worden of vals-positieve uitslagen kan veroorzaken. Daarom wordt er naar nieuwe, meer specifieke PET-tracers gezocht. FLT is hiervan een voorbeeld. Welke rol zou FLT-PET kunnen spelen in de klinische oncologie? FLT-PET kan solide tumoren detecteren en onderscheid maken tussen tumor en ontsteking zoals aangetoond is in een diermodel en in een aantal klinische pilot studies. De selectiviteit van FLT werd slechts in één specifiek (acuut) ontstekingsmodel onderzocht. Er is vervolgonderzoek nodig in verschillende tumor-ontstekingsmodellen en verschillende vormen van ontsteking in patiënten om meer inzicht te verkrijgen in de achtergronden en toepassingsmogelijkheden van FLT.

De rol van FLT-PET in de klinische oncologie zal vooral beperkt blijven tot kankervormen met een (zeer) hoge delingsactiviteit. De opname van FLT in tumoren met een lage delingsactiviteit is namelijk lager dan die van FDG; tumoren met een lage delingsactiviteit worden beter afgebeeld met FDG dan met FLT. Daarom zal het vervolgonderzoek naar de toepassingsmogelijkheden van FLT gelegen zijn bij tumoren met een hoge delingsactiviteit zoals het oesofaguscarcinoom en B-celmyeloom. FLT-PET dient daarnaast onderzocht te worden bij de detectie van hersentumoren. Immers hersentumoren hebben een hoge delingsactiviteit terwijl er een lage fysiologische opname van FLT in het brein is. Wanneer FDG-PET, spiraal-CT of MRI geen onderscheid kunnen maken tussen door bestraling veroorzaakte fibrose en een mogelijk tumorrecidief, zou de waarde van FLT-PET als complementaire afbeeldingstechniek onderzocht kunnen worden.

De mate van FLT-opname weerspiegelt de DNA-synthese, die een afspiegeling zou kunnen zijn van het effect van behandeling. Onderzoek is nodig om de opnamemechanismen van FLT in relatie tot de verschillende chemotherapeutica bij diverse tumorsoorten te begrijpen en te onderzoeken wat de veranderingen in FLT-opname gedurende en na chemotherapie betekenen voor de effectiviteit van de behandeling.

FLT heeft ook nadelen. Bij de bereiding van FLT is de radiochemische opbrengst te laag om meerdere patiënten uit één opbrengst te kunnen scannen. Het is te verwachten

dat er betere productiemethoden ontwikkeld zullen worden. Vooralsnog is het daarom niet mogelijk om grootschalig onderzoek met deze tracer uit te voeren.

Slechts een fractie van maligne cellen is in de late G<sub>1</sub>- of S-fase. Een beperkt aantal cellen zal dus FLT kunnen opnemen. De meerderheid van de maligne cellen is, net als ontstekingscellen die de tumor omgeven, metabool actief, wat leidt tot een hoge FDG-opname. Dit is waarschijnlijk een belangrijke reden waarom de FDG opname hoger is dan de FLT-opname in tumoren. De fosforyleringssnelheid van FLT is slechts 30% van die van thymidine, wat ook een reden voor verminderde intracellulaire FLT-opname kan zijn. Wanneer de FLT-opname in tumoren onder de detectiegrens komt, worden deze tumoren niet met FLT-PET gedetecteerd. FLT wordt gemetaboliseerd in de lever en daarnaast opgenomen in het beenmerg. FLT is daarom een onnauwkeurige tracer voor de detectie van levertumoren, levermetastasen en botmetastasen. Het is nog onduidelijk waarom er false-positieve opnamen worden gevonden in lymfklieren.

Toekomstig onderzoek met FLT-PET zal zich moeten richten op de selectieve detectie, stadiëring en therapie-evaluatie van kankervormen met een hoge delingsactiviteit. Met name voor deze indicaties zou FLT-PET mogelijk een waardevolle complementaire diagnostische techniek kunnen zijn.

# Dankwoord

Allereerst wil ik de patiënten, die aan dit onderzoek hebben meegedaan bedanken. Ondanks de belasting die de diagnose kanker met zich mee brengt en de onzekerheid van de waarde van FLT-PET bij hun vorm van kanker, waren velen bereid deel te nemen aan dit onderzoek. Daarnaast wil ik de KWF-Kankerbestrijding met al hun vrijwilligers en donateurs bedanken voor mogelijkheid de waarde van FLT-PET bij patiënten met kanker te kunnen onderzoeken.

Promoveren is een teamgebeuren en het team bij deze promotie is groot. Behalve de directe begeleiders, was een intensieve samenwerking tussen het PET-centrum en de afdelingen Chirurgische Oncologie, Pathologie en Laboratoriumgeneeskunde, KNO en Longziekten onontbeerlijk bij het tot stand komen van deze promotie. Ik zou iedereen willen bedanken die direct of indirect hieraan meegewerkt heeft. Daarnaast wil ik een aantal mensen in het bijzonder noemen:

Professor Hoekstra, beste Harald, jouw eindeloos enthousiasme, brede wetenschappelijke interesse, en ongelooflijk snelle manuscriptcorrectie hebben zeer motiverend gewerkt. Bijna elke patiënt die op jouw poli kwam, wist jij te overtuigen van de waarde van PET-onderzoek. Jij nam de binnenbocht van de haarspeldbocht als dat nodig was.

Professor Vaalburg, beste Wim, bedankt voor alle steun en vrijheid, die ik van jou kreeg om het onderzoek zelfstandig uit voeren met alle medewerkers en faciliteiten op het PET-centrum, where science meets medicine.

Dr. Elsinga, beste Philip, voor jou was dit het eerste KWF-project(leiderschap) (en gelukkig niet het laatste); voor mij was dit de eerste ervaring met PET-techniek, radiochemie, fysici en (radio)chemici. Je deur stond altijd voor mij open. Jouw nuchterheid, inzicht in het beta-denken (0 of 1 en heel soms 0,5), diplomatie en nuchtere wetenschappelijke houding zijn erg belangrijk geweest voor het traject van tracer tot en met publicaties. Daarnaast hebben de FLT-dreamteam borrels, etentjes en het congres in New Orleans geleid tot veel humor, hilariteit en gevleugelde uitspraken als: "Sergeant Cobben en Kletsmajoor Elsinga", "Dr E en Dr D", "no tracer, no fun", "proud to serve you", "for your own safety", "don't wanna rush ya, but...", etc.

Dr. Suurmeijer, beste Albert, jouw nauwkeurige beoordelingen van coupes en kleuringen, gortdroge humor en "wat willen we weten en wat kunnen meten"-houding, hebben geleid tot zeer gedegen en pragmatische oplossingen en goed te volgen publicaties.

Dr. Jager, beste Piet, jij was de ideale wetenschapper en clinicus met inzicht van de kliniek en de (on)mogelijkheden van PET. De artikelen wilde ik niet wegsturen voordat jij er naar gekeken had. Jij bent ook erg belangrijk geweest bij het bedenken van de proefdierstudie. Naast de wetenschap heb ik erg veel en hard met jou gelachen. Ook jij bent een belangrijk lid van het FLT-dreamteam, Mr. Jager-Applejuice...

I want to thank Prof. Dr. Ooyen, Prof. Dr. Roodenburg and Prof. Dr. Machulla for taking place in my "leescommissie".

Dr. van Waarde, beste Aren, bedankt voor het uitvoeren en opzetten van de proefdierstudie. En natuurlijk het geduld met de DEC.... We zijn nu de eerste groep die "de claim" van FLT onderzocht heeft en het vormt een belangrijke basis van proefschrift.

Het PET-centrum was mijn (uitvals)basis. Hier werken veel mensen die mij geholpen hebben bij mijn onderzoek. Beste Bram, bedankt voor al het (ontwikkelings)werk van FLT. Verder zorgde jij voor alle metabolietenbepalingen en dynamische bepalingen en de daarbij behorend heldere uitleg. Daarnaast heb je hetzelfde gevoel voor humor als ik en dat kan ik erg op waarde schatten. Ik vind het niet meer dan normaal dat jij mijn paranimf bent. Hilde en Moniek, jullie hadden als FLT-backup-team een 100% succespercentage, waarvoor mijn grote dank. Alle medisch nucleair werkers, Judith, Johan, Sabine, Yvonne, Arwin, en Remco bedankt voor jullie hulp en langer blijven bij de soms bewerkelijke protocollen. Beste Arja en Erna, bedankt voor alle hulp bij het plannen en verzetten van patiënten voor deze studie. Annie, bedankt voor alle logistiek en financiële zaken achter de schermen, die zorgden dat ik me alleen maar hoefde te richten op mijn promotie-onderzoek.

Ik wil alle medewerkers van de afdelingen Chirurgische Oncologie, KNO, Longziekten, Radiotherapie en Nucleaire Geneeskunde bedanken voor hun directe en indirecte betrokkenheid bij de inclusie van patiënten en de logistieke consequenties die dit met zich meebracht. Een aantal van hen wil ik hier apart bedanken. Beste Kees, Robert en Klaas, jullie waren altijd precies op de hoogte van potentiële patiënten(stromen) en gaven alvast een "voorzet" op de poli. Beste Bernard en Marianne, de samenwerking met jullie en jullie niet-aflatend enthousiasme heeft geleid tot een hoofdstuk en een onderzoekslijn die nu nog loopt. Harry, John en Nick voor het enthousiast maken van vaak zeer zieke patiënten om nog een extra PET-scan te ondergaan. Tom voor alle radiotherapeutisch achtergrondinformatie, humor en vriendschap en Alof voor zijn humor en het eenvoudig

oplossen van mijn "printproblemen". Riemer en Jan jullie waren altijd bereid tot uitleg van de bevindingen op PET en het aanpassen van planning.

Daarnaast heb ik de indicatiebesprekingen van de chirurgische oncologie, hoofd-hals oncologie, de mammawerkgroep, het longpanel en de directe samenwerking met stafleden, fellows en CHIVO's van de chirurgische oncologie als erg leerzaam en prettig ervaren.

Dr. Boeve, beste Jan-Willem, bedankt voor jouw kritische correctie van de inleiding van het proefschrift, in het bijzonder op het gebied van de radiologie.

De PET-onderzoekers, Remge, Liesbet, Carolien, Anne-Rixt en Lukas. Samen hebben we stoom kunnen afblazen en het onderzoek kunnen relativeren, waardoor de ontwikkeling van mijn zitblaren op het einde een stuk verdraagzamer was. FLT-PET voor de detectie van mammacarcinoom, de therapie-evaluatie van weke-delen sarcomen, primair larynxcarcinoom en non-seminoma testes is nog niet af. Ik ben daarom erg blij dat Lukas Been het stokje van me overneemt. Jij bent de juiste man op de juiste plek.

Collega onderzoekers bij chirurgie, in het bijzonder Erik, Tjeerd, Martin en Esther. De lunch liep vaak uit op POG (Promotie-ontwijkend gedrag). Heerlijk!

Beste Martijn, onze extra-curriculaire activiteiten zijn altijd erg gezellig en zorgen voor de juiste dosis ontspanning. Jouw goedlachse instelling en tips bij de overgang van onderzoek naar de chirurgie zijn zeer waardevol gebleken. Nog even doorbijten en dan sta jij hier. Met jou als paranimf, in combinatie met Bram, weet ik zeker dat jullie zorgen voor leuke dag.

Alle arts-assistenten chirurgie wil ik bedanken voor de prettige werksfeer waarin ik terecht ben gekomen als broekie. Jullie hebben mijn liefde in het voetbal weer aangewakkerd op het veld. Ik hoop dat nu duidelijk is dat Cobben zich moeilijk van de bal laat af zetten...

Simon, Jan, Khay en Reimon. Ik wil jullie bedanken voor alle agressie en stress, die ik kwijt mocht raken in de tennisballen die jullie om de oren vlogen elke vrijdag.

Lieve Tom, broeder, ik wil graag onderzoek doen en mensen opereren; jij wilt niets liever dan dieren opereren. Onze grote huisdieren hebben deze ambities regelmatig aan den lijve mogen ondervinden... Nog even en dan mag ik jou assisteren en hebben we wat meer tijd om bij te kletsen en je Belgische biertjes te "nuttigen". Jij ook succes met de laatste loodjes.

Lieve pap en mam, jullie ben ik veel dank verschuldigd. Met veel liefde, warmte en humor werd en word ik door jullie omringd en hebben jullie mij gestimuleerd en gesteund om mijn ambities te verwezenlijken.

Allerliefste Brigitte, het is bijna onmogelijk om mijn dank kort uit te drukken. Ik weet niet waar jij je energie en parate statistische kennis vandaan haalt, maar ik ben altijd erg blij als ik wat van de jouwe mocht en mag lenen. Daar heb ik gretig gebruik van gemaakt zonder dat je daar officieel bedankt voor wilde worden (tja...). Jouw glimlach en lichtjes in je ogen doen alles even stilstaan. Deze dag is ook om jou te bedanken en alvast een voorproefje...

## **Curriculum Vitae**

David Cobben werd geboren op 8 juni 1974 te Maastricht. Na het behalen van het VWO diploma in 1992 te Meerssen begon hij met de studie Geneeskunde aan de Universiteit Maastricht. Vanaf zijn tweede studiejaar werkte hij als student–onderzoeker achtereenvolgens bij de afdelingen Bewegingswetenschappen, Neurologie en Heelkunde. Zijn wetenschappelijke stage volgde hij bij de afdeling Heelkunde in het Academisch Ziekenhuis Maastricht (AZM), getiteld "The role of renal arginine during endotoxemia in the rat". In 1999 behaalde hij na een stage Emergency Medicine in Toronto, Canada, het artsexamen. Hierna werkte hij een half jaar als arts–onderzoeker bij de afdeling Heelkunde aan de Vrije Universiteit in Amsterdam. Daarna was hij 7 maanden werkzaam als arts–assistent bij de afdeling Heelkunde in het Academisch Ziekenhuis Groningen (AZG). Van 1 september 2000 tot 1 september 2003 is hij werkzaam geweest als arts–onderzoeker bij het PET–centrum en de afdeling Chirurgische Oncologie in het AZG, waar dit proefschrift tot stand kwam. Op 1 september 2003 is hij begonnen met de opleiding Heelkunde in het AZG (opleider Prof. Dr. H.J. ten Duis).



## Publications

Hallemeesch M, Cobben D, Dejong C, Soeters P, Deutz N. Renal amino acid metabolism during endotoxemia in the rat. *Journal of Surgical Research* 2000; 92: 193-200.

Hallemeesch M, Cobben D, Soeters P, Deutz N. Differential effects of selective and non-selective NOS inhibition on renal arginine and protein metabolism during endotoxemia in rats. *Clinical Nutrition* 2002; 21: 111-117.

Cobben D, Koopal S, Tiebosch A, Jager P, Elsinga P, Wobbles Th, Hoekstra H. New diagnostic techniques in staging in the surgical treatment of cutaneous malignant melanoma. *European Journal of Surgical Oncology* 2002; 28: 692-700.

Havenga K, Cobben D, Oyen W, Nienhuijs S, Hoekstra H, Ruers T, Wobbles Th. Fluorodeoxyglucose-positron emission tomography and sentinel lymph node biopsy in staging primary cutaneous melanoma. *European Journal of Surgical Oncology* 2003; 2: 662-664.

Cobben D, Jager P, Elsinga P, Maas B, Suurmeijer A, Hoekstra H. 3'-<sup>18</sup>F-fluoro-3'-deoxy-L-thymidine; a new tracer for staging metastatic melanoma? *Journal of Nuclear Medicine* 2003; 44: 1927-1932.

Cobben D, Elsinga P, van Waarde A, Jager P. Correspondence re: H. Barthel et al., 3'-deoxy-3'-[(18)F]fluorothymidine as a new marker for monitoring tumor response to antiproliferative therapy in vivo with positron emission tomography. *Cancer Research* 2003; 63: 3791-3798. *Cancer Research* 2003; 63: 8558-8559.

Bastiaannet E, Groen H, Jager P, Cobben D, van der Graaf W, Vaalburg W, Hoekstra H. The value of FDG-PET in the detection and grading of soft tissue and bone sarcomas; a systematic review and meta-analysis. *Cancer Treatment Reviews* 2004; 30: 83-101

Cobben D, van der Laan B, Maas B, Vaalburg W, Suurmeijer A, Hoekstra H, Jager P, Elsinga P. <sup>18</sup>F-FLT PET for visualization of laryngeal cancer: comparison with <sup>18</sup>F-FDG PET. *Journal of Nuclear Medicine* 2004; 45: 226-231.

Van Waarde A, Cobben D, Suurmeijer A, Maas B, Vaalburg W, de Vries E, Jager P, Hoekstra H, Elsinga P. Selectivity of 3'-deoxy-3'-[<sup>18</sup>F]fluorothymidine (FLT) and 2-[<sup>18</sup>F]fluoro-2-deoxy-D-glucose (FDG) for tumor versus inflammation in a rodent model. *Journal of Nuclear Medicine* 2004. In press.

Cobben D, Elsinga P, Suurmeijer A, Vaalburg W, Maas B, Jager P, Hoekstra H. Detection and grading of soft tissue sarcomas of the extremities with 3'[<sup>18</sup>F]fluoro-3'-deoxy-L-thymidine. *Clinical Cancer Research* 2004; *10*: 1685-90.

Cobben D, Elsinga P, Hoekstra P, Suurmeijer A, Vaalburg W, Maas B, Jager P, Groen H. Is <sup>18</sup>F-3'-fluoro-3'-deoxy-L-thymidine useful for staging and restaging of patients with non-small cell lung cancer? Submitted.

Been L, Cobben D, Jager P, Suurmeijer A, Hoekstra H, Elsinga P. [<sup>18</sup>F]FLT-PET in oncology; an overview of preclinical and clinical data. Submitted.

Positron emission tomography in patients with breast cancer using [<sup>18</sup>F]-fluoro-3'-deoxy-3'-L-fluorothymidine (FLT). A feasibility study. Been L, Cobben D, Elsinga P, Maas B, Jager P, de Vries J, Vaalburg W, Hoekstra H, Suurmeijer A. Submitted.